MAKING UP YOUR MIND:
WIRING THE DOPAMINE SYSTEM

Ewoud Schmidt

'To explore the human condition is to scientifically disentangle the mechanisms of our existence, to artistically testify about the very nature of being in existence, and to religiously hope that we are seen and recognized, that our existence as a drift through time is ultimately justified.'

COLOPHON

The research described in this thesis was performed at the Department of Translational Neuroscience, Brain Center Rudolf Magnus, University Medical Center Utrecht, the Netherlands.

Research in this thesis was financially supported by the Toptalent grant from the Netherlands Organisation for Scientific Research (NWO).

Publication of this thesis was financially supported by the Brain Center Rudolf Magnus, Carl Zeiss Microscopy and the Parkinson Vereniging.

The cover of this thesis was inspired by '*La trahison des images*' by René Magritte.

Cover & layout: Ewoud R. E. Schmidt
Printing: Ridderprint BV, Ridderkerk, the Netherlands
ISBN: 978-90-393-6118-4

MAKING UP YOUR MIND:

WIRING THE DOPAMINE SYSTEM

Ontwikkeling van het Brein:
de Aanleg van Dopaminerge Circuits
(met een samenvatting in het Nederlands)

PROEFSCHRIFT

ter verkrijging van de graad van doctor aan de Universiteit Utrecht
op gezag van de rector magnificus, prof. dr. G. J. van der Zwaan,
ingevolge het besluit van het college voor promoties
in het openbaar te verdedigen

op dinsdag 15 april 2014 des middags te 2.30 uur

door

Ewoud Roberto Eduard Schmidt

geboren op 5 februari 1985 te Rotterdam

Promotoren: Prof. dr. R. J. Pasterkamp
Prof. dr. J. P. H. Burbach

Voor mijn ouders

'Science aims to give us theories which are empirically adequate; and acceptance of a theory involves as belief only that it is empirically adequate.'

-Bas van Fraassen

CONTENTS

'The fact is, however, that the truths that are most evident are also the hardest to explain.'

- Roger Scruton

Chapter 1

General Introduction

PREFACE

Proper functioning of the nervous system relies on highly precise synaptic connectivity between millions of neurons. The formation of these connections relies on intricate cellular and molecular processes, in which axons are guided over long distances towards their targets, innervate appropriate subdomains and selectively connect with their synaptic partner neurons. Once laid out, these connections show various degrees of plasticity necessary to accommodate different aspects of behavior. Studies into the cellular and molecular mechanisms that control these processes have uncovered complex molecular interactions between axons and the extracellular environment and axon-axon interactions between different types of axons within larger axon tracts. However, despite these advances, the development of many brain regions remains poorly understood. Studying these processes is further complicated by the heterogeneous nature of many brain regions, with different classes of neurons grouped together into single brain nuclei or laminae. Though part of the same brain region, these different neuronal subtypes show distinct connectivity patterns and require unique but sometimes overlapping molecular mechanisms for proper circuit formation. A striking example of a brain region where heterogeneity is crucial for coordinating complex physiological and cognitive functions is the mesodiencephalic dopamine (mdDA) system. Disturbances in molecular mechanisms controlling the formation of mdDA neuronal circuitry have been implicated in various neurological and psychiatric diseases, including Parkinson's disease and schizophrenia. Still, our knowledge of the molecular events that underlie the formation of dopaminergic circuitry is still very limited. This thesis explores how molecular mechanisms orchestrate the formation of mdDA neuronal circuitry and aims at developing new tools to support future studies into the molecular and cellular basis of dopaminergic pathway development.

WIRING THE BRAIN: MECHANISMS FOR SHAPING CONNECTIVITY

A hallmark of the central nervous system (CNS) is the highly specific pattern of synaptic connectivity between large varieties of neuronal subtypes. The formation of these precise connections is crucial for the assembly of functional neural circuits. Remarkably, many of these connections are established simultaneously during embryonic and early postnatal development, which poses a challenging task coordinating the formation of these circuits. The following sections present a brief summary of our present knowledge of the molecular mechanisms controlling axon pathfinding and target innervation, processes which are essential for the development of neuronal connectivity.

AXON PATHFINDING

Developing neurons extend their axons over long distances in order to form connections with appropriate synaptic partners. This process of axon guidance is controlled by a group of molecules collectively known as axon guidance molecules. These molecules have classically been presented as cues in the environment, which act either as attractants or repellants and thereby direct axons towards there appropriate targets (Figure 1; Chilton, 2006; Dickson, 2002). In addition, these molecules can either be secreted or membrane-bound, which determines their range of action. Secreted molecules form gradients allowing them to signal over large distances, while membrane-bound cues display a restricted distribution and function locally. Growing axons detect these molecules via highly motile structures at their leading tip, called growth cones, which express specialized cell surface receptors. Binding of axon guidance proteins to the appropriate receptors on the growth cone of an extending axon induces activation of intracellular signaling cascades and results in the subsequent remodeling of the cytoskeleton and growth cone steering (Chilton, 2006; Dickson, 2002; Huber et al., 2003).

Over the past decades, different families of axon guidance proteins, including morphogens and growth factors, have been identified, which has allowed for detailed studies on the molecular mechanisms underlying axon guidance (Kolodkin and Pasterkamp, 2013; Kolodkin and Tessier-Lavigne, 2011). These studies have shown that axon guidance is not a unidirectional mechanism where the growth cone passively receives information through its growth cone receptor. Instead, the expression of

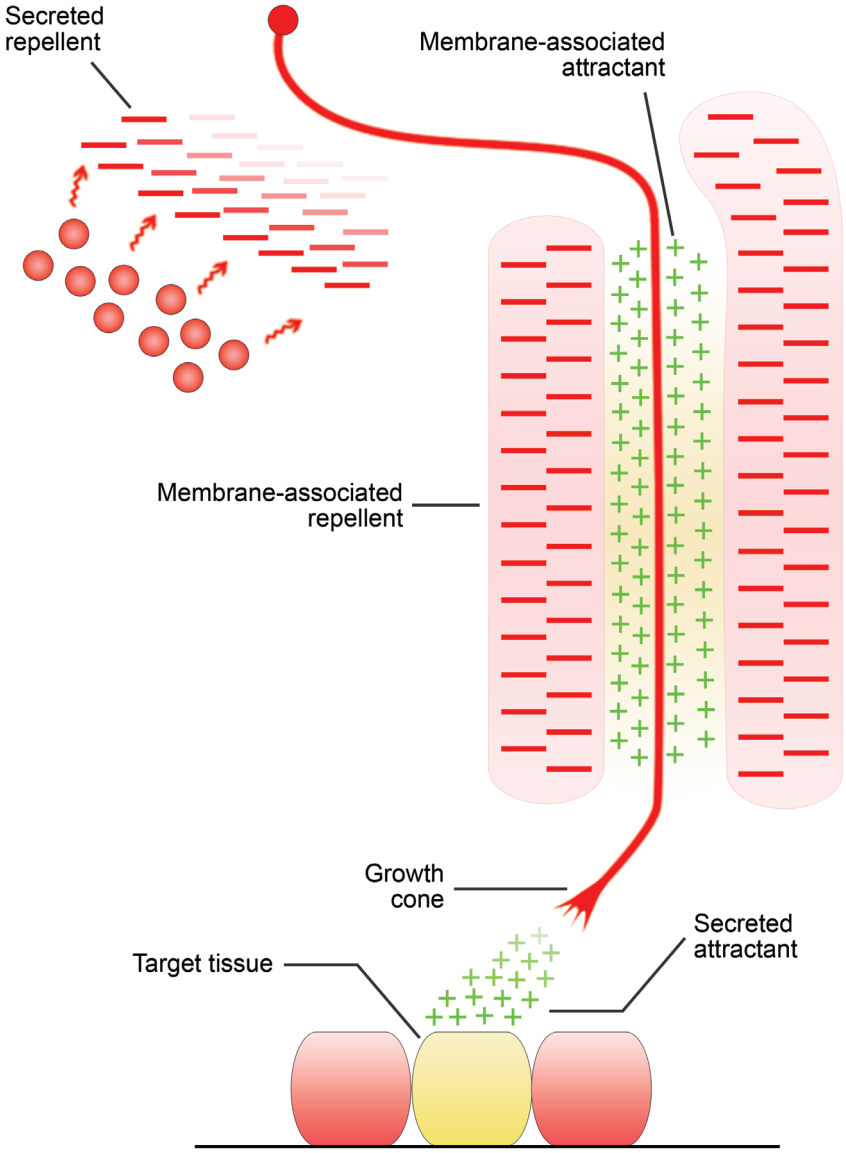

Figure 1. Principles of Axon Guidance.

Axon guidance is a multi-step process controlled by repellent (red minus) or attractant (green plus) molecules in the extracellular environment. These cues can be either secreted, forming long distance gradients, or membrane-associated, forming corridors through which axons travel. These guidance molecules are detected by the growth cone, a motile structure at the leading edge of the axon. Adapted from Schmidt et al., 2009.

these receptors is dynamically regulated via both cell and non-cell autonomous processes, which enables the growth cone to actively change its response to guidance molecules in the environment. In addition, interactions between different guidance molecules and/or downstream signaling pathways can have a synergistic effect, which is different from when these molecules act in isolation (Pasterkamp and Kolodkin, 2013; Raper and Mason, 2010).

AXON-AXON INTERACTIONS

During early development, the first extending axons, or pioneer axons, grow in a relatively axon-free environment in which they are guided by so-called guidepost cells to form the initial axon tracts. These tracts are then used by later extending axons for guidance towards their target, a process mediated by axon-axon interactions (Raper and Mason, 2010; Wang and Marquardt, 2013). For example, within the peripheral nervous system (PNS), axon-axon interactions play a crucial role in wiring sensory connections. Here it was shown that dorsal root sensory axons rely on earlier extending motor axons for guidance towards their targets (Figure 2A). Sensory axons recognize motor axons, a process which is mediated by EphA/ephrin-A signaling, and follow these axons towards their target. Loss of motor axons or changes in their molecular identity results in abnormal guidance of sensory axons (Gallarda et al., 2008; Wang et al., 2011). Similar mechanisms may play a role in guidance of corticothalamic axons (CTAs) and thalamocortical axons (TCAs). In contrast to the peripheral system, CTAs and TCAs extend in opposite directions and meet halfway their trajectory (Figure 2B). Selective ablation of these axon tracts, or selective changes in their trajectory perturbs the growth of the reciprocal tract, indicating a dependency between these two axonal populations (Deck et al., 2013; Hevner et al., 2002). Interestingly, this dependency was postulated almost twenty years ago as the 'handshake-hypothesis' in an attempt to explain how different subpopulations of TCAs are guided towards their appropriate subdomains in the cortex (Molnár and Blakemore, 1995). Although the dependency between CTAs and TCAs is now established, it remains unknown whether these axon-axon interactions are required for subdomain targeting and which molecular mechanisms mediate these types of reciprocal interactions.

Many of the major axon tracts in the CNS and PNS are composed of multiple types of axons. For example, the corpus callosum is composed of axons originating

in cortical layers II/III and V derived from different anatomical domains, such as the visual and sensorimotor cortex. These different axonal subtypes are segregated and organized along the rostrocaudal and ventrodorsal axis (Fame et al., 2011). Heterotypic organization of axon tracts can also be recognized in the PNS, where peripheral nerves are composed of segregated, but tightly bundled sensory and motor projections (Gallarda et al., 2008). The segregation of different axonal subtypes is crucial for the proper wiring of these projections, and in both the CNS and PNS involves EphA/ephrin-A signaling which functions as contact-dependent repulsive cues (Gallarda et al., 2008; Nishikimi et al., 2011). As has been shown for the thalamus and olfactory system (Imai et al., 2009; Lokmane et al., 2013), this segregation may serve as a sorting mechanism where the position of an axon within the tract is directly related to its final mapping in the target region, a mechanism which in the olfactory system is controlled by Semaphorin3A/Neuropilin-1 signaling (Imai et al., 2009).

TARGET SPECIFICITY

Upon arrival in the target region, afferent axons need to make connections with their appropriate synaptic partners, which are often located within subdomains of larger brain nuclei or laminated structures. Our current knowledge of the molecular mechanisms that control this selective targeting of axons is mainly derived from work done on laminated structures and involves complex interactions between axon guidance and cell adhesion molecules. Initially, a combination of repulsive and attractive molecules directs afferent axons to their appropriate layers. For example, repulsive membrane-bound cues, such as transmembrane semaphorins, direct retinal projections and mossy fibers to appropriate lamina in the mouse retina and hippocampus, respectively (Matsuoka et al., 2011a, 2011b; Suto et al., 2007), while the secreted repellent Slit1 regulates layered connectivity in the zebrafish tectum (Xiao et al., 2011). Similarly, Netrin-B acts as a secreted attractant in *Drosophila*, where it mediates lamina-restricted targeting of axons in the medulla of the optic lobe (Timofeev et al., 2012). Following the laminar targeting of axons by guidance molecules, combinatorial expression of homophilic cell surface molecules facilitates the recognition and stabilization of contacts between matched pre- and postsynaptic neurons. For example, Sidekicks and DsCAMs mediate precise synaptic connectivity between different retina neuron subtypes in the inner plexiform layer (IPL) of the chick retina (Yamagata and Sanes, 2008). Homophilic cell adhesion molecules such as

N-Cadherin and Capricious serve analogous functions in the *Drosophila* visual system (Nern et al., 2008; Shinza-Kameda et al., 2006). Similar to laminated structures such as the retina, brain nuclei are often subdivided into smaller subdomains comprising small clusters of related neurons. Recent progress supports the idea that repulsive and adhesive molecules may assist in the targeting of afferent axons to distinct (sub) nuclei (Osterhout et al., 2011; Pecho-Vrieseling et al., 2009). However, the cellular and molecular mechanisms that control subnucleus-specific wiring events remain largely unknown.

The precise pattern of pre- and postsynaptic connectivity largely determines the functional properties of brain regions. Understanding how connections are established and maintained is crucial for grasping the complex workings of the brain. Moreover, emerging evidence indicates the involvement of axon guidance molecules and potential wiring defects in several neurological diseases (Goshima et al., 2012; Lin et al., 2009; Nugent et al., 2012; Schmidt et al., 2009; Yaron and Zheng, 2007). This further underlines the importance of studying how these molecules control

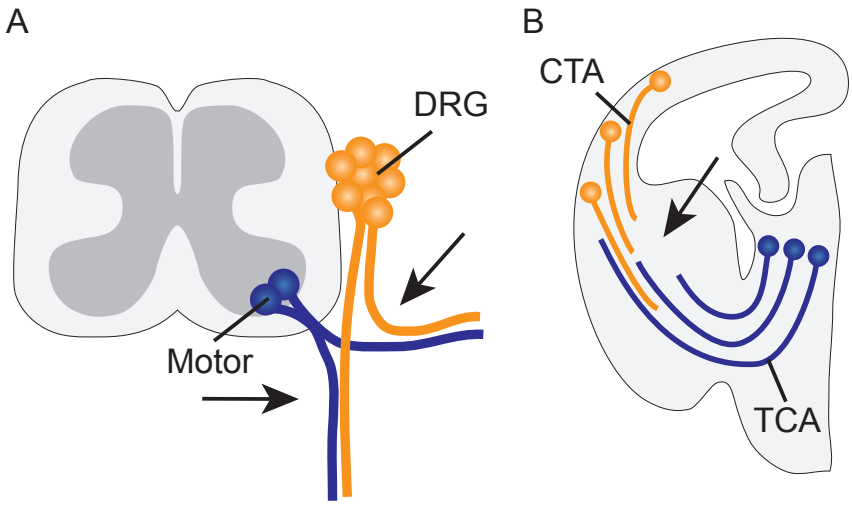

Figure 2. Axon-Axon Interactions Are Crucial for Axon Guidance.

(**A**) Dorsal root ganglion (DRG) axons interact (arrows) with earlier extending motor axons for proper guidance towards their targets. Upon making contact, DRG axons bundle together with motor axons, but remain segregated within the peripheral nerve.

(**B**) Corticothalamic axons (CTA) and thalamocortical axons (TCA) meet halfway along their trajectories in the subpallium (arrow). Interaction between these reciprocal projections is crucial for proper guidance as it determines which subdomain of the cortex or thalamus they innervate.

formation of neuronal circuitry. In this thesis, the mesodiencephalic dopamine (mdDA) system is studied within this context for two reasons: (1) it is a well described and accessible system, making it suitable for studying the development of neuronal connectivity in the CNS; (2) the mdDA system is directly and indirectly associated with many neurological and psychiatric diseases and advancing our knowledge of the development of this system is crucial for developing successful therapeutic strategies. The next sections will specify the midbrain dopamine system in more detail and discuss our current knowledge of the development of mdDA neuronal connectivity.

THE MESODIENCEPHALIC DOPAMINE SYSTEM

The mdDA system comprises a group of dopaminergic neurons located within the ventral midbrain. The mdDA system is essential for controlling voluntary movement and motivational behavior and is affected in many neurological and neuropsychiatric diseases, including Parkinson's disease, depression, schizophrenia, and drug addiction (Björklund and Dunnett, 2007a; Bromberg-Martin et al., 2010;

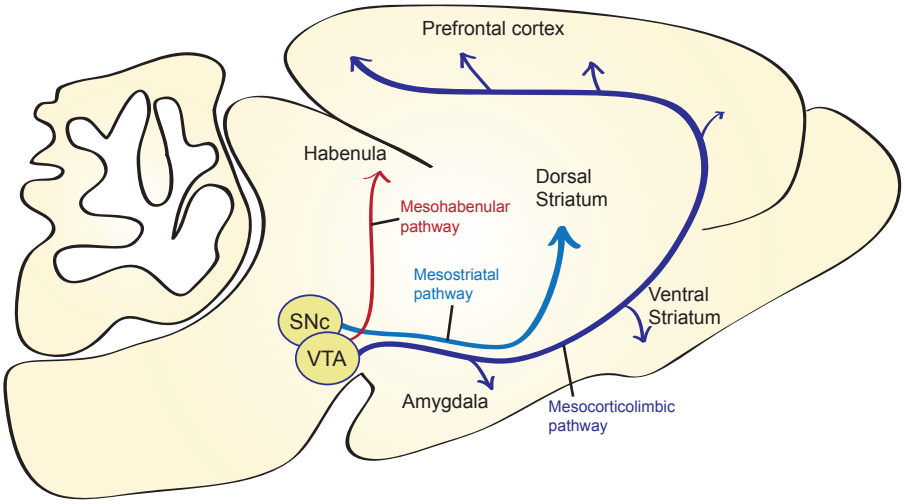

Figure 3. Projections of the Mesodiencephalic Dopamine System.

The mesodiencephalic (mdDA) system sends out projections to various regions in the brain. The substantia nigra pars compacta (SNc) primarily projects to the dorsal striatum, forming the mesostriatal pathway. Projections originating in the ventral tegmental area (VTA) form the mesocorticolimbic pathway, which projects to targets such as the amygdala, ventral striatum, and prefrontal cortex. A small group of axons projects dorsally towards the habenula, forming the mesohabenular pathway.

Dunlop and Nemeroff, 2007; Iversen and Iversen, 2007; Sesack and Carr, 2002; Sulzer, 2007). It contains approximately 20,000-30,000 neurons in mice and up to 400,000-600,000 neurons in humans, which are anatomically organized into three distinct subdomains. Located laterally is the substantia nigra pars compacta (SNc), which mainly sends out its projections towards the dorsal striatum forming the mesostriatal pathway (Figure 3). This mesostriatal pathway is mainly involved in controlling voluntary movement and its degeneration, together with the selective loss of SNc neurons, is the hallmark of Parkinson's disease. In contrast, the ventral tegmental area (VTA) and retrorubral field (RRF) have prominent projections towards the ventral striatum and medial prefrontal cortex (mPFC), known as the mesocorticolimbic pathway (Figure 3), which are involved in controlling motivational behavior (Björklund and Dunnett, 2007b; Van den Heuvel and Pasterkamp, 2008). The mesostriatal and the mesocorticolimbic pathways initially run together through the medial forebrain bundle (MFB) after which they segregate in the forebrain to innervate their prospective targets. In contrast, a small group of axons arising from neurons within the VTA, project dorsally towards the habenula. These projections are known as the mesohabenular pathway (Figure 3). The habenula plays an important role in signaling negative reward and has been associated with psychiatric diseases, such as major depressive disorder (Li et al., 2011, 2013; Matsumoto and Hikosaka, 2007, 2009). It comprises two subdomains, the medial habenula (mHb) and lateral habenula (lHb). The mHb primarily innervates the interpeduncular nucleus, while the lHb innervates monoaminergic nuclei, including the mdDA system. Moreover, the lHb is the only subdomain which receives reciprocal dopaminergic input from the mesohabenular pathway. The function of the mesohabenular pathway is still poorly understood, but recent results suggest it may act as a feedback loop by modulating habenular activity, and as such is important for coordinating reward related behaviors (Bianco and Wilson, 2009; Gruber et al., 2007; Kowski et al., 2009; Lecourtier and Kelly, 2007; Shen et al., 2012; Stamatakis et al., 2013). Mesohabenular axons run through the fasciculus retroflexus (FR), which is also the major output bundle of the habenula. The FR contains efferents from the habenula, which intermingle with afferents targeting the habenula. Interestingly, early tracing and lesion studies have shown that axons within the FR are organized into different subdomains (Araki et al., 1988; Ellison, 1992, 2002). Whether organization of axon tracts, such as in the FR, plays a role in guidance of mdDA axons remains unexplored. As will be

discussed in Chapter 3, the mesohabenular pathway provides a unique opportunity for studying how such processes control wiring of the mdDA system.

The identification of anatomically and functionally distinct mdDA subsets has provided important insights into how the mdDA system controls cognitive and motor behavior (Ikemoto, 2007; Roeper, 2013). Recent studies have further unraveled this diversity on a molecular and physiological level (Chung et al., 2005; Greene et al., 2005; Lammel et al., 2008; Di Salvio et al., 2010; Simeone et al., 2011; Veenvliet et al., 2013). However, our understanding of the underlying development and function of these neuronal subsets is lagging behind, and many aspects, such as how subset-specific connectivity is established, are still poorly understood (Van den Heuvel and Pasterkamp, 2008; Smidt and Burbach, 2007). Studies addressing these questions have been hindered by a lack of tools to reliably identify these subsets, an issue which will be further discussed in Chapter 5.

DEVELOPMENT OF THE MDDA SYSTEM

The formation of mdDA neuronal circuitry involves a series of stereotypic cellular and molecular events which control the guidance of mdDA axons towards appropriate target areas. The following sections will discuss our current knowledge of how mdDA axons are routed towards their targets and the molecular mechanisms that dictate the formation of this circuitry during development.

EARLY GUIDANCE WITHIN THE MIDBRAIN

Upon leaving the ventral midbrain, mdDA axons follow a dorsal trajectory after which they turn and grow in a rostral direction towards the forebrain (Figure 4A). Interactions between different classes of repellent and attractant axon guidance proteins play a role in this initial outgrowth and turning. Slits, known for their potent repulsive effect, are expressed in the hindbrain and the caudal and dorsal midbrain, whereas mdDA neurons express the cognate receptors Robo1 and Robo2 (Dugan et al., 2011; Lin et al., 2005; Marillat et al., 2002). This distribution of Slit proteins together with *in vitro* data showing the repulsive effect of Slits on mdDA axon outgrowth, strongly suggests these Slits prevent mdDA axons from aberrantly extending into the caudal or dorsal midbrain. This is further supported by pathfinding errors observed in *Slit1/2* and *Robo1/2* mutant mice (Dugan et al., 2011; Lin et al.,

2005; Marillat et al., 2002). Similarly, Semaphorin3F (Sema3F) is expressed dorsal and caudal of the mdDA system and is required for the rostral orientation of mdDA axons by repelling these axons rostrally (Yamauchi et al., 2009). In contrast, Sema3C is expressed in the prospective path along which mdDA axons travel towards the forebrain and acts as an attractant for these axons *in vitro* (Hernández-Montiel et al., 2008), supporting a role in guiding axons towards the forebrain. In addition to these axon guidance molecules, morphogens, such as Wnts, have recently been implicated in the rostral orientation of mdDA axons (Fenstermaker et al., 2010). Wnt5a and Wnt7b are expressed in opposing gradients along the rostrocaudal axis in the ventral midbrain, with Wnt5a showing low rostral/high caudal and Wnt7b high rostral/low caudal expression. Consistent with their role in controlling early mdDA pathfinding, Wnt5a acts as a repellent for mdDA axons, whereas Wnt7b has an attractive effect. Both Wnts signal through PCP receptor molecules expressed on mdDA axons and both PCP and Wnt5 mutant mice show defects in the rostral orientation of mdDA axons (Fenstermaker et al., 2010).

The expression of repellent molecules, such as Slits, Sema3F and Wnt5, in the ventral midbrain, is crucial for the proper rostral orientation and guidance of mdDA axons towards the forebrain. However, it is important to note that a small group of mdDA axons needs to traverse the dorsal midbrain to reach the habenula. As will be discussed in Chapter 3, these axons make use of a permissive pathway laid out by axons from the lHb, which provides a permissive corridor for these mesohabenular neurons.

GUIDANCE THROUGH THE MEDIAL FOREBRAIN BUNDLE

As mdDA axons enter the diencephalon, they tightly fasciculate into the medial forebrain bundle (MFB; Figure 4B). This process is controlled by surround repulsion mediated by Sema3F, which is expressed around the presumptive MFB. In addition, Sema3F is required for maintaining rostral growth through the lateral hypothalamic region (Kolk et al., 2009). Similarly, Wnt5a plays a role in fasciculating mdDA axons, since abnormal fasciculation of the MFB was observed in Wnt5a mutant mice (Blakely et al., 2011). In addition, a combination of molecules expressed at the ventral midline, including Netrin-1, Slit-1/Slit-2 and Sema3A, maintains the ipsilateral projection of mdDA axons by preventing aberrant midline crossing (Dugan et al., 2011; Kawano, 2003; Lin et al., 2005; Xu et al., 2010). Finally, a combination

of repellent and attractant cues in structures along the route of the MFB, such as expression of Slits and Sonic hedgehog (Shh) in the hypothalamus, may be involved in ensuring guidance of mdDA axons towards their targets within the forebrain (Deschamps et al., 2010; Hammond et al., 2009; Prestoz et al., 2012).

INNERVATION OF FOREBRAIN TARGETS

After traveling through the MFB, mdDA axons reach the forebrain, from where they innervate their targets (Figure 4C). In the adult, SNc neurons target the dorsolateral striatum, while VTA neurons predominantly target the ventrolateral striatum and prefrontal cortex (PFC). However, the dorsal and ventral striatum are initially innervated by both SNc and VTA neurons. Correct mapping of mdDA projections within the striatum is subsequently achieved by eliminating inappropriate axon collaterals during late embryonic development (Hu et al., 2004). Innervation and correct mapping of mdDA projections within the striatum may in part be controlled by the Eph/Ephrin family of axon guidance molecules. High expression of Ephrin-B2 is detected in ventromedial striatum, while expression is low in the dorsolateral striatum. Ephrin-B2 functions as a repulsive ligand for EphB1 expressing axons. Interestingly, SNc neurons, which target the dorsolateral striatum, express EphB1. No EphB1 expression is detected in VTA neurons which target the ventromedial striatum (Yue et al., 1999). Although this suggests a possible role for Ephrin-B2 as a pruning factor, analysis of *EphB1* mutant mice did not reveal any defects in the mapping of mdDA axons within the striatum (Richards et al., 2007). This may be explained by compensatory mechanism of other Ephs or Ephrins expressed within this system, or could indicate that Ephrin-B2 signals through other receptor molecules (Cooper et al., 2008; Passante et al., 2008; Sun et al., 2010).

Axons originating in the VTA densely innervate the prefrontal cortex (PFC). Although the molecular mechanisms controlling this innervation remain largely unknown, Sema3F and Nrp2 have been implicated in controlling innervation of the developing cortical plate (Kolk et al., 2009). Sema3F functions as a chemoattractant by reorienting and redirecting Nrp2-expressing mdDA axons in the subplate towards the cortical plate. This is surprising, as Sema3F functions as a repellent at earlier stages of development when these axons grow through the MFB. This demonstrates the potential of mdDA axons to actively change their response to environmental cues and underlines the complexity of mdDA circuit development.

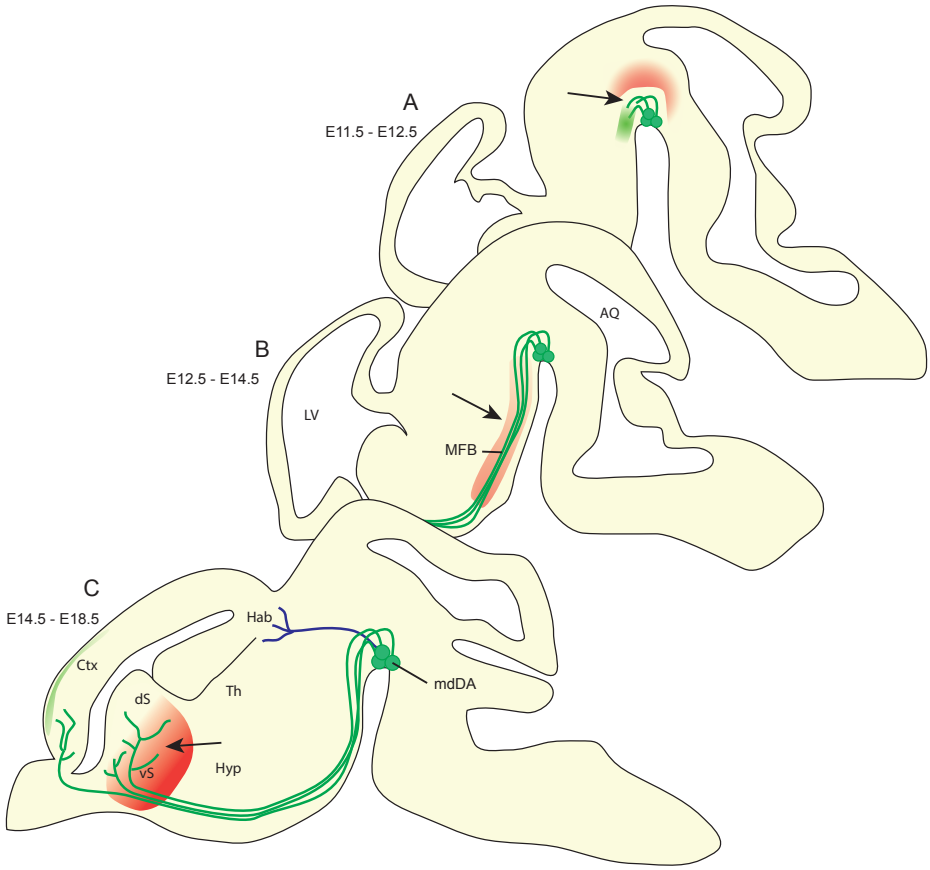

Figure 4. Development of Mesodiencephalic Projections.

(**A-C**) Developing mdDA axons are guided by a combination of repellent (red) and attractant (green) molecules that direct these axons towards their targets in the forebrain. MdDA axons initially extend in a dorsal direction after which they redirect rostrally (arrow) towards the forebrain. This process is mediated by chemorepulsive activity in the caudal and dorsal midbrain and chemoattractive activity along the presumptive trajectory of mdDA axons towards the forebrain (**A**). Next, mdDA axons fasciculate (arrow) in the medial forebrain bundle (MFB), which is mediated by surround repulsion around the MFB, after which they continue their journey ventrally in a rostral direction (**B**). Upon arrival at their target regions in the forebrain, mdDA axons defasciculate and innervate their appropriate targets (arrow). A gradient of chemorepulsive cues mediates mapping of mdDA axons in the striatum. Chemoattractive activity in the cortex directs mdDA axons towards their appropriate cortical layers (**C**). Mechanisms controlling development of mdDA axons targeting the habenula (blue) are discussed in Chapter 3. AQ, aquaduct; Ctx, cortex; dS, dorsal striatum; Hab, habenula; Hyp, hypothalamus; LV, lateral ventricle; Th, thalamus; vS, ventral striatum.

FUNCTION AND MAINTENANCE

After the initial formation of mdDA circuitry, several classes of guidance molecules remain expressed within mdDA neurons and their target areas at postnatal stages and during adulthood. These molecules may be important for the late phases of development, such as the innervation of the PFC, which continues until early adulthood. In addition, they may function to control neuronal plasticity and maintain neuronal connections throughout life (Prestoz et al., 2012; Rosenberg and Lewis, 1995). The mdDA system has been implicated in various neuropsychiatric disorders and changes in the mdDA circuitry during perinatal development or adulthood may underlie or contribute to these disorders (Flores, 2011). Recent studies have begun to unravel how axon guidance molecules, in particular Netrin-1 and its transmembrane receptors Deleted in Colorectal Cancer (DCC), control functional changes in mdDA circuitry during postnatal and adult stages. Changes in the level of DCC, using DCC heterozygous mutant mice, results in a reduced sensitization to amphetamine. Interestingly, this effect was not present in juvenile or peripubertal mice, consistent with the idea that the presence of axon guidance molecules at adult stages is crucial for maintaining proper functional connectivity in response to extrinsic stimuli (Flores et al., 2005; Grant et al., 2007). Moreover, corresponding structural changes in the PFC were found at both the pre- and postsynaptic level (Manitt et al., 2011). It should be noted that Netrin-1 is a bifunctional guidance protein and its role as an attractant or repellent is determined by its interaction with DCC or UNC5H, respectively (Muramatsu et al., 2010). In Chapter 4 the possible role of UNC5H in controlling functional changes in mdDA circuitry will be further discussed.

CONCLUDING REMARKS

Our current knowledge of the cellular and molecular mechanisms controlling the formation and maintenance of mdDA circuitry is still very limited. The mdDA system consists of a heterogeneous group of neurons located within different anatomical domains. However, besides this anatomical diversity, recent studies have identified new neuronal subtypes at a molecular and physiological level (Chung et al., 2005; Greene et al., 2005; Lammel et al., 2008; Di Salvio et al., 2010; Simeone et al., 2011; Veenvliet et al., 2013). This has provided important new insights into how the mdDA system controls cognitive and motor behaviors (Ikemoto, 2007; Roeper,

2013), but our understanding of the development and function of these neuronal subsets is rather limited and many aspects, such as how subset-specific connectivity is established and maintained, are still poorly understood (Van den Heuvel and Pasterkamp, 2008; Smidt and Burbach, 2007).

AIM AND OUTLINE OF THIS THESIS

Formation of precise synaptic connectivity is controlled by a myriad of molecular interactions between axons and the extracellular environment, and interactions between axons in larger axon tracts. Disturbances in the formation of neuronal circuits have been implicated in various neuropsychiatric disorders. In particular, disruptions in the development of mdDA circuitry may contribute to the underlying pathology of diseases such as Parkinson's disease and schizophrenia. Still, very little is known about the molecular mechanisms underlying the development of mdDA circuitry. Studies into the development of these circuits have been hampered by a lack of tools to identify and characterize different subsets of mdDA neurons. This thesis is aimed at unraveling the molecular principles that dictate mdDA circuit formation by 1) using a combination of molecular, cellular and mouse genetic approaches to study the development of mdDA circuitry, and 2) develop new tools to facilitate future in-depth studies into the molecular mechanisms that control mdDA circuit development. Our findings can be summarized as follows:

Chapter 2: Dissection and Culture of Mouse Dopaminergic and Striatal Explants in Three-Dimensional Collagen Matrix Assays

Molecules that affect mdDA axon guidance and targeting can be studied *in vitro* by culturing mdDA explants together with explants of their target areas, such as the striatum, in a collagen matrix assay. In this chapter, we describe methods for the purification of rat tail collagen, microdissection of dopaminergic and striatal explants, their culture in collagen gels, and subsequent immunohistochemical and quantitative analysis.

Chapter 3: Subdomain-Mediated Axon-Axon Signaling and Chemoattraction Cooperate to Regulate Afferent Innervation of the Lateral Habenula

Axons originating in the VTA specifically target the lHb. However, how this specific innervation of the lHb is established remains largely unknown. In this chapter, we demonstrate that the lHb sends out efferent projections that guide dopaminergic afferents to the lHb, a process mediated by the cell adhesion molecule LAMP. Upon arrival, Netrin-1 secretion by the lHb controls axon target entry to ensure specific innervation of the lHb.

Chapter 4: *Unc5C* Haploinsufficient Phenotype: Striking Similarities with the *DCC* Haploinsufficiency Model

The guidance cue receptors DCC and UNC5 homologues (UNC5H) are expressed by mesocorticolimbic dopamine neurons. In this chapter, we demonstrate that *Unc5C* haploinsufficiency results in diminished amphetamine-induced locomotion which is observed after adolescence. Tyrosine hydroxylase expression in *Unc5C* haploinsufficient mice is increased in the medial prefrontal cortex, but not in the nucleus accumbens. The striking similarity between the DCC and the Unc5C haploinsufficient phenotypes supports the possibility that the reported effects are mediated by DCC/UNC5C receptor complex.

Chapter 5: Transgenic Strategy for Analyzing Midbrain Dopamine Neuron Diversity

In this chapter, we present a genetic strategy, called *Pitx3-ITC*, which relies on subset-specific Cre or Flp expression for labeling of two mdDA subsets in a single mouse. In addition, we present *Nrp2-FlpO* and *Gucy2c-iCre* mice which, together with *Pitx3-ITC* mice, sparsely label mdDA neurons. Initial characterization of these mice reveals previously unknown axonal organization of mdDA subsets, as well as characteristic, but poorly understood, connectivity patterns at both the pre- and postsynaptic level.

Chapter 6: General Discussion

In this chapter, we discuss the results described in this thesis in the light of what is currently known about mechanisms controlling formation of neuronal circuits. Our findings provide new insights into fundamental mechanisms dictating neuronal circuit formation and provide new tools for future studies into the development of the mdDA system.

REFERENCES

Araki, M., McGeer, P.L., and Kimura, H. (1988). The efferent projections of the rat lateral habenular nucleus revealed by the PHA-L anterograde tracing method. Brain Res. *441*, 319–330.

Bianco, I.H., and Wilson, S.W. (2009). The habenular nuclei: a conserved asymmetric relay station in the vertebrate brain. Philos. Trans. R. Soc. Lond. B. Biol. Sci. *364*, 1005–1020.

Björklund, A., and Dunnett, S.B. (2007a). Fifty years of dopamine research. Trends Neurosci. *30*, 185–187.

Björklund, A., and Dunnett, S.B. (2007b). Dopamine neuron systems in the brain: an update. Trends Neurosci. *30*, 194–202.

Blakely, B.D., Bye, C.R., Fernando, C. V, Horne, M.K., Macheda, M.L., Stacker, S. A., Arenas, E., and Parish, C.L. (2011). Wnt5a regulates midbrain dopaminergic axon growth and guidance. PLoS One *6*, e18373.

Bromberg-Martin, E.S., Matsumoto, M., and Hikosaka, O. (2010). Dopamine in motivational control: rewarding, aversive, and alerting. Neuron *68*, 815–834.

Chilton, J.K. (2006). Molecular mechanisms of axon guidance. Dev. Biol. *292*, 13–24.

Chung, C.Y., Seo, H., Sonntag, K.C., Brooks, A., Lin, L., and Isacson, O. (2005). Cell type-specific gene expression of midbrain dopaminergic neurons reveals molecules involved in their vulnerability and protection. Hum. Mol. Genet. *14*, 1709–1725.

Cooper, M. A., Kobayashi, K., and Zhou, R. (2008). Ephrin-A5 regulates the formation of the ascending midbrain dopaminergic pathways. Dev. Neurobiol. *69*, 36–46.

Deck, M., Lokmane, L., Chauvet, S., Mailhes, C., Keita, M., Niquille, M., Yoshida, M., Yoshida, Y., Lebrand, C., Mann, F., et al. (2013). Pathfinding of Corticothalamic Axons Relies on a Rendezvous with Thalamic Projections. Neuron *77*, 472–484.

Deschamps, C., Morel, M., Janet, T., Page, G., Jaber, M., Gaillard, A., and Prestoz, L. (2010). EphrinA5 protein distribution in the developing mouse brain. BMC Neurosci. *11*, 105.

Dickson, B.J. (2002). Molecular mechanisms of axon guidance. Science *298*, 1959–1964.

Dugan, J.P., Stratton, A., Riley, H.P., Farmer, W.T., and Mastick, G.S. (2011). Midbrain dopaminergic axons are guided longitudinally through the diencephalon by Slit/Robo signals. Mol. Cell. Neurosci. *46*, 347–356.

Dunlop, B.W., and Nemeroff, C.B. (2007). The role of dopamine in the pathophysiology of depression. Arch. Gen. Psychiatry *64*, 327–337.

Ellison, G. (1992). Continuous amphetamine and cocaine have similar neurotoxic effects in lateral habenular nucleus and fasciculus retroflexus. Brain Res. *598*, 353–356.

Ellison, G. (2002). Neural degeneration following chronic stimulant abuse reveals a weak link in brain, fasciculus retroflexus, implying the loss of forebrain control circuitry. Eur. Neuropsychopharmacol. *12*, 287–297.

Fame, R.M., MacDonald, J.L., and Macklis, J.D. (2011). Development, specification, and diversity of callosal projection neurons. Trends Neurosci. *34*, 41–50.

Fenstermaker, A.G., Prasad, A. A., Bechara, A., Adolfs, Y., Tissir, F., Goffinet, A., Zou, Y., and Pasterkamp, R.J. (2010). Wnt/planar cell polarity signaling controls the anterior-posterior organization of monoaminergic axons in the brainstem. J. Neurosci. *30*, 16053–16064.

Flores, C. (2011). Role of netrin-1 in the organization and function of the mesocorticolimbic dopamine system. J. Psychiatry Neurosci. *36*, 296–310.

Flores, C., Manitt, C., Rodaros, D., Thompson, K.M., Rajabi, H., Luk, K.C., Tritsch, N.X., Sadikot, A. F., Stewart, J., and Kennedy, T.E. (2005). Netrin receptor deficient mice exhibit functional reorganization of dopaminergic systems and do not sensitize to amphetamine. Mol. Psychiatry *10*, 606–612.

Gallarda, B.W., Bonanomi, D., Müller, D., Brown, A., Alaynick, W. A., Andrews, S.E., Lemke, G., Pfaff, S.L., and Marquardt, T. (2008). Segregation of Axial Motor and Sensory Pathways via Heterotypic Trans-Axonal Signaling. Science *320*, 233–236.

Goshima, Y., Sasaki, Y., Yamashita, N., and Nakamura, F. (2012). Class 3 semaphorins as a therapeutic target. Expert Opin. Ther. Targets *16*, 933–944.

Grant, A., Hoops, D., Labelle-Dumais, C., Prévost, M., Rajabi, H., Kolb, B., Stewart, J., Arvanitogiannis, A., and Flores, C. (2007). Netrin-1 receptor-deficient mice show enhanced mesocortical dopamine transmission and blunted behavioural responses to amphetamine. Eur. J. Neurosci. *26*, 3215–3228.

Greene, J.G., Dingledine, R., and Greenamyre, J.T. (2005). Gene expression profiling of rat midbrain dopamine neurons: implications for selective vulnerability in parkinsonism. Neurobiol. Dis. *18*, 19–31.

Gruber, C., Kahl, A., Lebenheim, L., Kowski, A., Dittgen, A., and Veh, R.W. (2007). Dopaminergic projections from the VTA substantially contribute to the mesohabenular pathway in the rat. Neurosci. Lett. *427*, 165–170.

Hammond, R., Blaess, S., and Abeliovich, A. (2009). Sonic hedgehog is a chemoattractant for midbrain dopaminergic axons. PLoS One *4*, e7007.

Hernández-Montiel, H.L., Tamariz, E., Sandoval-Minero, M.T., and Varela-Echavarría, A. (2008). Semaphorins 3A, 3C, and 3F in mesencephalic dopaminergic axon pathfinding. J. Comp. Neurol. *506*, 387–397.

Van den Heuvel, D.M.A., and Pasterkamp, R.J. (2008). Getting connected in the dopamine system. Prog. Neurobiol. *85*, 75–93.

Hevner, R.F., Miyashita-Lin, E., and Rubenstein, J.L.R. (2002). Cortical and thalamic axon pathfinding defects in Tbr1, Gbx2, and Pax6 mutant mice: evidence that cortical and thalamic axons interact and guide each other. J. Comp. Neurol. *447*, 8–17.

Hu, Z., Cooper, M., Crockett, D.P., and Zhou, R. (2004). Differentiation of the midbrain dopaminergic pathways during mouse development. J. Comp. Neurol. *476*, 301–311.

Huber, A.B., Kolodkin, A.L., Ginty, D.D., and Cloutier, J-F. (2003). Signaling at the growth cone: ligand-receptor complexes and the control of axon growth and guidance. Annu. Rev. Neurosci. *26*, 509–563.

Ikemoto, S. (2007). Dopamine reward circuitry: two projection systems from the ventral midbrain to the nucleus accumbens-olfactory tubercle complex. Brain Res. Rev. *56*, 27–78.

Imai, T., Yamazaki, T., Kobayakawa, R., Kobayakawa, K., Abe, T., Suzuki, M., and Sakano, H. (2009). Pre-target axon sorting establishes the neural map topography. Science *325*, 585–590.

Iversen, S.D., and Iversen, L.L. (2007). Dopamine: 50 years in perspective. Trends Neurosci. *30*, 188–193.

Kawano, H. (2003). Aberrant trajectory of ascending dopaminergic pathway in mice lacking Nkx2.1. Exp. Neurol. *182*, 103–112.

Kolk, S.M., Gunput, R.-A.F., Tran, T.S., van den Heuvel, D.M.A., Prasad, A.A., Hellemons, A.J.C.G.M., Adolfs, Y., Ginty, D.D., Kolodkin, A.L., Burbach, J.P.H., et al. (2009). Semaphorin 3F is a bifunctional guidance cue for dopaminergic axons and controls their fasciculation, channeling, rostral growth, and intracortical targeting. J. Neurosci. *29*, 12542–12557.

Kolodkin, A.L., and Pasterkamp, R.J. (2013). SnapShot: Axon Guidance II. Cell *153*, 722–722.e1.

Kolodkin, A.L., and Tessier-Lavigne, M. (2011). Mechanisms and molecules of neuronal wiring: a primer. Cold Spring Harb. Perspect. Biol. *3*, 1–14.

Kowski, A. B., Veh, R.W., and Weiss, T. (2009). Dopaminergic activation excites rat lateral habenular neurons in vivo. Neuroscience *161*, 1154–1165.

Lammel, S., Hetzel, A., Häckel, O., Jones, I., Liss, B., and Roeper, J. (2008). Unique properties of mesoprefrontal neurons within a dual mesocorticolimbic dopamine system. Neuron *57*, 760–773.

Lecourtier, L., and Kelly, P.H. (2007). A conductor hidden in the orchestra? Role of the habenular complex in monoamine transmission and cognition. Neurosci. Biobehav. Rev. *31*, 658–672.

Li, B., Piriz, J., Mirrione, M., Chung, C., Proulx, C.D., Schulz, D., Henn, F., and Malinow, R. (2011). Synaptic potentiation onto habenula neurons in the learned helplessness model of depression. Nature *470*, 535–539.

Li, K., Zhou, T., Liao, L., Yang, Z., Wong, C., Henn, F., Malinow, R., Yates, J.R., and Hu, H. (2013). βCaMKII in lateral habenula mediates core symptoms of depression. Science *341*, 1016–1020.

Lin, L., Rao, Y., and Isacson, O. (2005). Netrin-1 and slit-2 regulate and direct neurite growth of ventral midbrain dopaminergic neurons. Mol. Cell. Neurosci. *28*, 547–555.

Lin, L., Lesnick, T.G., Maraganore, D.M., and Isacson, O. (2009). Axon guidance and synaptic maintenance: preclinical markers for neurodegenerative disease and therapeutics. Trends Neurosci. *32*, 142–149.

Lokmane, L., Proville, R., Narboux-Nême, N., Györy, I., Keita, M., Mailhes, C., Léna, C., Gaspar, P., Grosschedl, R., and Garel, S. (2013). Sensory map transfer to the neocortex relies on pretarget ordering of thalamic axons. Curr. Biol. *23*, 810–816.

Manitt, C., Mimee, A., Eng, C., Pokinko, M., Stroh, T., Cooper, H.M., Kolb, B., and Flores, C. (2011). The netrin receptor DCC is required in the pubertal organization of mesocortical dopamine circuitry. J. Neurosci. *31*, 8381–8394.

Marillat, V., Cases, O., Nguyen-Ba-Charvet, K.T., Tessier-Lavigne, M., Sotelo, C., and Chédotal, A. (2002). Spatiotemporal expression patterns of slit and robo genes in the rat brain. J. Comp. Neurol. *442*, 130–155.

Matsumoto, M., and Hikosaka, O. (2007). Lateral habenula as a source of negative reward signals in dopamine neurons. Nature *447*, 1111–1115.

Matsumoto, M., and Hikosaka, O. (2009). Representation of negative motivational value in the primate lateral habenula. Nat. Neurosci. *12*, 77–84.

Matsuoka, R.L., Nguyen-Ba-Charvet, K.T., Parray, A., Badea, T.C., Chédotal, A., and Kolodkin, A.L. (2011a). Transmembrane semaphorin signalling controls laminar stratification in the mammalian retina. Nature *470*, 259–263.

Matsuoka, R.L., Chivatakarn, O., Badea, T.C., Samuels, I.S., Cahill, H., Katayama, K., Kumer, S., Suto, F., Chedotal, A., Peachey, N.S., et al. (2011b). Class 5 Transmembrane Semaphorins Control Selective Mammalian Lamination and Function. Neuron *71*, 460–473.

Molnár, Z., and Blakemore, C. (1995). How do thalamic axons find their way to the cortex? Trends Neurosci. *18*, 389–397.

Muramatsu, R., Nakahara, S., Ichikawa, J., Watanabe, K., Matsuki, N., and Koyama, R. (2010). The ratio of "deleted in colorectal cancer" to "uncoordinated-5A" netrin-1 receptors on the growth cone regulates mossy fibre directionality. Brain *133*, 60–75.

Nern, A., Zhu, Y., and Zipursky, S.L. (2008). Local N-cadherin interactions mediate distinct steps in the targeting of lamina neurons. Neuron *58*, 34–41.

Nishikimi, M., Oishi, K., Tabata, H., Torii, K., and Nakajima, K. (2011). Segregation and pathfinding of callosal axons through EphA3 signaling. J. Neurosci. *31*, 16251–16260.

Nugent, A. a, Kolpak, A.L., and Engle, E.C. (2012). Human disorders of axon guidance. Curr. Opin. Neurobiol. *22*, 837–843.

Osterhout, J.A., Josten, N., Yamada, J., Pan, F., Wu, S., Nguyen, P.L., Panagiotakos, G., Inoue, Y.U., Egusa, S.F., Volgyi, B., et al. (2011). Cadherin-6 Mediates Axon-Target Matching in a Non-Image-Forming Visual Circuit. Neuron *71*, 632–639.

Passante, L., Gaspard, N., Degraeve, M., Frisén, J., Kullander, K., De Maertelaer, V., and Vanderhaeghen, P. (2008). Temporal regulation of ephrin/Eph signalling is required for the spatial patterning of the mammalian striatum. Development *135*, 3281–3290.

Pasterkamp, R.J., and Kolodkin, A.L. (2013). SnapShot: Axon Guidance. Cell *153*, 494–494.e2.

Pecho-Vrieseling, E., Sigrist, M., and Yoshida, Y. (2009). Specificity of sensory–motor connections encoded by Sema3e–Plxnd1 recognition. Nature *459*, 842–846.

Prestoz, L., Jaber, M., and Gaillard, A. (2012). Dopaminergic axon guidance: which makes what? Front. Cell. Neurosci. *6*, 32.

Raper, J., and Mason, C. (2010). Cellular strategies of axonal pathfinding. Cold Spring Harb. Perspect. Biol. *2*, a001933.

Richards, A. B., Scheel, T. A., Wang, K., Henkemeyer, M., and Kromer, L.F. (2007). EphB1 null mice exhibit neuronal loss in substantia nigra pars reticulata and spontaneous locomotor hyperactivity. Eur. J. Neurosci. *25*, 2619–2628.

Roeper, J. (2013). Dissecting the diversity of midbrain dopamine neurons. Trends Neurosci. *36*, 336–342.

Rosenberg, D.R., and Lewis, D.A. (1995). Postnatal maturation of the dopaminergic innervation of monkey prefrontal and motor cortices: a tyrosine hydroxylase immunohistochemical analysis. J. Comp. Neurol. *358*, 383–400.

Di Salvio, M., Di Giovannantonio, L.G., Omodei, D., Acampora, D., and Simeone, A. (2010). Otx2 expression is restricted to dopaminergic neurons of the ventral tegmental area in the adult brain. Int. J. Dev. Biol. *54*, 939–945.

Schmidt, E.R.E., Pasterkamp, R.J., and van den Berg, L.H. (2009). Axon guidance proteins: novel therapeutic targets for ALS? Prog. Neurobiol. *88*, 286–301.

Sesack, S.R., and Carr, D.B. (2002). Selective prefrontal cortex inputs to dopamine cells: implications for schizophrenia. Physiol. Behav. *77*, 513–517.

Shen, X., Ruan, X., and Zhao, H. (2012). Stimulation of Midbrain Dopaminergic Structures Modifies Firing Rates of Rat Lateral Habenula Neurons. PLoS One *7*, e34323.

Shinza-Kameda, M., Takasu, E., Sakurai, K., Hayashi, S., and Nose, A. (2006). Regulation of layer-specific targeting by reciprocal expression of a cell adhesion molecule, capricious. Neuron *49*, 205–213.

Simeone, A., Di Salvio, M., Di Giovannantonio, L.G., Acampora, D., Omodei, D., and Tomasetti, C. (2011). The role of otx2 in adult mesencephalic-diencephalic dopaminergic neurons. Mol. Neurobiol. *43*, 107–113.

Smidt, M.P., and Burbach, J.P.H. (2007). How to make a mesodiencephalic dopaminergic neuron. Nat. Rev. Neurosci. *8*, 21–32.

Stamatakis, A.M., Jennings, J.H., Ung, R.L., Blair, G.A., Weinberg, R.J., Neve, R.L., Boyce, F., Mattis, J., Ramakrishnan, C., Deisseroth, K., et al. (2013). A Unique Population of Ventral Tegmental Area Neurons Inhibits the Lateral Habenula to Promote Reward. Neuron *80*, 1039–1053.

Sulzer, D. (2007). Multiple hit hypotheses for dopamine neuron loss in Parkinson's disease. Trends Neurosci. *30*, 244–250.

Sun, J.H., Gao, Q., Zhang, J., Bao, L.H., Dong, H.M., Liang, N., Li, G.B., Li, Z.H., and Gao, Y.M. (2010). Ephrinb3 induces mesostriatal dopaminergic projection to the striatum. Biochem. Biophys. Res. Commun. *400*, 194–199.

Suto, F., Tsuboi, M., Kamiya, H., Mizuno, H., Kiyama, Y., Komai, S., Shimizu, M., Sanbo, M., Yagi, T., Hiromi, Y., et al. (2007). Interactions between plexin-A2, plexin-A4, and semaphorin 6A control lamina-restricted projection of hippocampal mossy fibers. Neuron *53*, 535–547.

Timofeev, K., Joly, W., Hadjieconomou, D., and Salecker, I. (2012). Localized netrins act as positional cues to control layer-specific targeting of photoreceptor axons in Drosophila. Neuron *75*, 80–93.

Veenvliet, J. V., Dos Santos, M.T.M., Kouwenhoven, W.M., von Oerthel, L., Lim, J.L., van der Linden, A.J.A., Koerkamp, M.J.A.G., Holstege, F.C.P., Smidt, M.P. (2013). Specification of dopaminergic subsets involves interplay of En1 and Pitx3. Development *140*, 4116–4116.

Wang, L., and Marquardt, T. (2013). What axons tell each other: axon-axon signaling in nerve and circuit assembly. Curr. Opin. Neurobiol. 1–9.

Wang, L., Klein, R., Zheng, B., and Marquardt, T. (2011). Anatomical coupling of sensory and motor nerve trajectory via axon tracking. Neuron *71*, 263–277.

Xiao, T., Staub, W., Robles, E., Gosse, N.J., Cole, G.J., and Baier, H. (2011). Assembly of lamina-specific neuronal connections by slit bound to type IV collagen. Cell *146*, 164–176.

Xu, B., Goldman, J.S., Rymar, V. V, Forget, C., Lo, P.S., Bull, S.J., Vereker, E., Barker, P. A., Trudeau, L.E., Sadikot, a F., et al. (2010). Critical roles for the netrin receptor deleted in colorectal cancer in dopaminergic neuronal precursor migration, axon guidance, and axon arborization. Neuroscience *169*, 932–949.

Yamagata, M., and Sanes, J.R. (2008). Dscam and Sidekick proteins direct lamina-specific synaptic connections in vertebrate retina. Nature *451*, 465–469.

Yamauchi, K., Mizushima, S., Tamada, A., Yamamoto, N., Takashima, S., and Murakami, F. (2009). FGF8 signaling regulates growth of midbrain dopaminergic axons by inducing semaphorin 3F. J. Neurosci. *29*, 4044–4055.

Yaron, A., and Zheng, B. (2007). Navigating their way to the clinic: emerging roles for axon guidance molecules in neurological disorders and injury. Dev. Neurobiol. *67*, 1216–1231.

Yue, Y., Widmer, D. A., Halladay, A. K., Cerretti, D.P., Wagner, G.C., Dreyer, J.L., and Zhou, R. (1999). Specification of distinct dopaminergic neural pathways: roles of the Eph family receptor EphB1 and ligand ephrin-B2. J. Neurosci. *19*, 2090–2101.

'All of us would like realism to be true; we would like to think that science works because it has got a grip on how things really are. But such claims have yet to be made out.'

-Larry Laudan

Chapter 2

Dissection and Culture of Mouse Dopaminergic and Striatal Explants in Three-Dimensional Collagen Matrix Assays

Ewoud R.E. Schmidt, Francesca Morello, and R. Jeroen Pasterkamp

Department of Neuroscience and Pharmacology, Rudolf Magnus Institute for Neuroscience, University Medical Center Utrecht, Universiteitsweg 100, 3584 CG, Utrecht, the Netherlands

Journal of Visualized Experiments, 2012 (61), e3691

Video link: http://www.jove.com/details.php?id=3691

ABSTRACT

Midbrain dopamine (mdDA) neurons project via the medial forebrain bundle towards several areas in the telencephalon, including the striatum[1]. Reciprocally, medium spiny neurons in the striatum that give rise to the striatonigral (direct) pathway innervate the substantia nigra[2]. The development of these axon tracts is dependent upon the combinatorial actions of a plethora of axon growth and guidance cues including molecules that are released by neurites or by (intermediate) target regions[3,4]. These soluble factors can be studied *in vitro* by culturing mdDA and/or striatal explants in a collagen matrix which provides a three-dimensional substrate for the axons mimicking the extracellular environment. In addition, the collagen matrix allows for the formation of relatively stable gradients of proteins released by other explants or cells placed in the vicinity (e.g. see references 5 and 6). Here we describe methods for the purification of rat tail collagen, microdissection of dopaminergic and striatal explants, their culture in collagen gels and subsequent immunohistochemical and quantitative analysis. First, the brains of E14.5 mouse embryos are isolated and dopaminergic and striatal explants are microdissected. These explants are then (co)cultured in collagen gels on coverslips for 48 to 72 hours *in vitro*. Subsequently, axonal projections are visualized using neuronal markers (e.g. tyrosine hydroxylase, DARPP32, or βIII tubulin) and axon growth and attractive or repulsive axon responses are quantified. This neuronal preparation is a useful tool for *in vitro* studies of the cellular and molecular mechanisms of mesostriatal and striatonigral axon growth and guidance during development. Using this assay, it is also possible to assess other (intermediate) targets for dopaminergic and striatal axons or to test specific molecular cues.

PROTOCOL

1. PREPARATION OF RAT TAIL COLLAGEN

1.1) Collect 6-10 adult rat tails (it is possible to store the tails at -20°C until use).

1.2) Soak the tails in 95% ethanol overnight at room temperature (RT).

Dissection of rat tails (in tissue culture hood; keep tools in 70% ethanol when not using them and make sure that all solutions, tools and glassware used throughout this procedure are sterile).

1.3) To collect tendons from the tails, cut off the tip of the tail. Hold large end of the tail with a pair of forceps. Use another pair of forceps to hold, bend and break the tail close to the other forceps. Pull apart and the tendons will be left behind (Fig. 1A,B).

1.4) Collect the tendons in sterile H_2O and after collecting all tendons move them to a new petridish with sterile H_2O.

1.5) Take 2-3 tendons and shred them using 2 pairs of forceps in a new petridish with sterile H_2O. Remove non-tendon tissue such as veins (tendon tissue is shiny and reflective; Fig. 1C). After removal of all non-tendon tissue, each tail yields approximately 100-150 mg of tendons.

1.6) Transfer the tendons to 300 ml of sterile 3% acetic acid and stir slowly overnight at 4°C.

1.7) Add an additional 200 ml of sterile 3% acetic acid and stir slowly overnight at 4°C.

1.8) Centrifuge the acetic acid solution containing the tendons at ~2700x*g* for 120 min at 4°C to pellet non-dissolved tendons and non-tendon tissue.

1.9) During centrifugation prepare dialysis tubing:
- cut pieces of 40 cm
- boil in 500 µM EDTA for 5 min
- cool in sterile H_2O

1.10) Tie a knot at one end of the dialysis tubing and fill the tubing with the supernatant of the centrifuged tendon solution on ice in the tissue culture hood using an automatic pipetter and a 25 ml pipet. Avoid producing bubbles. Knot the other end of the tubing and store tubing on sterile aluminum foil on ice until all pieces of tubing are filled (Fig. 1D).

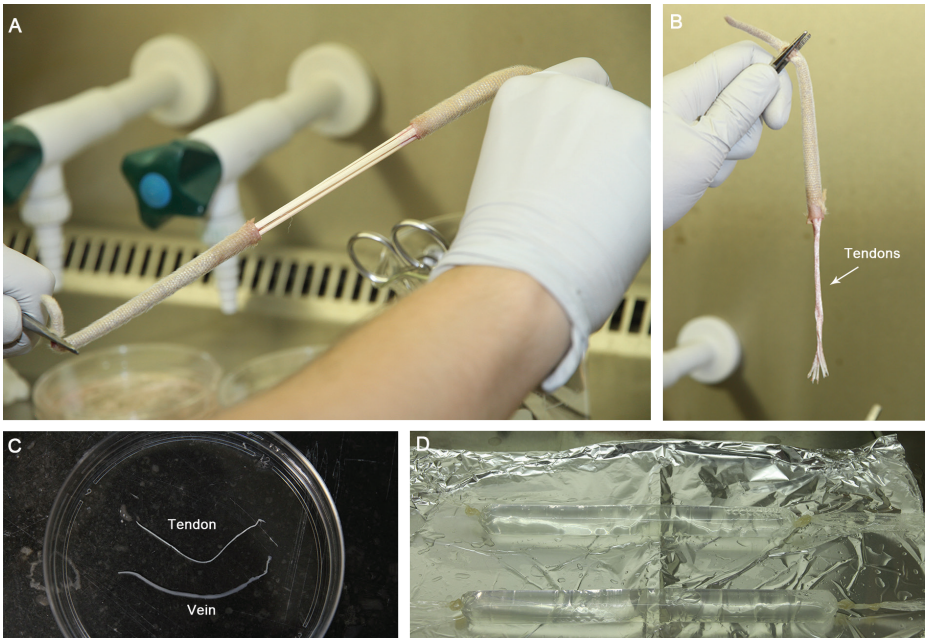

Figure 1. Photos Illustrating the Preparation of Collagen From Rat Tail Tendons.

(**A**) Pulling apart the rat tail exposes the tendons.

(**B**) Tendons are visible as rope-like bundles.

(**C**) The tendons are easy to distinguish from veins by their shiny white appearance.

(**D**) After dissolving the tendons in acetic acid, the solution is transferred to dialysis tubing. To keep the dissolved collagen cold, tubes are placed on sterile aluminum foil on ice.

1.11) Prepare 10 l of sterile 0.1X MEM, pH 4.0, in the tissue culture hood. Add floater to pieces of tubing and add these to the pre-cooled 0.1X MEM solution in a 10 l beaker. Dialyze overnight at 4°C while slowly stirring. This dialysis removes excess acid while keeping the pH low.

1.12) Replace with new pre-cooled 10 l 0.1X MEM and stir overnight at 4°C.

1.13) Repeat the previous step by replacing with new pre-cooled 10 l 0.1X MEM and stir overnight at 4°C.

1.14) Aliquot collagen solution into sterile 50 ml tubes. Store aliquots at 4°C. Keep 6-12 months, only handle the collagen stock in the tissue culture hood.

1.15) It is important to test whether the purified collagen needs to be diluted (in 0.1x MEM) to obtain optimal results in the collagen matrix assay. Therefore, generate a collagen dilution series (undiluted collagen, 1:1, 1:2 and 1:5 diluted) and perform collagen matrix assays as described below to determine the optimal collagen dilution.

2. DISSECTION OF THE DOPAMINERGIC MIDBRAIN[7,8]

2.1) Dissect E14.5 mouse embryos from the uterus of the mother and keep in L15 medium on ice until needed.

All subsequent dissection steps are performed in L15 medium on ice.

2.2) Dissect out the brain.

2.3) Remove the telencephalon by cutting along the medial part of each telencephalic vesicle (use the telencephalic vesicles for striatal explants).

2.4) Remove the meningeal sheath.

2.5) Make a dorsoventral cut just rostral of the mesencephalic flexure.

2.6) Make another dorsoventral cut just caudal of the mesencephalic flexure.

2.7) Make a rostrocaudal cut along the dorsal midline using a microdissection knife to expose the underlying ventral midbrain tissue. Be careful not to hit the ventral midbrain tissue as it contains the dopaminergic neurons (Fig. 2).

2.8) Make two rostrocaudal cuts lateral and parallel to the ventral midline to remove dorsal midbrain tissue.

2.9) Divide the remaining ventral midbrain tissue into explants using a microdissection knife.

2.10) Store the explants in L15 medium containing 5% FBS on ice until use.

3. DISSECTION OF THE STRIATUM

All dissection steps are performed in L15 medium on ice.

3.1) Use telencephalic vesicles dissected during midbrain dissection.

3.2) Remove the thalamus by cutting in between the thalamus and the striatum using forceps.

3.3) Make a mediolateral cut rostral to the striatum to remove rostral structures such as the olfactory bulb. Repeat this step for tissue located caudally to the striatum.

3.4) Position the remaining slice to obtain a coronal view of the striatum (Fig. 2).

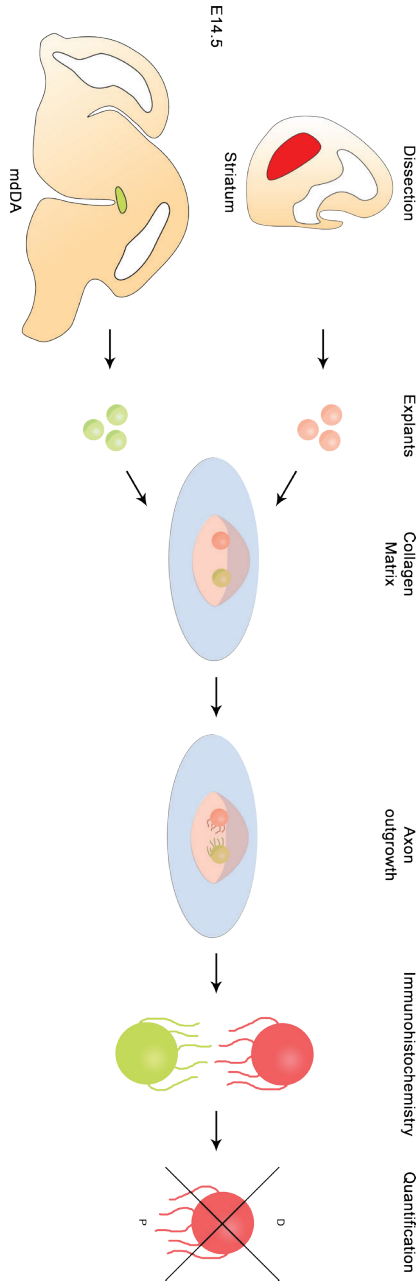

Figure 2. Schematic Indicating the Different Steps of the Procedure.

Appropriate brain regions are dissected and cut to generate explants. A single midbrain and striatal explant are positioned in close proximity in a collagen matrix and left to grow for 48-72 hours at 37°C. Axons are visualized by fluorescence immunohistochemistry and a P/D ratio is calculated to quantify chemotropic responses.

3.5) The striatum can be recognized as a slightly less dense (more transparent) part of tissue. Dissect out the striatum and cut into explants using a microdissection knife. Avoid the slightly darker tissue close to the midline, which contains migrating neurons of the lateral and medial ganglionic eminence.

4. ASSEMBLY COLLAGEN MATRIX ASSAYS

Preparation of the collagen (all steps on ice, use cooled pipet tips).

4.1) Mix 860 µl of diluted collagen with 100 µl of 10x MEM and 40 µl of 1M sodium bicarbonate ($NaHCO_3$) and keep on ice. If at this point the collagen warms up it will solidify.

4.2) Add a drop of 20 µl (approximately 5 mm in diameter) of prepared collagen to a coverslip in a well of a 4-well Nunc dish and let it stand in a CO_2 incubator at 37°C and 5% CO_2 for 30 min (ambient O_2 concentration is sufficient). During this incubation the collagen will gelatinize.

Setup co-culture in collagen gel.

4.3) After the collagen has gelatinized, use a pipet with a 200 µl tip to transfer a dopaminergic or striatal explant to the collagen.

4.4) Move the explants in close proximity to each other using a needle. Keep them apart at a distance of approximately the diameter of one explant (~200-300 µm) (Fig. 2).

4.5) Remove excess medium and add 20 µl of prepared collagen on top of the explants. This will often cause the explants to move around. Reposition the explants using a needle as described in 4.4.

4.6) Let the collagen solidify for 15 min at RT followed by 30 min at 37°C and 5% CO_2.

4.7) After the collagen has set, add 400µl of explant medium and grow for 2-3 days in a CO_2 incubator at 37˚C and 5% CO_2.

5. ANALYSIS BY IMMUNOHISTOCHEMISTRY AND QUANTIFICATION

Immunohistochemistry.

5.1) To fix explants, gently add 400 µl of 8% paraformaldehyde (PFA) in PBS to 400 µl of medium (thereby diluting the PFA to 4%) and let stand for 1 hour at RT.

5.2) Wash 3x 15min in PBS at RT.

5.3) Incubate in blocking buffer (BB; PBS + 1% FBS + 0.1% Triton X-100) for 2 hours.

5.4) Incubate overnight with primary antibody in BB at 4˚C. For dopaminergic axons use anti-tyrosine hydroxylase antibodies (1:1000)[7], for striatal axons anti-Darpp32 antibodies (1:500)[9] and for visualizing all axons anti-βIII tubulin (1:3000)[7].

5.5) Wash 5x 1 hour in PBS at RT.

5.6) Incubate with secondary antibody conjugated to the appropriate fluorophore (1:500) in BB overnight at 4˚C. From this step on minimize exposure of the explants to light (e.g. cover them with aluminum foil).

5.7) Wash overnight in PBS at 4˚C followed by several washes during the next day.

5.8) Mount explants on microscope slides using Prolong Antifade reagent mounting medium. Add a drop of ~10 µl on a glass microscope slide. Take the coverslip and gently place it on the drop of mounting medium with the explant side facing down. Avoid trapping any air under de coverslip by very gently lowering it on the drop of mounting medium.

Quantification by calculating P/D ratio.

5.9) Acquire digital images of the explants using an epifluorescence microscope (Fig. 3).

5.10) Using these images, divide each explant into quadrants to generate a proximal quadrant (i.e. part of the explant closest to the adjacent explant) and a distal quadrant (part of the explant farthest away from the adjacent explant) (Fig. 2, 4).

5.11) Measure the length of 20 longest neurites emerging from the explant both in the proximal and distal quadrants.

5.12) Use the average length of the 20 longest neurites to calculate the P/D ratio for each individual explant. A P/D ratio > 1 indicates axon attraction, while a ratio < 1 indicates axon repulsion.

5.13) In some cases, the dense growth of neurites prevents the assessment of individual neurite length. In these situations, quantification can be performed by measuring the distance between the edge of the explant and the leading front of axon growth in the proximal and distal quadrants.

REPRESENTATIVE IMAGES

After successful culture of dopaminergic and striatal explants a large number of axons are visible using bright field microscopy or as visualized by anti-βIII tubulin immunocytochemistry (not shown). A subset of these axons will be dopaminergic or striatal axons as visualized using immunocytochemistry (Fig. 3). By dividing the explants into quadrants as described and determining P/D ratios, a putative axon attractive or repulsive effect can be quantified (Fig. 3E).

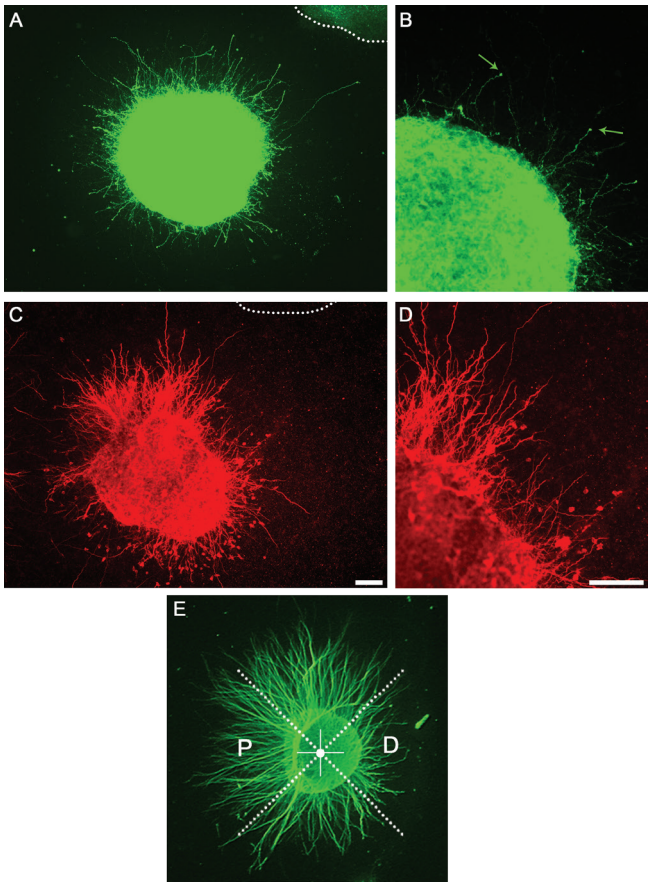

Figure 3. Representative Results Showing Axon Growth in a Collagen Matrix Culture.
(**A-B**) Midbrain explant stained with anti-tyrosine hydroxylase antibody revealing axon outgrowth. Dotted line indicates adjacent explant. (**B**) Magnification of **A** showing individual neurites and growth cones (arrows).
(**C-D**) Striatal explant stained with anti-Darpp32. (**D**) Magnification of **C** showing individual neurites.
(**E**) Example of P/D ratio quantification. Explants are divided into equal quadrants. The proximal quadrant is facing the adjacent explant while the distal quadrant is facing away from it. Scale bars indicate 100 μm.

DISCUSSION

The collagen matrix assay described here has been used and improved by many different labs in the past decades to investigate a variety of axon guidance molecules and neuronal systems (e.g. see references 5-8). These studies have shown that this assay is a powerful tool for studying the effects and regulation of axon guidance molecules secreted by different (intermediate) target tissues.

However, it should be noted that the collagen matrix is a substitute for the extracellular environment (ECM) but clearly lacks many proteins normally present in the ECM. Components of the ECM are known to influence the effects of axon guidance molecules[10]. Nevertheless, the collagen matrix assay is particularly useful for investigating basic molecular mechanisms *in vitro* and in combination with other tissue culture approaches (e.g. organotypic slice cultures[11]) or the analysis of genetically engineered animal models.

Several factors determine the success of the collagen matrix assay. First, the size of the explants is crucial for optimal axon growth. Large dopaminergic and striatal explants often display limited axon growth, while small explants show irregular and fasciculated outgrowth. Furthermore, the distance between the individual explants greatly influences the effect a secreted molecule can exert on adjacent explants. If the explants are too far apart, diffusible molecules will fail to reach the explants. Conversely, when the distance is too small axons may grow into the adjacent explants, making it difficult to qualitatively and quantitatively assess axon growth and guidance. Finally, the quality of the rat tail collagen is important and is directly correlated with the outgrowth of axons and survival of explants.

The assay described here can be modified in different ways to address specific research questions. For instance, addition of function blocking antibodies to the growth medium allows for the functional inhibition of (candidate) molecules. In addition, explants can be combined with cell aggregates secreting specific axon growth and guidance factors. Finally, explants could be obtained from GFP reporter mice in which specific neuronal populations and their axons are labeled. Using this setup, axons can be followed during the course of the collagen matrix assay.

TABLE OF SPECIFIC REAGENTS

Name of the reagent	Company	Catalogue number
Fetal Calf Serum	BioWhittaker	14-801F
Glutamine (200mM)	PAA	M11-004
Hepes	VWR International	441476L
β-Mercaptoethanol	Merck	444203
Minimum Essential Media (MEM)	Gibco	61100-087
Neurobasal	Gibco	21103-049
B27	Gibco	17504-044
Leibovitz's L-15 Medium	Gibco	11415-049
Penicillin-Streptomycin	Gibco	15070-063
Prolong Gold Antifade Reagent	Invitrogen	P36930
Dialysis tubing	Spectrum Labs	132660
Rabbit anti-Tyrosine Hydroxylase	Pel-Freez	P40101-0
Rabbit anti-Darpp32 (H-62)	Santa-Cruz	Sc-11365
Mouse anti-βIII tubulin	Sigma	T8660
Alexa Fluor labeled secondary antibodies	Invitrogen	

ACKNOWLEDGEMENTS

The collagen matrix assay has been developed and improved by the work of many different research groups during the past two to three decades. The approaches described here for dopaminergic and striatal explants greatly benefit from these studies. In addition, the authors would like to thank Asheeta Prasad for her help in setting up striatal explant cultures. Work in the lab was funded by the Human frontier Science Program Organization (Career Development Award), the Netherlands Organization of Health Research and Development (ZonMW-VIDI and ZonMW-TOP), the Europanian Union (mdDA-NeuroDev, FP7/2007-2011, Grant 222999) (to RJP), and the Netherlands Organization for Scientific Research (TopTalent; to ERES).

REFERENCES

1. Van den Heuvel, D.M., Pasterkamp, R.J. Getting connected in the dopamine system. Prog. Neurobiol. 85, 75-93, (2008).

2. Lobo, M.K. Molecular profiling of striatonigral and striatopallidal medium spiny neurons past, present, and future. Int. Rev. Neurobiol. 89, 1-35, (2009).

3. Dickson, B.J. Molecular mechanisms of axon guidance. Science 298, 1959-1964, (2002).

4. Chilton, J.K. Molecules mechanisms of axon guidance. Dev. Biol. 292, 13-24, (2006).

5. Lumsden, A.G., Davies, A.M. Chemotropic effect of specific target epithelium in the developing mammalian nervous system. Nature 323, 538-539, (1986).

6. Tessier-Lavigne, M., Placzek, M., Lumsden, A.G., Dodd, J., Jessel, T.M., Chemotropic guidance of developing axons in the mammalian central nervous system. Nature 336, 775-778, (1988).

7. Kolk, S.M., Gunput, R.A., Tran, T.S., van den Heuvel, D.M., Prasad, A.A., Hellemons, A.J., Adolfs, Y., Ginty, D.D., Kolodkin, A.L., Burbach, J.P., Smidt, M.P., Pasterkamp, R.J. Semaphorin 3F is a bifunctional guidance cue for dopaminergic axons and controls their fasciculation, channeling, rostral growth, and intracortical targeting. J. Neurosci. 29, 12542-12557, (2009).

8. Fenstermaker, A.G., Prasad, A.A., Bechara, A., Adolfs, Y., Tissir, F., Goffinet, A., Zou, Y., Pasterkamp, R.J. Wnt/planar cell polarity signaling controls the anterior-posterior organization of monoaminergic axons in the brainstem. J. Neurosci. 30, 16053-16064, (2010).

9. Arlotta, P., Molyneaux, B.J., Jabaudon, D., Yoshida, Y., Macklis, J.D. Ctip2 controls the differentiation of medium spiny neurons and the establishment of the cellular architecture of the striatum. J. Neurosci. 28, 622-632, (2008)

10. De Wit, J., Toonen, R.F., Verhage, M. Matrix-dependent local retention of secretory vesicle cargo in cortical neurons. J. Neurosci. 29, 23-37, (2009)

11. Gähwiler, B.H., Capogna, M., Debanne, D., McKinney, R.A., Thompson, S.M. Organotypic slice cultures: a technique has come of age. Trends Neurosci. 20, 471-477, (1997)

'Induction is the glory of science and the scandal of philosophy.'

-Charlie Dunbar Broad

Chapter 3

Subdomain-Mediated Axon-Axon Signaling and Chemoattraction Cooperate to Regulate Afferent Innervation of the Lateral Habenula

Ewoud R. E. Schmidt[1], Sara Brignani[1], Youri Adolfs[1], Jeroen Demmers[2], Marina Vidaki[3], Amber-Lee S. Donahoo[4], Linda J. Richards[4], Domna Karagogeos[3], Sharon M. Kolk[1,5], and R. Jeroen Pasterkamp[1]

[1]Department of Translational Neuroscience, Brain Center Rudolf Magnus, University Medical Center Utrecht, Universiteitsweg 100, 3584 CG, Utrecht, the Netherlands
[2]Proteomics Centre and Department of Cell Biology, Erasmus University Medical Centre, Rotterdam 3015 GE, the Netherlands
[3]Department of of Basic Science, Faculty of Medicine, University of Crete and Institute of Molecular Biology and Biotechnology, FoRTH, Heraklion, Greece 71110
[4]The University of Queensland, Queensland Brain Institute and The School of Biomedical Sciences, Brisbane, Queensland, 4067, Australia
[5]Present address: Department of Molecular Animal Physiology, Donders Institute for Brain, Cognitive and Behaviour, Radboud University Nijmegen, Nijmegen, the Netherlands

Under Revision

ABSTRACT

A pervasive feature of neural circuitry is the organization of neuronal projections and synapses into specific brain nuclei or laminae. Lamina-specific connectivity is controlled by selective expression of extracellular guidance and adhesion molecules in the target field. However, how (sub)nucleus-specific connections are established and whether axon-derived cues contribute to subdomain targeting is largely unknown. Here we demonstrate that the lateral subnucleus of the habenula (lHb) determines its own afferent innervation by sending out efferent projections that express the cell adhesion molecule LAMP to reciprocally collect, sort and guide dopaminergic afferents to the lHb – a phenomenon we term subdomain-mediated axon-axon signaling. This process of reciprocal axon-axon interactions cooperates with lHb-specific chemoattraction mediated by Netrin-1, which controls axon target entry, to ensure specific innervation of the lHb. We propose that cooperation between pre-target reciprocal axon-axon signaling and subdomain-restricted instructive cues provides a highly precise and general mechanism to establish subdomain-specific neural circuitry.

INTRODUCTION

The formation of highly specific patterns of synaptic connectivity between afferent axons and their partner neurons is essential for the assembly of functional neural circuits that underlie all behavior. The organization of the nervous system in two main anatomical units, i.e. brain nuclei and laminated structures, facilitates this process by spatially grouping synaptic partners and by enabling subdomain-restricted expression of instructive molecular cues. Despite the important role of these organizing principles, our understanding of the cellular and molecular basis of lamina- or subnucleus-specific circuit development is still limited.

Our current knowledge of subdomain-specific axon targeting mainly derives from work on laminated structures and recent studies have uncovered different molecular strategies that control lamina-specific targeting independent of neural acitvity. This work shows that initially target-derived membrane-associated or secreted guidance cues function to direct axon projections to or exclude them from specific layers. Subsequently, combinatorial expression of cell adhesion molecules facilitates the recognition and stabilization of contacts between matched pre- and postsynaptic neurons (Baier, 2013; Huberman et al., 2010; Robles and Baier, 2012; Sanes and Yamagata, 2009; Williams et al., 2010). Similar to laminated structures, brain nuclei are often subdivided into smaller subdomains comprising small clusters of related neurons (e.g. Aizawa et al., 2012; Molnár et al., 2012). A striking example of a brain nucleus in which subdomain-specific connectivity coordinates complex physiological functions is the habenula. The habenula receives afferent inputs from many forebrain regions, mediates reward related behavior and is linked to psychiatric disease (Li et al., 2011, 2013; Matsumoto and Hikosaka, 2007, 2009). It comprises two main subdomains, the medial habenula (mHb) and lateral habenula (lHb). The mHb primarily projects axons to the interpeduncular nucleus, while the lHb can directly innervate monoaminergic nuclei, including dopaminergic neurons (Bianco and Wilson, 2009; Hikosaka et al., 2008). The lHb is the only subdomain that receives reciprocal dopaminergic innervation (Gruber et al., 2007), which acts as a feedback loop to inhibit lHb activity (Kowski et al., 2009; Shen et al., 2012; Shumake et al., 2010; Stamatakis et al., 2013). However, our understanding of how subdomain-specific innervation patterns in the habenula, as well as in other brain nuclei, are established is rather limited.

During development, axons do not only rely on molecular gradients presented in the surrounding environment for guidance (Pasterkamp and Kolodkin, 2013), but also on signals provided by other axons. Although axon-axon signaling serves critical roles in nervous system wiring, the underlying mechanisms are incompletely understood. Furthermore, our understanding of the function and mechanisms of axon-axon interactions mainly derives from studies on axon types extending alongside as part of the same nerve, or bundle (Grueber and Sagasti, 2010; Imai and Sakano, 2011; Luo and Flanagan, 2007; Tessier-Lavigne and Goodman, 1996; Wang and Marquardt, 2013). In contrast, molecular mechanisms that drive instructive interactions between reciprocally projecting axons, e.g. those between the habenula and dopamine system, and the functional contribution of such interactions to neural circuit assembly remain largely unresolved (Deck et al., 2012). This is surprising as reciprocal connections between brain regions function as important feedback and feedforward loops in many neural circuits.

Here, we show that the habenular nucleus integrates different, previously uncharacterized cellular and molecular mechanisms to control its subdomain-specific innervation by dopaminergic axons. Alhough dopaminergic afferents inhibit the activity and function of the lHb through unique non-canonical signaling pathways (Stamatakis et al., 2013), how these mesohabenular connections are established is unknown. We demonstrate that during development neurons in the lHb send out axon projections that selectively express the neural cell adhesion molecule limbic system-associated membrane protein (LAMP; Pimenta et al., 1995) to reciprocally guide afferent dopaminergic axons from the midbrain specifically to the lHb. These observations unveil a novel role for axon-axon signaling by showing that a specific subdomain sends out molecularly labeled efferent projections in a larger axon bundle to collect, sort and guide its own reciprocal afferent projections in a subdomain-restricted manner. Furthermore, we find that selective innervation of the lHb by dopaminergic afferents not only relies on axon-axon signaling but also requires subdomain-restricted expression of the secreted attractant Netrin-1 (Lai Wing Sun et al., 2011) to mediate the entry of these afferents into the lHb. This function of Netrin-1 in axon target entry is distinct from its previously reported roles in vertebrate neural circuit assembly. Together, our findings identify conceptually novel axonal wiring principles in the developing habenular system that may also apply more generally to other brain nuclei or laminated structures.

RESULTS

The habenula receives complex, subdomain-restricted afferent inputs, including those from dopaminergic neurons in the ventral tegmental area (VTA). However, despite the important physiological role of these dopaminergic afferents (Stamatakis et al., 2013), how dopaminergic innervation of the habenula is established is unknown. To determine how dopaminergic afferents specifically innervate the lHb (Fig. 1A), we first characterized their ontogeny using immunohistochemistry for tyrosine hydroxylase (TH), the rate-limiting enzyme in dopamine synthesis. TH-positive axons started to project towards the habenula around E12.5 and arrived at this structure by E13.5 (Fig. 1B; data not shown). At E16.5, TH-positive axons had entered the lHb, but not the mHb, and two days later, at E18.5, this subdomain-specific innervation was further increased (Fig. 1C, D). Thus, during development dopaminergic axons selectively innervate the lHb without expanding into the mHb.

NETRIN-1 IS A SUBNUCLEUS-SPECIFIC ATTRACTANT FOR DOPAMINERGIC AXONS

How is the selective innervation of the lHb achieved? To address this question, we searched for molecular differences between the mHb and lHb by using laser capture microdissection in combination with mass spectrometry (Fig. 1E). This analysis identified 2880 unique proteins and revealed differential expression of several classes of proteins with established roles in neural circuit development, e.g. axon guidance and cell adhesion molecules (Table S1). Expression of these candidates was either restricted to the mHb, lHb or markedly enriched in one of the two subdomains. Analysis of the expression of several of these candidates, and of their ligands or binding partners, revealed subdomain-specific expression for *Netrin-1* and its receptor *DCC* in the habenula. Netrin-1 is a secreted protein that induces axon repulsion or attraction through specific cell surface receptors, including DCC (Lai Wing Sun et al., 2011). *DCC* strongly labeled the mHb at E16.5, while *Netrin-1* expression was confined to the lHb (Fig. 1F). *DCC* was also expressed in the dopaminergic midbrain with strong expression in the VTA, the origin of the dopaminergic projections that innervate the lHb (Gruber et al., 2007; Phillipson and Griffith, 1980) (Fig. 1G). To confirm that DCC protein is expressed on dopaminergic axons growing towards the lHb, we performed immunohistochemistry for DCC in *Pitx3-GFP* mice, because of an inability to combine DCC and TH antibodies for double immunostaining. In

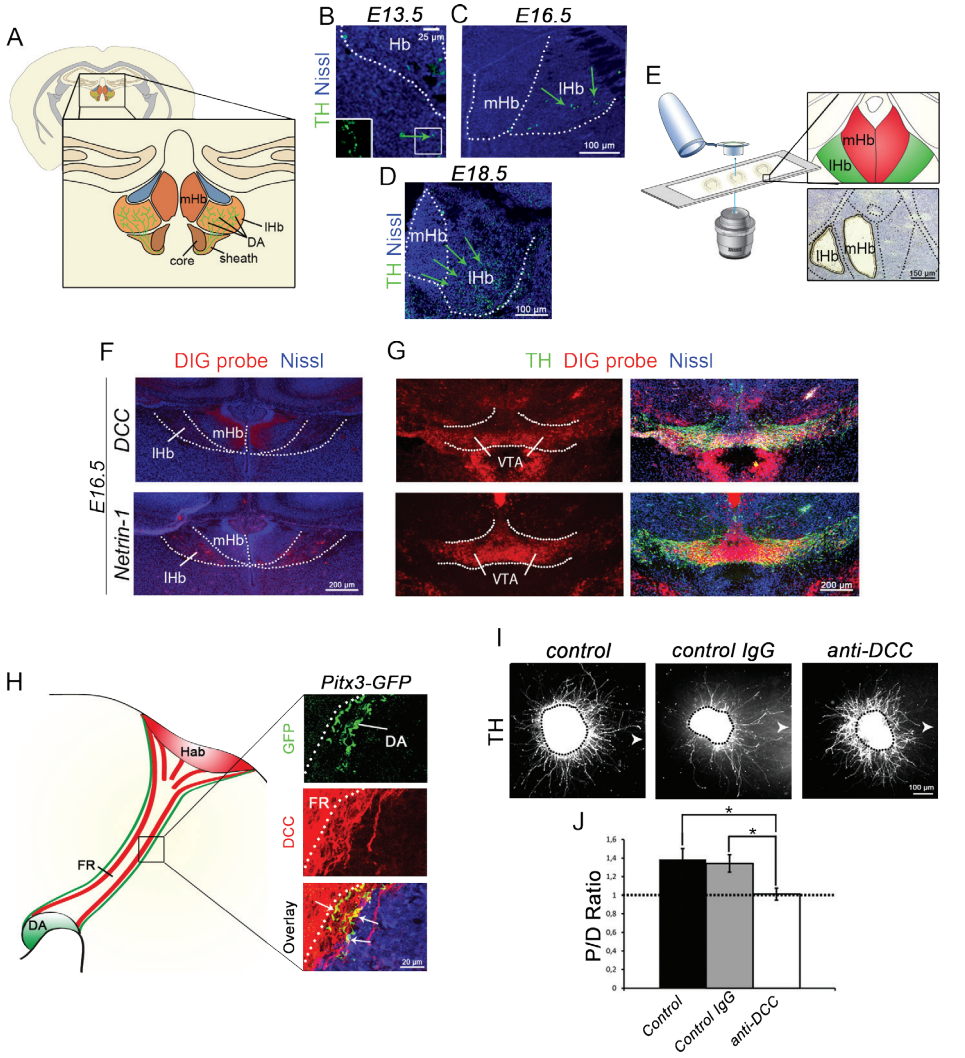

Figure 1. Netrin-1 is a Subnucleus-Specific Attractant for Dopaminergic Axons.

(**A**) Schematic of a coronal section of the mouse brain depicting the medial habenula (mHb), lateral habenula (lHb) and the fasciculus retroflexus (FR). The FR is the major output bundle of the habenula. Dopaminergic (DA) innervation of the habenula is restricted to the lHb.

(**B-D**) Immunohistochemistry for tyrosine hydroxylase (TH) on coronal sections of the embryonic habenula. Green arrows indicate TH-positive axons. Inset in **B** shows a higher magnification of the boxed area in **B**.

(**E**) Laser capture microdissection was performed on the mHb or lHb in E16.5 mouse brain sections.

(**F, G**) *In situ* hybridization for *DCC* and *Netrin-1* in coronal sections of the habenula (**F**) and dopaminergic midbrain (**G**). Immunohistochemistry for TH labels the dopamine system (delineated by dashed line) (**G**). VTA, ventral tegmental area.

(**H**) Schematic of a sagittal section of the mouse brain depicting the habenula, dopaminergic midbrain (DA) and

Pitx3-GFP mice, midbrain dopamine neurons and their axons express GFP (Zhao et al., 2004). At E14.5, GFP-positive axons heading towards the habenula expressed DCC and were surrounded by reciprocally projecting DCC-positive, GFP-negative habenular axons (Fig. 1H).

The expression of DCC on dopaminergic axons and *Netrin-1* in the lHb suggested that this ligand-receptor pair may regulate the dopaminergic innervation of the lHb. To test this model, we first determined whether dopaminergic VTA axons respond to Netrin-1 *in vitro*. VTA explants were combined with transiently transfected 293 cells secreting Netrin-1, or control cells, in a collagen matrix (Schmidt et al., 2012). In line with the reported chemoattractive effect of Netrin-1 in other neural systems, dopaminergic VTA axons were attracted by Netrin-1 (Fig. S1). Next, explant co-culture assays were performed by combining VTA and lHb explants. Axons emanating from VTA explants were attracted towards lHb explants and this effect was blocked by the addition of DCC function blocking antibodies, but not IgG control antibodies (P/D ratio 1.39 ± 0.12 for control (n = 16), 1.34 ± 0.09 for control IgG (n = 12) and 1.01 ± 0.06 for anti-DCC (n = 10); $P < 0.05$; Fig. 1I, J). Together, these data show that Netrin-1 secreted by the lHb acts as an attractant for DCC-expressing dopaminergic axons.

NETRIN-1 CONTROLS DOPAMINERGIC AXON TARGET ENTRY IN THE LHB

To examine whether DCC and Netrin-1 are required *in vivo* for subdomain-specific innervation of the lHb, dopaminergic targeting of the lHb was analyzed in $DCC^{-/-}$ and $Netrin\text{-}1^{-/-}$ mice at E18.5, when dopaminergic fibers occupy most of the lHb (Fig. 1D). Genetic ablation of *DCC* resulted in an almost complete loss of lHb innervation (27.7% ± 4.8% of control, n = 4 for control and $DCC^{-/-}$; $P < 0.001$; Fig. 2A, B) and TH-positive axons were found to accumulate at the ventral border of the lHb in $DCC^{-/-}$ mice instead of entering this structure (Fig. 2A, B, insets). $Netrin\text{-}1^{-/-}$ mice

FR. Immunohistochemistry for DCC and GFP on *Pitx3-GFP* mouse brain sections reveals expression of DCC on GFP-positive dopaminergic axons in the FR (arrows). Dashed line indicates border between core and sheath region.
(**I**) Immunocytochemistry for TH on collagen matrix assays combining E14.5 VTA and lHb explants in the absence of antibody (control) or in the presence of IgG control or anti-DCC function blocking antibodies. Arrowheads indicate position of adjacent lHb explants.
(**J**) Average P/D ratio for control, control IgG and anti-DCC conditions. * P < 0.05. Error bars indicate SEM. See also Figure S1 and Table S1.

displayed similar phenotypes, although some innervation of the lHb was observed, most likely because this mouse mutant is a hypomorph displaying residual Netrin-1 expression (41.3% ± 12.3% of control, n = 3 and n = 4 for control and *Netrin-1*$^{-/-}$, respectively; $P < 0.05$; Fig. 2A, C) (Serafini et al., 1996). To determine whether lack of dopaminergic innervation of the lHb in *DCC*$^{-/-}$ mice is due to removal of DCC from habenular or dopaminergic axons, we next genetically ablated *DCC* in the habenula or in the dopaminergic midbrain. To remove DCC from the habenula, a bacterial artificial chromosome (BAC) mouse was generated expressing Cre recombinase under the control of *Tag-1* promotor sequences. Tag1 is a marker of the habenula and *Tag-1-Cre*:*ROSA26-eYFP* mice revealed robust recombination in the habenula but not in dopaminergic neurons (Fig. 2D). Crossing *Tag1-Cre* mice with *DCC*$^{fl/fl}$ mice (Krimpenfort et al., 2012) resulted in loss of DCC expression in the habenula but did not change the number of dopaminergic axons in the lHb (90.4% ± 9.4% of control, n = 3; n.s.; Fig. 2E, G; not shown). To remove DCC from dopaminergic axons, *DCC* conditional mutants were crossed with *Engrailed*(*En1)-Cre* mice, which drive Cre recombinase expression at early stages of midbrain development but not in the habenula (Kimmel et al., 2000). We tested several other Cre-lines with reported expression in dopaminergic neurons (e.g. *Pitx3-Cre*, *DAT-Cre*), but none of these lines induced recombination at sufficiently early stages of dopaminergic development (not shown). Loss of DCC in midbrain dopamine neurons in *En1-Cre:DCC*$^{fl/fl}$ mice resulted in reduced innervation of the lHb (39.7% ± 9.9% of control, n = 3; $P < 0.05$; Fig. 2F, H). This reduction was somewhat less severe in *En1-Cre:DCC*$^{fl/fl}$

Figure 2. Subdomain-Specific Innervation of the Habenula by Dopaminergic Afferents Requires *In Vivo* DCC/Netrin-1 Signaling.

(**A**) Immunohistochemistry for tyrosine hydroxylase (TH) in coronal sections of the E18.5 habenula of wild-type (WT), *DCC*$^{-/-}$ or *Netrin-1*$^{-/-}$ mice. Insets show a higher magnification of the boxed areas showing the ventral border of the lateral habenula (lHb). Green arrows point to aberrant accumulation of dopaminergic axons.

(**B, C**) Quantification of the dopaminergic innervation of the lHb in *DCC*$^{-/-}$ (**B**) and *Netrin-1*$^{-/-}$ (**C**) mice.

* $P < 0.05$, *** $P < 0.001$. Error bars indicate SEM.

(**D**) Immunohistochemistry for GFP and TH on coronal sections of E18.5 *Tag1-Cre:Rosa26-eYFP* mice showing GFP expression in the habenula and FR, but not in dopamine neurons in the ventral tegmental area (VTA).

(**E, F**) Immunohistochemistry for tyrosine hydroxylase (TH) in coronal sections of E18.5 *Tag1-Cre:DCC*$^{wt/wt}$ and *Tag1-Cre:DCC*$^{fl/fl}$ mice (**E**) or *En1-Cre:DCC*$^{wt/wt}$ and *En1-Cre:DCC*$^{fl/fl}$ mice (**F**). White arrows indicate dopaminergic axons in the lHb. Arrowhead in F indicates accumulation of dopaminergic axons at the ventral border of the lHb

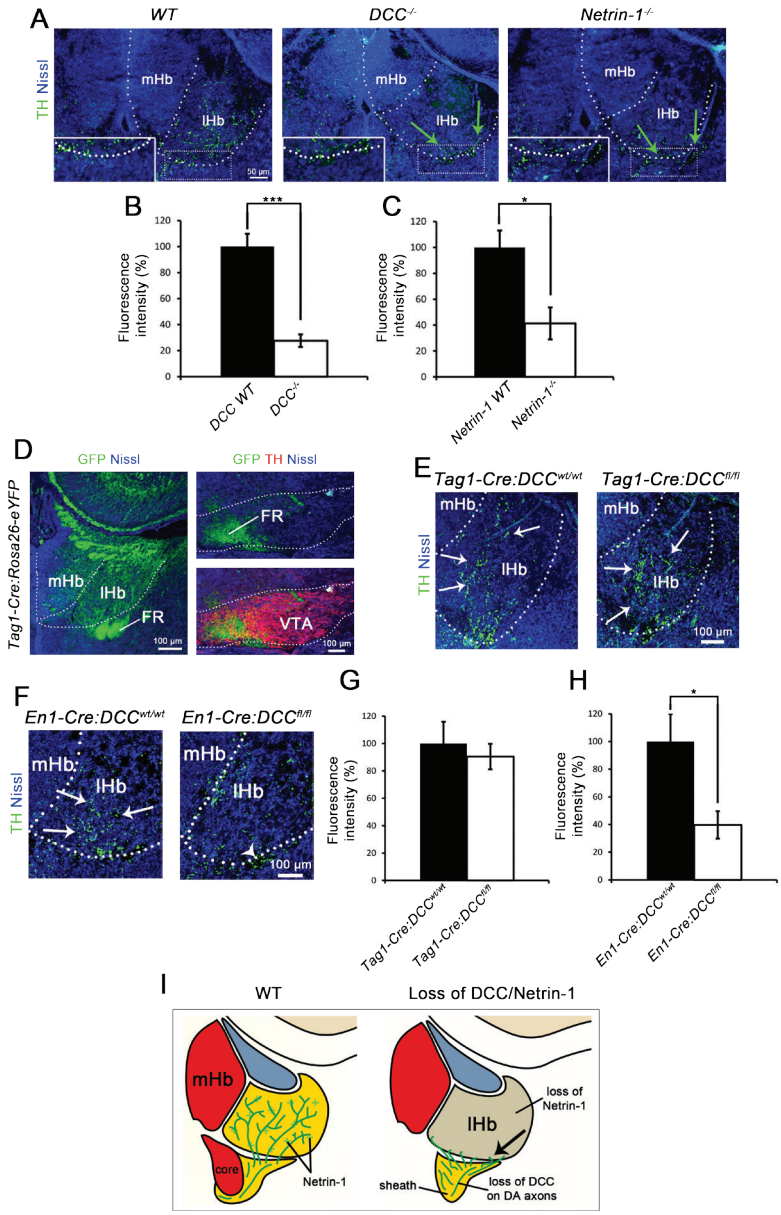

(**G, H**) Quantification of the dopaminergic innervation of the lHb in *Tag1-Cre:DCC* (**G**) and *En1-Cre:DCC* (**H**) conditional knockout mice. Innervation is not affected in *Tag1-Cre:DCC$^{fl/fl}$* mice, but is dramatically reduced in *En1-Cre:DCC$^{fl/fl}$* mice. * $P < 0.05$. Error bars indicate SEM.

(**I**) Schematic representation of the defects in dopaminergic innervation of the lHb observed following loss of DCC or Netrin-1. Dopaminergic axons fail to enter the lHb and accumulate at the ventral border of this subnucleus (arrow). mHb, medial habenula.

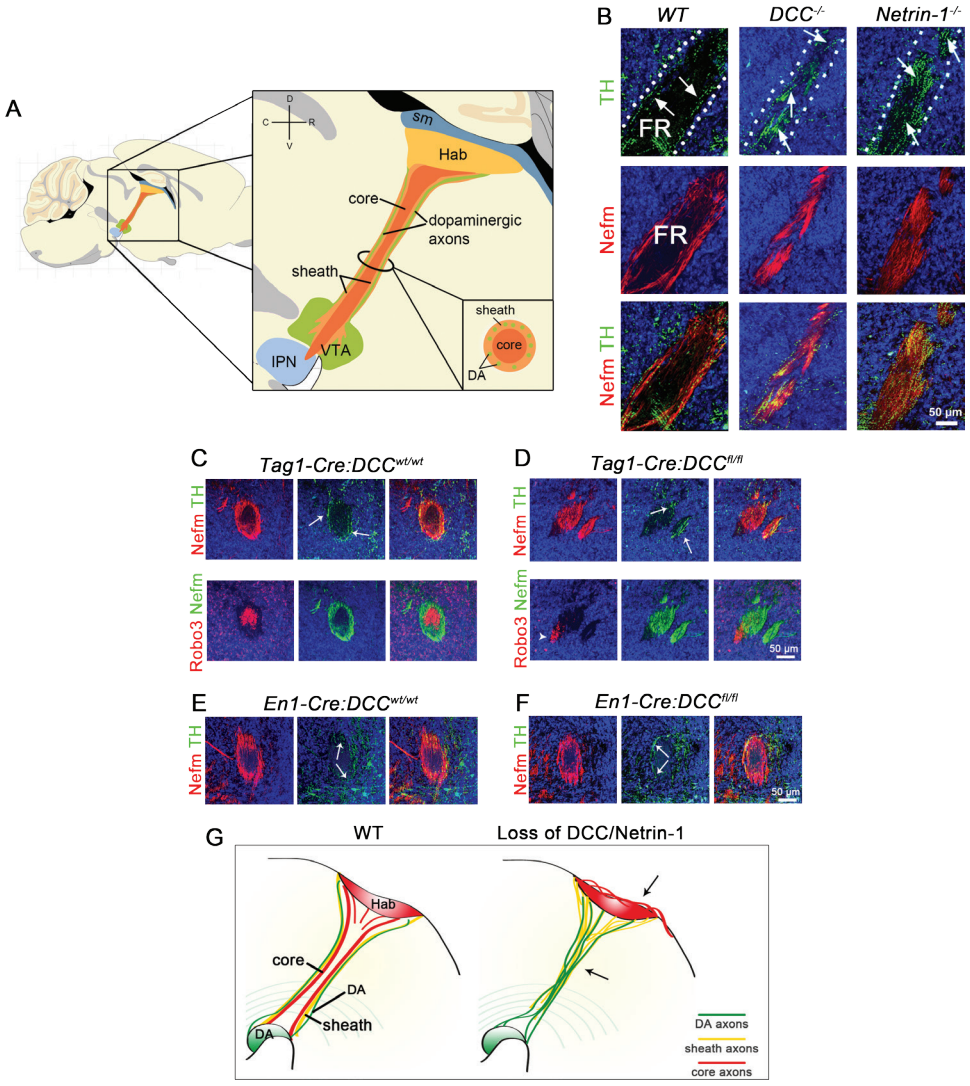

Figure 3. Abnormal Organization of the FR in *DCC* and *Netrin-1* Knockout Mice.

(**A**) Schematic of a sagittal section of the mouse brain showing the segregated organization of habenular (Hab) and dopaminergic axons in the fasciculus retroflexus (FR). Axons from medial habenula (mHb) neurons run in the core of the FR, while lateral habenula (lHb) and dopaminergic (DA) axons are closely associated in the sheath of the FR. IPN, interpeduncular nucleus; sm, stria medullaris; VTA, ventral tegmental area.

(**B**) Double-immunohistochemistry for tyrosine hydroxylase (TH) and neurofilament medium polypeptide (Nefm) on sagittal sections. In E18.5 *DCC* and *Netrin-1* knockout mice, thick bundles of TH-positive axons and Nefm-positive habenular axons intermingle throughout the entire FR (arrows), contrasting their normal lateral distribution in the FR in wild-type (WT, arrows) mice.

(**C, D**) Immunohistochemistry for Robo3, Nefm and TH on coronal sections of the FR of E18.5 *Tag1-Cre:DCC*

mice as compared to *DCC* full knockout mice, presumably because En1 levels vary among dopaminergic neurons (Veenvliet et al., 2013). Nevertheless, the majority of dopaminergic axons accumulated at the border of the lHb in *En1-Cre:DCC$^{fl/fl}$* mice and did not enter the lHb, as we also observed following complete ablation of DCC (Fig. 2A, F). Collectively, these data show that Netrin-1 expressed in the lHb instructs dopaminergic axons expressing DCC to enter the lHb (Fig. 2I).

RECIPROCAL AXON-AXON INTERACTIONS GUIDE DOPAMINERGIC AFFERENTS TO THE LHB

Although dopaminergic axons did reach the lHb in *DCC$^{-/-}$* and *Netrin-1$^{-/-}$* mice, we observed that their organization in the fasciculus retroflexus (FR) was severely disrupted. The FR is the major output bundle of the habenula in which efferent habenular axons are intermingled with specific afferent projections. Habenular efferents display a characteristic segregated distribution in the FR, with axons from the mHb projecting in the core of the bundle and lHb axons forming a sheath around this core (Fig. 3A) (Bianco and Wilson, 2009). To analyze this organization in relation to dopaminergic afferents in *DCC$^{-/-}$* and *Netrin-1$^{-/-}$* mice, we identified and applied new markers for mHb and lHb axons, Robo3 and Neurofilament medium polypeptide (Nefm), respectively (Fig. S2A). In E18.5 wild-type mice, TH-positive axons were restricted to the Nefm-postive sheath region and absent from the Robo3-positive core (Fig. 3A, B; Fig. S2A). In contrast, in *DCC$^{-/-}$* and *Netrin-1$^{-/-}$* mice thick bundles of TH-positive axons traversed the entire width of the FR (Fig. 3B). The mutant FR consisted mainly of Nefm-positive axons, while only few Robo3-positive axons were detected. Instead an aberrant population of Robo3-positive mHb axons was detected at the dorsal roof of the habenula, suggesting that mHb axons redirect dorsally in the absence of Netrin-1–DCC signaling (Fig. S2B). Interestingly, TH-positive axons in the FR in *DCC$^{-/-}$* and *Netrin-1$^{-/-}$* mice were

conditional knockout mice. The organization of the FR is severly disrupted in *Tag1-Cre:DCC$^{fl/fl}$* mice: TH-positive axons intermingle with lHb axons throughout the FR (arrow), while a small number of Robo3-positive mHb axons is situated outside of the sheath (arrowhead).

(**E, F**) Immunohistochemistry for Nefm and TH on coronal sections of the FR of E18.5 *En1-Cre:DCC* conditional knockout mice.

(**G**) Schematic representation of the disrupted organization of the FR following loss of Netrin-1 or DCC. Misrouted core axons are observed at the dorsal roof of the habenula and closely associated lHb and dopaminergic axons occupy the entire FR (arrows). See also Figure S2.

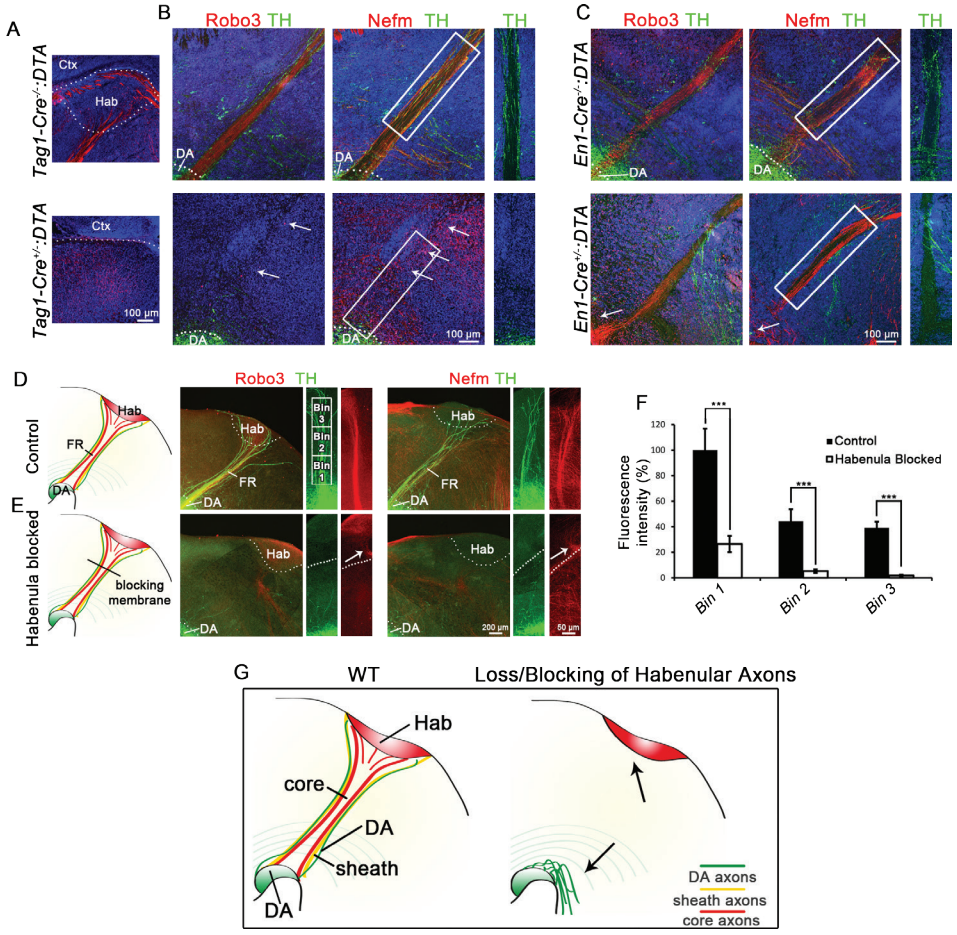

Figure 4. Lateral Habenula Axons Serve as a Scaffold for Dopaminergic Afferents Targeting this Subnucleus.

(**A-C**) Immunohistochemistry for neurofilament medium polypeptide (Nefm), Robo3 and/or tyrosine hydroxylase (TH) on sagittal sections of E18.5 *Tag1-Cre:DTA* and *En1-Cre:DTA* mice. The habenula (Hab, **A**) and the fasciculus retroflexus (FR) are absent in *Tag1-Cre*$^{+/-}$*:DTA* mice (**B**, white arrows) and TH-positive dopaminergic (DA) axons fail to project to the habenula (**B**). In *En1-Cre*$^{+/-}$*:DTA* mice midbrain DA neurons are absent (white arrows), but the FR is intact (**C**). Boxed areas are shown at a higher magnification at the right. Ctx, cortex.

(**D, E**) E12.5 organotypic slices were cultured for 3 days *in vitro* (DIV) and subjected to immunohistochemistry for Robo3, TH and Nefm. Insertion of blocking membranes (dotted lines) redirected habenular axons (white arrows) and prevented growth of DA axons towards the habenula (**E**). Squares in **D** show bins used for quantification shown in **F**.

(**F**) Growth of DA axons was quantified using the bins shown in **D**. All bins were normalized to Bin 1 of the control condition. *** $P < 0.001$. Error bars indicate SEM.

(**G**) Schematic representation of the effect of Hab or FR ablation or the insertion of blocking membranes on dopaminergic axon growth towards the Hab. See also Figure S3 and S4.

restricted to regions occupied by Nefm-positive lHb axons, resembling their close association in the sheath region of wild-type mice. Furthermore, the overall number of TH-positive axons reaching the lHb in mutant mice was comparable to control (not shown). Ablation of DCC in the habenula in *Tag1-Cre:DCC$^{fl/fl}$* mice induced similar phenotypes: intermingling of TH and lHb axons throughout the width of the FR and a dorsal redirection of most Robo3-positive mHb axons (Fig. 3C, D; Fig. S2C). In contrast, loss of DCC in dopaminergic axons in *En1-Cre:DCC$^{fl/fl}$* mice did not affect the organization of the FR (Fig. 3E, F). These results show that Netrin-1 and DCC are required for the guidance of mHb axons to the midbrain and suggest that dopaminergic axons utilize lHb efferents to reach the lHb (Fig. 3G). This latter hypothesis is in line with our observation that during development habenular axons first extend to the ventral midbrain following which dopaminergic axons reciprocally project to the habenula along the developing FR (Fig. S3).

To evaluate a model in which dopaminergic axons use lHb efferents to reach the lHb and to study whether such dependency would be uni- or bidirectional, we performed *in vivo* genetic ablation studies. DTA mice, which conditionally express subunit A of the diphtheria toxin, were crossed with *Tag1-Cre* mice to ablate the habenula. *Tag1-Cre:DTA* embryos displayed a loss of the habenula and the FR, in addition to other Tag1-positive structures outside the midbrain (Fig. 4A). Furthermore, no dopaminergic projections extended to the habenula in *Tag1-Cre:DTA* mice, while other dopaminergic pathways in the brain were intact (Fig. 4B; Fig. S4). Thus, dopaminergic axons require the habenula and/or the FR for guidance towards the lHb. To assess whether, the converse, lHb axons depending on dopaminergic neurons or axons for guidance to the midbrain, is true, the region of the midbrain containing dopaminergic neurons was ablated by crossing *En1-cre* and *DTA* mice. Although *En1-cre:DTA* embryos showed complete loss of midbrain dopaminergic neurons and their axons, the projection and organization of mHb and lHb axons was intact (Fig. 4C).

Together these data unveil a dependency by dopaminergic axons on either long-distance instructive cues from the habenula or short-range cues on lHb axons in the sheath for guidance to the lHb. To discriminate between these two possibilities, we developed an organotypic culture assay that recapitulates the *in vivo* development of the habenular system in order to specifically block axonal growth from the habenula while leaving the habenula itself intact. A blocking membrane was placed at the

ventral border of the habenula in E13.5 mouse brain hemisections following which the hemisections were cultured for three days. The membrane contains pores that allow diffusion of secreted molecules but block the growth of axons (López-Bendito et al., 2006). In cultures without membrane insertion, a clear FR had formed with both mHb and lHb axons extending into the midbrain, as visualized by Robo3 and Nefm immunohistochemistry in combination with TH staining (Fig. 4D). In contrast, insertion of blocking membranes prevented the formation of the FR (Fig. 4E). In addition, the number of dopaminergic axons growing to the habenula was dramatically reduced (Bin 1, 26.4% ± 6.3% of control; Bin 2, 44.4% ± 9.3% for control and 5.3% ± 1.4% for blocked, n = 7 and n = 10 slices for control and blocked; $P < 0.001$; Fig. 4E, F), and no dopaminergic axons were detected directly at the habenula (Bin 3, 39.1% ± 2.8% for control and 1.9% ± 0.4% for blocked; $P < 0.001$; Fig. 4E, F). Thus, our expression, genetic and cell culture data show that dopaminergic axons depend on lHb axons for guidance towards the lHb (Fig. 4G). This suggests that the lHb sends out efferent projections to collect and guide its own afferent projections.

SUBDOMAIN-SPECIFIC AXON GUIDANCE AND CELL ADHESION MOLECULE EXPRESSION IN THE FR

Although our data show that dopaminergic projections rely on lHb axons for guidance towards the habenula, how this interaction is mediated at the molecular level is not known. To identify the underlying molecular mechanism, laser capture microdissection experiments were performed on the embryonic FR in combination with mass spectrometry analysis to identify subdomain-specific proteins in the FR at the time of dopaminergic axon pathfinding (Fig. 5A). Since axon guidance proteins and adhesion molecules are likely candidates for mediating axon-axon interactions, these proteins were selected from the mass spectrometry data and subjected to immunohistochemical analysis (Table S2 and Fig. 5B-D). Immunohistochemistry on transverse sections of the FR showed that these selected proteins can be grouped on basis of their subdomain localization within the FR. Candidates were either localized to the entire FR (Fig. 5B), the core (Fig. 5C) or the sheath domain (Fig. 5D). These results reveal subdomain-specific expression of various axon guidance and cell adhesion molecules in the developing FR, uncovering a molecular code that could underlie various aspects of FR organization, including the segregation of different axonal populations and their guidance towards specific subdomains.

AXON-DERIVED LAMP GUIDES DOPAMINERGIC AXONS TO THE LHB

Two FR proteins identified by mass spectrometry (Table S2) displayed sheath-specific expression; close homologue of L1 (CHL1) and limbic-system associated protein (LAMP) (Fig. 5D). Given their selective expression and reported role in cell adhesion and neurite outgrowth (Hillenbrand et al., 1999; Zhukareva and Levitt, 1995), we next assessed whether CHL1 or LAMP mediated interactions between lHb and dopaminergic axons. CHL1 is a type I transmembrane protein, while LAMP is tethered to the membrane via a glycosylphosphatidylinositol (GPI) anchor. We exploited these differences in membrane presentation by using the enzyme phosphatidylinositol-specific phospholipase C (PI-PLC) in combination with hemisection cultures. PI-PLC will remove GPI-linked proteins, such as LAMP, but leaves transmembrane proteins, such as CHL1, intact (Fig. 6A). Treatment with

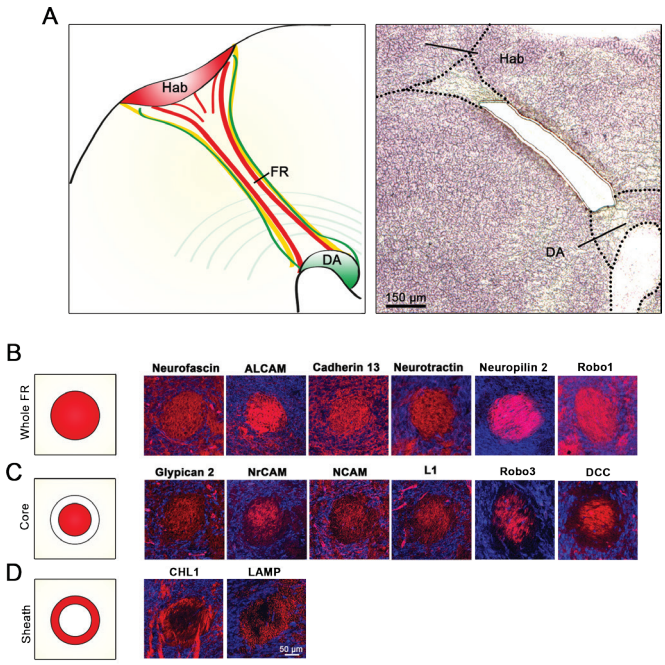

Figure 5. Laser Capture Microdissection of the Fasiculus Retroflexus Reveals Subdomain-Specific Expression of Axon Guidance and Cell Adhesion Molecules.

(**A**) Laser capture microdissection was performed on the fasciculus retroflexus (FR) in E16.5 sagittal mouse brain sections. Hab, habenula; DA, dopamine neuron pool.

(**B-D**) Immunohistochemistry on coronal sections of the FR using antibodies against different axon guidance and cell adhesion molecules. Proteins identified by mass spectrometry on FR samples display three modes of expression: throughout the FR (**B**), restricted to the core region of the FR (**C**), or specific to the sheath (**D**). See also Table S2.

PI-PLC did not affect the initial growth of TH-positive axons towards the habenula, indicating that this enzymatic treatment does not have a deleterious effect on axon growth (Bin 1, 102.9% ± 16.23% of control, n = 11 for both control and PI-PLC; P = 0.896; Fig. 6B, C). Despite this initial growth towards the habenula, dopaminergic axons did not reach this brain region following PI-PLC treatment but, rather, stalled or were redirected rostrally halfway along their normal trajectory (Bin 2, 82.8% ± 12.2% for control and 45% ± 7.8% for PI-PLC; $P < 0.05$; Fig. 6B, C). Most redirected axons eventually joined the medial forebrain bundle and, consequently, the habenula remained largely devoid of dopaminergic innervation (Bin 3, 63.1% ± 7.4% for control and 15% ± 2.3% for PI-PLC; $P < 0.001$; Fig. 6B, C). PI-PLC treatment did not alter the growth of habenular axons in the FR, as visualized by Nefm immunohistochemistry (Fig. 6B).

To confirm that the impaired growth of TH-positive axons towards the habenula following PI-PLC application resulted from the cleavage of LAMP, LAMP function blocking antibodies were applied to the hemisection cultures (Fig. 6D). In line with the effect of PI-PLC treatment (Fig. 6A-C), TH-positive axon growth towards the habenula was reduced, with many axons deviating towards the forebrain in the presence of anti-LAMP antibodies (Bin 1, 70.4% ± 4.3% of control, n = 15 and n = 17 for control and anti-LAMP; $P < 0.001$; Bin 2, 61.9% ± 4.9% for control and 35.1% ± 4.3% for anti-LAMP; $P < 0.001$; Bin 3, 48.3% ± 3.32% for control and 23.3% ± 3% for anti-LAMP; $P < 0.001$; Fig. 6E, F). Application of PI-PLC induced a greater reduction and redirection of TH-positive axons as compared to anti-LAMP antibody application. This could reflect an inability of the antibody to block all LAMP, perhaps due to limited tissue penetration, or a role for additional GPI-linked proteins in the development of dopaminergic projections to the lHb. Anti-LAMP antibody treatment did not alter the growth of habenular axons in the FR (Fig. 6E).

LAMP is a member of the IgLON family, which includes proteins that promote or inhibit cell adhesion and axon growth of specific neuronal populations (Gil et al., 2002; Keller et al., 1989; Zhukareva and Levitt, 1995). Therefore, we hypothesized that LAMP on lHb axons serves as an adhesive and growth promoting substrate for dopaminergic axons. To test this idea, dopaminergic explant cultures were grown on coverslips coated with control or LAMP substrate. In line with the PI-PLC and antibody blocking experiments, TH-positive axon growth was increased on LAMP

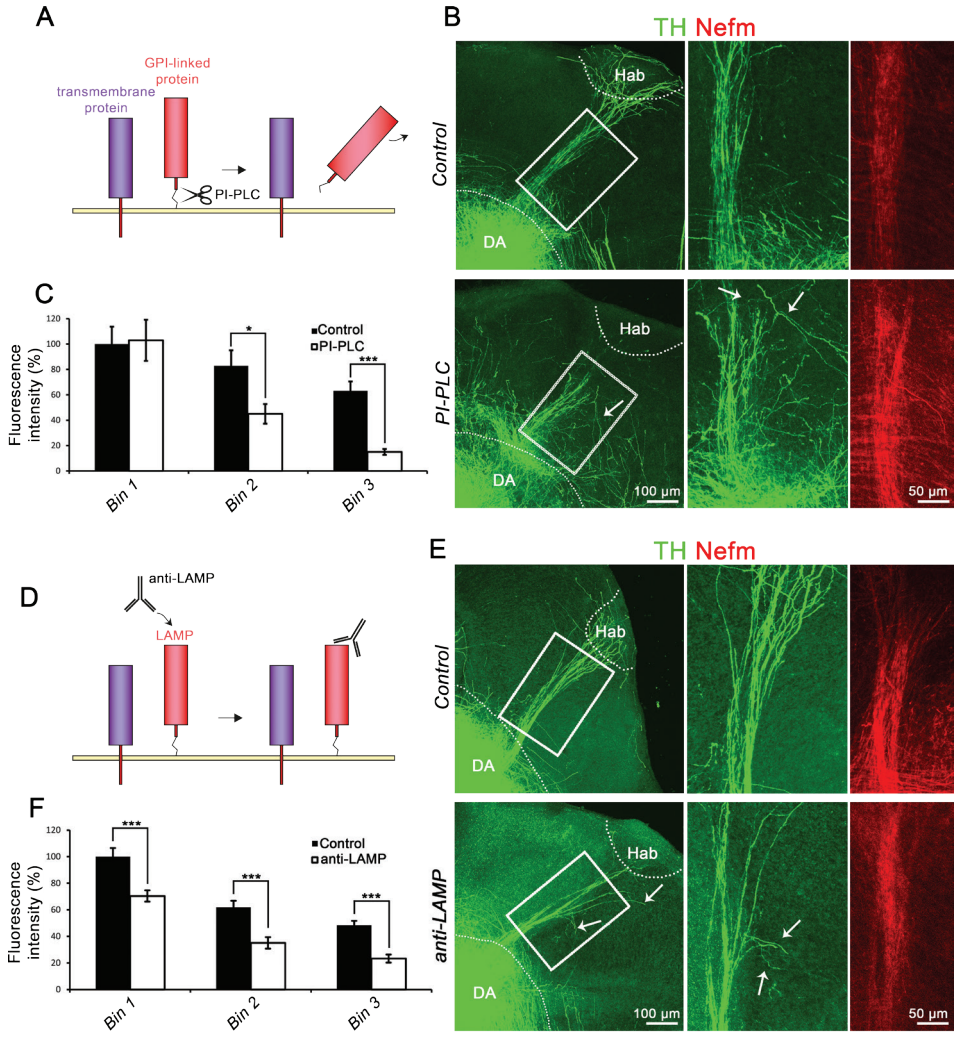

Figure 6. The GPI-linked Cell Adhesion Molecule LAMP Mediates Guidance of Dopaminergic Axons to the Habenula.

(**A, D**) Schematics showing the PI-PLC or function blocking antibody treatments to specifically remove glycophosphatidylinositol (GPI)-anchored molecules (**A**) or block limbic system associated protein (LAMP) (**D**).

(**B, E**) Immunohistochemistry for tyrosine hydroxylase (TH) and neurofilament medium polypeptide (Nefm) on E12.5 organotypic slice cultures treated with PI-PLC or anti-LAMP antibodies and cultured for 3 days *in vitro*. Boxed areas are shown at higher magnification in two right panels. White arrows indicate rostrally redirected axons. DA, dopaminergic; Hab, habenula.

(**C, F**) Quantification of PI-PLC or antibody treated cultures using bins as shown in Fig. 4D. * $P < 0.05$, *** $P < 0.001$. Error bars indicate SEM.

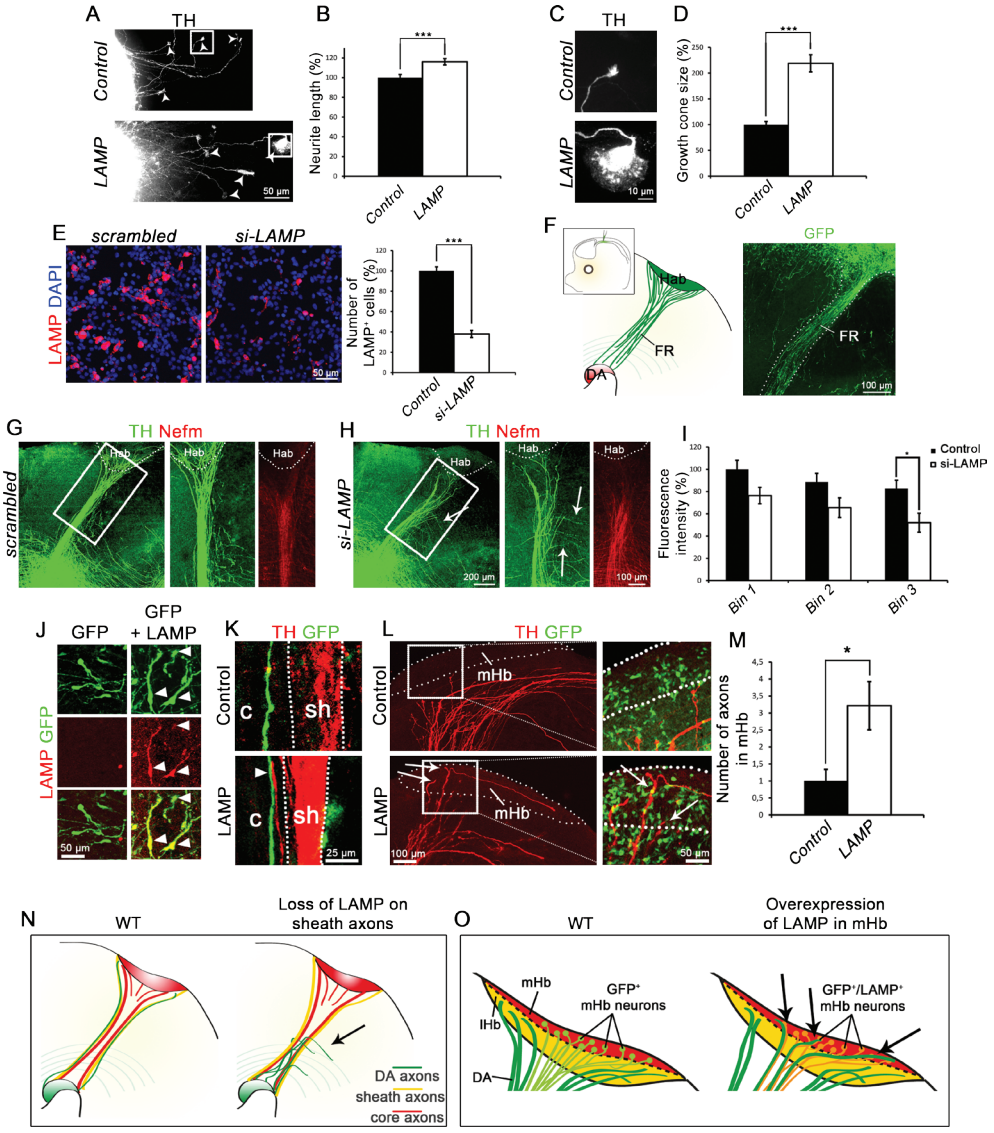

Figure 7. LAMP is Required on lHb Axons to Establish Subdomain-Restricted Innervation of the Habenula by Dopaminergic Afferents.

(**A-D**) Explants of the E14.5 dopamine system were grown on control or limbic system-associated protein (LAMP) substrate and subjected to immunocytochemistry for tyrosine hydroxylase (TH) (**A, C**). The length of TH-positive axons and the size of TH-positive growth cones are increased on LAMP as compared to control substrate. Arrowheads in **A** indicate growth cones. Boxed areas are shown at higher magnification in **C**. *** $P < 0.001$. Error bars denote SEM.

(**E**) HEK293 cells transfected with a LAMP expression vector show robust LAMP expression. Subsequent

as compared to control protein (116.1% ± 3.24% of control, n = 310 and n = 320 for control and LAMP; $P < 0.001$; Fig 7A, B). Furthermore, the size of growth cones at the leading tip of TH-positive axons was strongly increased (218.91% ± 16.72% of control, n = 304 and n = 314 for control and LAMP; $P < 0.001$; Fig. 7C, D). Together, these experiments show that LAMP serves as an adhesive and growth-promoting factor for dopaminergic axons.

To confirm the specificity of the antibody experiments and to establish that LAMP expressed by lHb axons, rather than other structures in the vicinity of the FR, guides dopaminergic axons, we directed siRNAs to the habenula during early stages of dopaminergic pathfinding using *ex vivo* electroporation. Transfection of an ON-TARGETplus pool of siRNAs against LAMP in HEK293 cells exogenously expressing this cell adhesion molecule resulted in effective knockdown of LAMP, as compared to scrambled control siRNAs (38% ± 3.5% of control, n = 12; P < 0.001; Fig. 7E). To confirm our ability to target the habenula by electroporation, a GFP expression vector was electroporated at E12.5. Subsequent analysis of GFP signals revealed strong and specific labeling of habenular neurons and projections in the FR (Fig. 7F). Next, siRNAs were introduced at E12.5 or E13.5 followed by immunohistochemical assessment of the trajectories of habenular and dopaminergic

transfection of siRNAs directed against *LAMP* (*si-LAMP*) but not of scrambled control siRNAs induces efficient knock-down of LAMP. *** $P < 0.001$. Error bars denote SEM.

(**F**) Schematic showing the injection site used for *ex vivo* electroporation of GFP and siRNAs. Electroporation of GFP into the habenula results in expression in both the habenula as well as axons projecting into the fasciculus retroflexus (FR). DA, dopamine neuron pool; Hab, habenula.

(**G, H**) Immunohistochemistry for tyrosine hydroxylase (TH) and neurofilament medium polypeptide (Nefm) following electroporation with scrambled or *LAMP* siRNAs. White arrows indicate rostrally redirected axons.

(**I**) Quantification of fluorescence intensty using bins as shown in Fig. 4D. * $P < 0.05$. Error bars denote SEM.

(**J**) Immunohistochemistry for LAMP and GFP following electroporation with a GFP or a combination of LAMP and GFP expression vectors. Electroporation of the LAMP expression vector induces ectopic expression of LAMP protein. Arrowheads indicate GFP-positive cells expressing ectopic LAMP in the medial habenula (mHb).

(**K, L**) Immunohistochemistry for TH and GFP on slice cultures 3 days after electroporation. Dotted lines in **K** indicate sheath region and arrowhead points to a TH-positive axon crossing over from the sheath region to a GFP/LAMP-positive core axon. Dotted line in **L** indicates mHb as determined by immunohistochemistry for Robo3. Boxed area is shown at higher magnification at the right. Arrow indicates TH-positive axons extending along GFP/LAMP-expressing cell bodies and processes in the mHb. c, core; sh, sheath.

(**M**) Quantification of the number of dopaminergic axons innervating the mHb. * $P < 0.05$. Error bars denote SEM.

(**N, O**) Schematics summarizing the effects of LAMP knockdown and ectopic LAMP expression in the mHb on dopaminergic axon guidance towards the habenula and subdomain targeting in the habenula.

axons three days later. Electroporation with scrambled control siRNAs did not visibly alter the growth or trajectory of habenular or dopaminergic axons. In contrast, LAMP knockdown induced a significant decrease in the outgrowth of TH-positive axons towards the habenula, causing a marked reduction in the dopaminergic innervation of this nucleus (Bin 3, 82.6% ± 7.5% for control (n = 13) and 52% ± 8.5% (n = 8) for si-LAMP; $P < 0.05$; Fig 7G-I). This effect was evident despite our observation that only a subset of habenular neurons is targeted by the *ex vivo* electroporation procedure. Furthermore, similar to our observations following PI-PLC treatment and antibody application, many TH-positive axons redirected rostrally halfway along their trajectory towards the habenula (Fig. 7H). LAMP knockdown did not visibly alter the growth of habenular axons in the FR, as visualized by Nefm immunohistochemistry (Fig. 7G, H).

Finally, to show that LAMP not only guides dopaminergic afferents to the lHb but also has an instructive role in the targeting dopaminergic axons specifcally towards the lHb, we ectopically expressed LAMP in the mHb using *ex vivo* electroporation. Co-electroporation of LAMP and GFP expression vectors confirmed the presence of LAMP protein in electroporated neurons and axons (Fig. 7J). LAMP or control expression vectors were electroporated at E13.5 and dopaminergic innervation of the FR and habenula was assessed three days later using immunohistochemistry. As expected, many GFP-positive neurons were present in the mHb and extended axons into the core of the FR. Interestingly, TH-positive axons from the sheath region often crossed over to nearby GFP/LAMP-positive axons in the core but never to axons expressing GFP only (Fig. 7K). This effect was also reflected at the level of the mHb. Robo3 was used to identify the mHb, which was devoid of dopaminergic axons after electroporation of GFP (Fig. 7L). In contrast, overexpression of GFP and LAMP induced aberrant dopaminergic innervation of the mHb (321,4% ± 70,8% of control, n = 11 for and n = 14 for control and LAMP, respectively; $P < 0.05$; Fig. 7L, M). Although only a small subset of mHb neurons was targeted by the *ex vivo* electroporation procedure, several dopaminergic axons were found to abnormally innervate the mHb along GFP-positive axons and continue along the cell bodies and processes of LAMP-expressing neurons in the mHb (Fig. 7L).

Together these results show that LAMP expressed on lHb axons in the sheath of the FR serves as a molecular scaffold for dopaminergic axons, guiding these axons to a specific subdomain of the habenula, the lHb (Fig. 7N, O). These data show that

pre-target reciprocal axon-axon signaling can contribute to subdomain-specific axon targeting and provide insight into the function of the poorly characterized IgCAM LAMP.

DISCUSSION

Numerous brain nuclei are distinguishable in the vertebrate nervous system and often these structures are further subdivided into smaller subdomains. Although clustering of neurons into (sub)nuclei facilitates the generation of highly specific patterns of synaptic connectivity, how brain nuclei are formed and innervated remains poorly understood. Here we show that reciprocal axon-axon interactions cooperate with subnucleus-restricted chemoattractive mechanisms to coordinate the dopaminergic innervation of the lateral subnucleus of the habenula (lHb). We demonstrate that the lHb determines its own pattern of afferent innervation by sending out LAMP-positive efferent projections that reciprocally guide dopaminergic afferents to the lHb. At the lHb, the secreted attractant Netrin-1 is required for their entry into this subnucleus (Fig. 8). Together, our findings identify pre-target axon-axon signaling as a novel mechanism to wire reciprocally connected brain regions in a subdomain-specific manner and reveal an unexpected role for chemoattraction in subnucleus-restricted axon target entry.

RECIPROCAL AXON-AXON SIGNALING GUIDES DOPAMINERGIC AFFERENTS

Although the guidance and targeting of axons by chemotropic cues in their environment has been well established (Pasterkamp and Kolodkin, 2013), less is known about the role of axon-derived cues. It is clear, however, that axon-axon interactions are used to establish complex neural circuits (Grueber and Sagasti, 2010; Imai and Sakano, 2011; Luo and Flanagan, 2007; Tessier-Lavigne and Goodman, 1996; Wang and Marquardt, 2013). Our knowledge of these interactions mainly derives from studies on afferent axons that extend alongside. For example, Eph/ephrin signaling between sensory and motor axons in the periphery mediates their segregation and guidance, while axon-derived semaphorins and their receptors mediate pre-target sorting of olfactory sensory axons (Gallarda et al., 2008; Imai et al., 2009; Joo et al., 2013; Lattemann et al., 2007; Wang et al., 2011). How interactions between

reciprocally projecting axon types are controlled or contribute to circuit assembly is poorly understood. This is remarkable given the critical role of reciprocal connections as feedback or feedforward loops in many neural circuits.

The habenula is an excellent system for studying axon-axon signaling. Neurons in the lHb and mHb give rise to well-characterized, anatomically segregated efferent projections in a large axon bundle, the FR. In addition, during early development many habenular afferents make a binary choice between the lHb and mHb, providing a sensitive assay for studies on axon target selection and innervation. Finally, the habenular system not only contains axon types that run alongside, but it also harbors reciprocal connections (Fig. 3A) (Bianco and Wilson, 2009). Here, we exploited these characteristics to reveal a requirement for reciprocal axon-axon signaling in the development of subdomain-specific dopaminergic connections. Remarkably, our data show that the lHb determines its own pattern of afferent innervation by sending out molecularly labeled efferents in a larger axon bundle that collect, sort and guide afferents and specifically deliver them in the lHb, a phenomenon we term subdomain-mediated axon-axon signaling (Fig. 8). Multiple lines of evidence support this model. First, expression data localize dopaminergic axons in the FR sheath intermingled with reciprocally projecting lHb axons. Second, dopaminergic axon targeting of the lHb is largely intact in *Tag1-Cre:DCC*$^{fl/fl}$ mice in which the FR is almost exclusively composed of lHb axons. Third, blockage of habenular axon growth *in vitro* and genetic ablation of the habenula and the FR *in vivo* precludes dopaminergic innervation of the lHb. Fourth, neutralization or knockdown of the lHb-specific cue LAMP prevents dopaminergic innervation of the lHb. Finally, ectopic LAMP expression in mHb neurons and their axons erroneously redirects dopaminergic afferents to the mHb.

One of the best-studied examples of reciprocal axon-axon interactions is the interdependency of thalamocortical and corticothalamic axons (Molnár et al., 2012). During development, thalamocortical axons traverse the subpallium to reach the cortex and are then used by corticothalamic afferents for reciprocal guidance through the subpallium (Deck et al., 2013). We observe a similar temporal sequence of axon progression: lHb efferents reach the midbrain following which dopaminergic afferents use these efferents to navigate towards the habenula. Our data do, however, not only confirm previous findings in another system but also uncover novel roles for reciprocal axon-axon signaling in axon sorting and targeting. Further, our study provides an

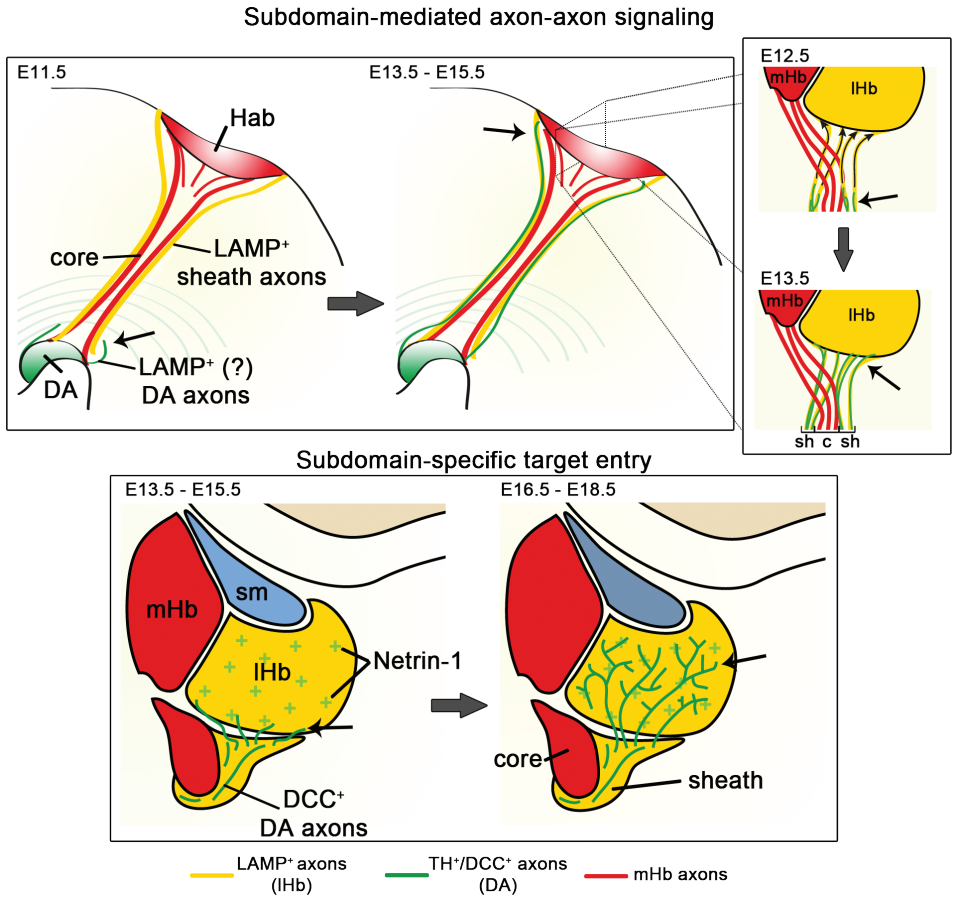

Figure 8. Subdomain-Specific Innervation of the Habenula Requires Cooperation Between Reciprocal Axon-Axon Signaling and Subnucleus-Restricted Chemoattraction.

In our model, the lateral subnucleus of the habenula (lHb) sends out efferent projections that selectively express the cell adhesion molecule limbic system-associated membrane protein (LAMP) to reciprocally guide afferent dopaminergic (DA) axons over a long distance and deliver these axons specifically at the border of the lHb, a process we refer to as subdomain-mediated axon-axon signaling. Upon arrival at the lHb, subdomain-restricted expression of the secreted attractant Netrin-1 is required for the entry of DCC-expressing dopaminergic afferents into this subnucleus. These findings reveal the first subnucleus-specific axonal targeting mechanisms and highlight novel axonal wiring principles that are likely to also apply to subdomain-specific wiring events in other reciprocally connected neural systems. See text for more details. c, core; Hab, habenula; mHb, medial habenula; lHb, lateral habenula; sh, sheath; sm, stria medullaris.

example of a protein that can mediate such reciprocal axon-axon interactions, LAMP. LAMP promotes dopaminergic axon extension and is expressed in dopaminergic neurons that project afferents to the habenula (Gruber et al., 2007) (Fig. 7, S5). This, together with the fact that the adhesive effects of LAMP are attributed to homophilic interactions (Zhukareva and Levitt, 1995) supports a model in which homophilic LAMP interactions guide dopaminergic axons (Fig. 8). Notably, LAMP is also expressed in reciprocally connected parts of the thalamus and cortex and *in vitro* it regulates the growth and guidance of the axonal projections connecting these structures (Mann et al., 1998). Further studies are needed to determine whether LAMP mediates interactions between thalamocortical and corticothalamic axons, or other reciprocal connections in the brain, analogous to its role in the habenular system.

AXON-AXON SIGNALING REGULATES SUBDOMAIN-SPECIFIC AXON TARGETING

The ordered distribution of different axon types in large axon tracts is a pervasive anatomical feature of neural circuits and underlies the generation of precise synaptic connections (Wang and Marquardt, 2013). Efferent projections from the mHb and lHb are segregated in the core and sheath regions of the FR, respectively. Although the molecular basis of this segregation is unknown, our findings show that lHb axon-derived LAMP localizes dopaminergic afferents to the FR sheath. In addition, misexpression of LAMP in the mHb and core axons aberrantly redirects dopaminergic afferents to the mHb revealing that LAMP-positive lHb axons not only guide dopaminergic afferents but also dictate their subdomain targeting. Our current understanding of the molecular basis of subdomain-specific axon targeting mainly derives from studies on laminar structures such as the hippocampus and the visual system. This work shows that target-derived guidance cues first direct axons to or away from specific laminae following which combinatorial expression of cell adhesion molecules facilitates the formation of (sub)lamina-specific synaptic contacts (Baier, 2013; Huberman et al., 2010; Robles and Baier, 2012; Sanes and Yamagata, 2009; Williams et al., 2010). Our data show that subdomain-mediated axon-axon signaling provides an additional strategy to regulate subdomain-specific circuit assembly that relies on axon-axon interactions rather than target restricted cues. Previous studies have implicated axon-axon signaling in different aspects of

target selection, innervation and mapping (Imai et al., 2009; Lattemann et al., 2007; Mizumoto and Shen, 2013; Schwabe et al., 2013; Sweeney et al., 2007; Takeuchi et al., 2010). However, our findings are conceptually distinct from these previous reports: we find that molecular interactions between reciprocal efferent and afferent axons target dopaminergic afferents to the lHb, rather than signaling between afferent projections heading for the same target. Further, they reveal one of the first subnucleus-specific targeting mechanisms and it will be interesting to determine whether similar mechanisms operate in other nuclei or even in laminated structures.

NETRIN-1 IS A SUBDOMAIN-SPECIFIC CUE REGULATING SUBNUCLEAR AXON TARGET ENTRY

Although one might predict that dopaminergic axons would simply follow LAMP-positive axons into the lHb to meet their synaptic targets, our data identify a requirement for Netrin-1 in the entry of dopaminergic afferents into this subnucleus (Fig. 8). In the absence of Netrin-1, or its receptor DCC, dopaminergic axons accumulate at their normal entry site at the lHb. Our data show that Netrin-1 secreted by the lHb serves as an attractant for dopaminergic axons expressing DCC. This is supported by the analysis of conditional and full *DCC* and *Netrin-1* knockout mice suggesting that *in vivo* Netrin-1 most likely functions as a short-range attractant, as axons arrive at the lHb in the absence of Netrin-1-DCC signaling but accumulate at its ventral border. This idea is in line with recent work on short-range attractive effects of Netrin-B during the lamina-specific targeting of R8 retinal axons in the medulla of the *Drosophila* optic lobe. Here, Netrin-B is released in the R8 axon-recipient layer M3 of the retina by afferent axonal projections and subsequently captured by neuron-associated Frazzled, the fly homologue of DCC. This results in a short-range Netrin-B signal that attracts ingrowing R8 axons into layer M3 (Timofeev et al., 2012). Our data extend these findings by showing that Netrin-1 mediates the entry of dopaminergic afferents into a specific subnucleus in vertebrate species. This indicates that Netrins play conserved roles in the subdomain-specific innervation of both laminated structures and brain nuclei and identifies a novel role for these cues distinct from previously reported functions in for example axon guidance, topographic sorting and synaptogenesis ((Bielle et al., 2011; Goldman et al., 2013; Lai Wing Sun et al., 2011; Manitt et al., 2011; Poon et al., 2008; Powell et al., 2008) and references therein).

Our work further shows that at least two distinct mechanisms are needed to control the dopaminergic innervaton of the lHb. A possible explanation for this cooperation between axon-axon signaling and chemoattraction is that lHb axons act to deliver dopaminergic axons specifically at the lHb following which Netrin-1 uncouples these axons. This would allow other (non-)axonal molecular signals within the lHb to guide dopaminergic axons to their partner neurons. Furthermore, Netrin-1 may not only facilitate axon entry but could subsequently confine these axons to the lHb. Netrin-B serves an analogous role in the *Drosophila* visual system, where it not only attracts but also confines R8 axonal afferents to layer M3, preventing their progression into deeper layers (Timofeev et al., 2012). It is possible that Netrin-1 cooperates with repulsive signals in the mHb to safeguard subdomain-specificity. Interesting candidates would be Slits, which have recently been implicated in the layer-specific organization of the zebrafish tectum (Xiao et al., 2011) and display habenular subnucleus-specific expression, e.g. the repulsive cue *Slit2* is specifically expressed in the mHb (E.R.E.S. and R.J.P., unpublished observations). Further studies will be needed to dissect the mechanistic details of Netrin-1-mediated axon target entry and to test whether Netrin-1 is required for confining dopaminergic afferents to the lHb.

Despite its important physiological functions and its implication in disorders such as major depressive disorder (MDD) (Hikosaka, 2010), the mechanisms underlying habenular circuit development in mammals remain largely unknown (Chen et al., 2000; Funato et al., 2000; Giger et al., 2000; Kantor et al., 2004). Our study reveals mechanisms that enable the generation of highly specific patterns of afferent innervation in the habenula. These principles may not only apply to dopaminergic axons but also to the many other afferent projections targeting the habenula (Bianco and Wilson, 2009). Together, our work provides tools and a conceptual framework for the further dissection of habenular circuit assembly. More generally, our findings unveil an unexpected cooperation between subdomain-mediated axon-axon signaling and subnucleus-restricted chemoattraction in subdomain-specific axon targeting. Analogous combinatorial targeting strategies could be widely used because many brain nuclei and layered structures in the nervous system display subdomain-specific patterns of guidance cue expression and are interconnected with their afferent target regions though reciprocal axon projections.

MATERIALS AND METHODS

MOUSE LINES

Animal use and care was in accordance with local institutional guidelines. Generation of transgenic mice and all other mouse lines used in this study are described in the Supplemental Experimental Procedures.

IMMUNOHISTOCHEMISTRY AND *IN SITU* HYBRIDIZATION

Nonradioactive *in situ* hybridization and immunohistochemistry were performed as described previously (Kolk et al., 2009; Pasterkamp et al., 2007). Average fluorescence intensity was measured using the histogram function in Adobe Photoshop. Background was determined in areas without staining and subtracted from images after which mean signal intensity was determined. See Supplemental Experimental Methods for more details on reagents and protocols.

LASER CAPTURE MICRODISSECTION

Laser capture microdissection was performed using a PALM laser microscope system (Zeiss). Samples were subjected to SDS-PAGE and were sent for mass spectrometry analysis. See Supplemental Experimental Methods for a detailed description of the laser capture microdissection procedure.

EXPLANT AND ORGANOTYPC SLICE CULTURES

Three dimensional collagen matrix assays were performed as described previously (Kolk et al., 2009; Schmidt et al., 2012). See Supplemental Experimental Procedures for a detailed description of the antibody prepration, coating and quantification. For organotypic slice cultures, E12.5 mouse brains were dissected to produce two sagittal hemisections. Following three days in culture, hemisections were fixed in 4% PFA and stained using appropriate antibodies. See Supplemental Experimental Procedures for more detailed description of the culture conditions, immunohistochemistry and quantification.

EX VIVO ELECTROPORATION

To test siRNA knockdown efficiency, HEK 293 human embryonic kidney cells were plated onto poly-D-lysine coated coverslips. siRNAs (ON-TARGET plus SMARTpool; Dharmacon) were transfected using Lipofectamine 2000 (Invitrogen)

according to manufacturer's protocol. For electroporation, mouse embryos were collected at E13.5 and the third ventricle was injected with siRNA (25 μM) and DNA (1 μg/μl). After electroporation hemisections were cultured as described above for the organotypic slice cultures. See Supplemental Experimental Procedures for more details.

QUANTIFICATION AND STATISTICS METHODS

Statistical analyses were performed using IBM SPSS Statistics by Student's *t*-test. All data were expressed as means ± SEM and significance was defined as $P < 0.05$.

ACKNOWLEDGEMENTS

We thank members of the Pasterkamp laboratory for assistance and discussions and Alex Kolodkin and Gulermina Lopez-Bendito for reading the manuscript. We thank Marc Tessier-Lavigne, Anton Berns, Cecilia Flores, Wolfgang Wurst, Alain Chedotal, Meng Li and Marten Smidt for providing us with mouse lines. We would like to thank Nicoletta Kessaris for help and advice on BAC technology, cloning and reagents. We are grateful to Seiji Miyata and Helen Cooper for sharing reagents. We thank Jerre van Veluw for technical assistance on the laser capture microdissection. Anti-Tag1 and anti-LAMP anitbodies were obtained from the Developmental Studies Hybridoma Bank. This study is supported by grants from the Netherlands Organization for Scientific Research (TopTalent; to E.R.E.S.), Stichting Parkinson Fonds, the Netherlands Organization for Health Research and Development (VIDI, ZonMW-TOP), the European Union (mdDANeurodev, FP7/2007-2011, Grant 222999), and the People Programme (Marie Curie Actions) of the European Union's Seventh Framework Programme FP7/2007-2013/ under REA grant agreement n° [289581] (NPlast) (to R.J.P.). This study was partly performed within the framework of Dutch Top Institute Pharma Project T5-207 (to R.J.P.). This work was partly supported by project grants (631466 and1043045) from the National Health and Medical Research Council, Australia (NHMRC). LJR was supported by an NHMRC Principal Research fellowship and A-L S.D was supported by an Australian Post-graduate Award scholarship and a top-up scholarship from the Queensland Brain Institute.

REFERENCES

Aizawa, H., Kobayashi, M., Tanaka, S., Fukai, T., and Okamoto, H. (2012). Molecular characterization of the subnuclei in rat habenula. J. Comp. Neurol. *520,* 4051-4066.

Baier, H. (2013). Synaptic laminae in the visual system: molecular mechanisms forming layers of perception. Annu. Rev. Cell Dev. Biol. *29*, 385–416.

Bianco, I.H., and Wilson, S.W. (2009). The habenular nuclei: a conserved asymmetric relay station in the vertebrate brain. Philos. Trans. R. Soc. Lond. B. Biol. Sci. *364*, 1005–1020.

Bielle, F., Marcos-Mondéjar, P., Leyva-Díaz, E., Lokmane, L., Mire, E., Mailhes, C., Keita, M., García, N., Tessier-Lavigne, M., Garel, S., et al. (2011). Emergent growth cone responses to combinations of Slit1 and Netrin 1 in thalamocortical axon topography. Curr. Biol. *21*, 1748–1755.

Chen, H., Bagri, A., Zupicich, J.A., Zou, Y., Stoeckli, E., Pleasure, S.J., Lowenstein, D.H., Skarnes, W.C., Chédotal, A., and Tessier-Lavigne, M. (2000). Neuropilin-2 Regulates the Development of Select Cranial and Sensory Nerves and Hippocampal Mossy Fiber Projections. Neuron *25*, 43–56.

Deck, M., Lokmane, L., Chauvet, S., Mailhes, C., Keita, M., Niquille, M., Yoshida, M., Yoshida, Y., Lebrand, C., Mann, F., et al. (2013). Pathfinding of Corticothalamic Axons Relies on a Rendezvous with Thalamic Projections. Neuron *77*, 472–484.

Funato, H., Saito-Nakazato, Y., and Takahashi, H. (2000). Axonal growth from the habenular nucleus along the neuromere boundary region of the diencephalon is regulated by semaphorin 3F and netrin-1. Mol. Cell. Neurosci. *16*, 206–220.

Gallarda, B.W., Bonanomi, D., Müller, D., Brown, A., Alaynick, W. A. Andrews, S.E., Lemke, G., Pfaff, S.L., and Marquardt, T. (2008). Segregation of Axial Motor and Sensory Pathways via Heterotypic Trans-Axonal Signaling. Science *320*, 233–236.

Giger, R.J., Cloutier, J.F., Sahay, A., Prinjha, R.K., Levengood, D. V, Moore, S.E., Pickering, S., Simmons, D., Rastan, S., Walsh, F.S., et al. (2000). Neuropilin-2 is required in vivo for selective axon guidance responses to secreted semaphorins. Neuron *25*, 29–41.

Gil, O.D., Zhang, L., Chen, S., Ren, Y.Q., Pimenta, A., Zanazzi, G., Hillman, D., Levitt, P., and Salzer, J.L. (2002). Complementary expression and heterophilic interactions between IgLON family members neurotrimin and LAMP. J. Neurobiol. *51*, 190–204.

Goldman, J.S., Ashour, M. A., Magdesian, M.H., Tritsch, N.X., Harris, S.N., Christofi, N., Chemali, R., Stern, Y.E., Thompson-Steckel, G., Gris, P., et al. (2013). Netrin-1 Promotes Excitatory Synaptogenesis between Cortical Neurons by Initiating Synapse Assembly. J. Neurosci. *33*, 17278–17289.

Gruber, C., Kahl, A., Lebenheim, L., Kowski, A., Dittgen, A., and Veh, R.W. (2007). Dopaminergic projections from the VTA substantially contribute to the mesohabenular pathway in the rat. Neurosci. Lett. *427*, 165–170.

Grueber, W., and Sagasti, A. (2010). Self-avoidance and tiling: mechanisms of dendrite and axon spacing. Cold Spring Harb. Perspect. Biol. *2*, a001750.

Hikosaka, O. (2010). The habenula: from stress evasion to value-based decision-making. Nat. Rev. Neurosci. *11*, 503–513.

Hikosaka, O., Sesack, S.R., Lecourtier, L., and Shepard, P.D. (2008). Habenula: crossroad between the basal ganglia and the limbic system. J. Neurosci. *28*, 11825–11829.

Hillenbrand, R., Molthagen, M., Montag, D., and Schachner, M. (1999). The close homologue of the neural adhesion molecule L1 (CHL1): patterns of expression and promotion of neurite outgrowth by heterophilic interactions. Eur. J. Neurosci. *11*, 813–826.

Huberman, A.D., Clandinin, T.R., and Baier, H. (2010). Molecular and cellular mechanisms of lamina-specific axon targeting. Cold Spring Harb. Perspect. Biol. *2*, a001743.

Imai, T., and Sakano, H. (2011). Axon-axon interactions in neuronal circuit assembly: lessons from olfactory map formation. Eur. J. Neurosci. *34*, 1647–1654.

Imai, T., Yamazaki, T., Kobayakawa, R., Kobayakawa, K., Abe, T., Suzuki, M., and Sakano, H. (2009). Pre-target axon sorting establishes the neural map topography. Science *325*, 585–590.

Joo, W.J., Sweeney, L.B., Liang, L., and Luo, L. (2013). Linking cell fate, trajectory choice, and target selection: genetic analysis of Sema-2b in olfactory axon targeting. Neuron *78*, 673–686.

Kantor, D.B., Chivatakarn, O., Peer, K.L., Oster, S.F., Inatani, M., Hansen, M.J., Flanagan, J.G., Yamaguchi, Y., Sretavan, D.W., Giger, R.J., et al. (2004). Semaphorin 5A is a bifunctional axon guidance cue regulated by heparan and chondroitin sulfate proteoglycans. Neuron *44*, 961–975.

Keller, F., Rimvall, K., Barbe, M.F., and Levitt, P. (1989). A membrane glycoprotein associated with the limbic system mediates the formation of the septo-hippocampal pathway in vitro. Neuron *3*, 551–561.

Kimmel, R.A., Turnbull, D.H., Blanquet, V., Wurst, W., Loomis, C.A., and Joyner, A.L. (2000). Two lineage boundaries coordinate vertebrate apical ectodermal ridge formation. Genes Dev. 1377–1389.

Kolk, S.M., Gunput, R.-A.F., Tran, T.S., van den Heuvel, D.M.A., Prasad, A.A., Hellemons, A.J.C.G.M., Adolfs, Y., Ginty, D.D., Kolodkin, A.L., Burbach, J.P.H., et al. (2009). Semaphorin 3F is a bifunctional guidance cue for dopaminergic axons and controls their fasciculation, channeling, rostral growth, and intracortical targeting. J. Neurosci. *29*, 12542–12557.

Kowski, a B., Veh, R.W., and Weiss, T. (2009). Dopaminergic activation excites rat lateral habenular neurons in vivo. Neuroscience *161*, 1154–1165.

Krimpenfort, P., Song, J.-Y., Proost, N., Zevenhoven, J., Jonkers, J., and Berns, A. (2012). Deleted in colorectal carcinoma suppresses metastasis in p53-deficient mammary tumours. Nature *482*, 538–541.

Lai Wing Sun, K., Correia, J.P., and Kennedy, T.E. (2011). Netrins: versatile extracellular cues with diverse functions. Development *138*, 2153–2169.

Lattemann, M., Zierau, A., Schulte, C., Seidl, S., Kuhlmann, B., and Hummel, T. (2007). Semaphorin-1a controls receptor neuron-specific axonal convergence in the primary olfactory center of Drosophila. Neuron *53*, 169–184.

Li, B., Piriz, J., Mirrione, M., Chung, C., Proulx, C.D., Schulz, D., Henn, F., and Malinow, R. (2011). Synaptic potentiation onto habenula neurons in the learned helplessness model of depression. Nature *470*, 535–539.

Li, K., Zhou, T., Liao, L., Yang, Z., Wong, C., Henn, F., Malinow, R., Yates, J.R., and Hu, H. (2013). βCaMKII in lateral habenula mediates core symptoms of depression. Science *341*, 1016–1020.

López-Bendito, G., Cautinat, A., Sánchez, J.A., Bielle, F., Flames, N., Garratt, A.N., Talmage, D. a, Role, L.W., Charnay, P., Marín, O., et al. (2006). Tangential neuronal migration controls axon guidance: a role for neuregulin-1 in thalamocortical axon navigation. Cell *125*, 127–142.

Luo, L., and Flanagan, J.G. (2007). Development of continuous and discrete neural maps. Neuron *56*, 284–300.

Manitt, C., Mimee, A., Eng, C., Pokinko, M., Stroh, T., Cooper, H.M., Kolb, B., and Flores, C. (2011). The netrin receptor DCC is required in the pubertal organization of mesocortical dopamine circuitry. J. Neurosci. *31*, 8381–8394.

Mann, F., Zhukareva, V., Pimenta, A., Levitt, P., and Bolz, J. (1998). Membrane-associated molecules guide limbic and nonlimbic thalamocortical projections. J. Neurosci. *18*, 9409–9419.

Matsumoto, M., and Hikosaka, O. (2007). Lateral habenula as a source of negative reward signals in dopamine neurons. Nature *447*, 1111–1115.

Matsumoto, M., and Hikosaka, O. (2009). Representation of negative motivational value in the primate lateral habenula. Nat. Neurosci. *12*, 77–84.

Mizumoto, K., and Shen, K. (2013). Interaxonal interaction defines tiled presynaptic innervation in C. elegans. Neuron *77*, 655–666.

Molnár, Z., Garel, S., López-Bendito, G., Maness, P., and Price, D.J. (2012). Mechanisms controlling the guidance of thalamocortical axons through the embryonic forebrain. Eur. J. Neurosci. *35*, 1573–1585.

Pasterkamp, R.J., and Kolodkin, A.L. (2013). SnapShot: Axon Guidance. Cell *153*, 494–494.e2.

Pasterkamp, R.J., Kolk, S.M., Hellemons, A.J.C.G.M., and Kolodkin, A.L. (2007). Expression patterns of semaphorin7A and plexinC1 during rat neural development suggest roles in axon guidance and neuronal migration. BMC Dev. Biol. *7*, 98.

Phillipson, O.T., and Griffith, A. C. (1980). The neurones of origin for the mesohabenular dopamine pathway. Brain Res. *197*, 213–218.

Pimenta, A.F., Zhukareva, V., Barbe, M.F., Reinoso, B.S., Grimley, C., Henzel, W., Fischer, I., and Levitt, P. (1995). The limbic system-associated membrane protein is an Ig superfamily member that mediates selective neuronal growth and axon targeting. Neuron *15*, 287–297.

Poon, V.Y., Klassen, M.P., and Shen, K. (2008). UNC-6/netrin and its receptor UNC-5 locally exclude presynaptic components from dendrites. Nature *455*, 669–673.

Powell, A.A.W.A., Sassa, T., Wu, Y., Tessier-Lavigne, M., and Polleux, F. (2008). Topography of thalamic projections requires attractive and repulsive functions of Netrin-1 in the ventral telencephalon. PLoS Biol. *6*, e116.

Robles, E., and Baier, H. (2012). Assembly of synaptic laminae by axon guidance molecules. Curr. Opin. Neurobiol. *22*, 799–804.

Sanes, J.R., and Yamagata, M. (2009). Many paths to synaptic specificity. Annu. Rev. Cell Dev. Biol. *25*, 161–195.

Schmidt, E.R.E., Morello, F., and Pasterkamp, R.J. (2012). Dissection and culture of mouse dopaminergic and striatal explants in three-dimensional collagen matrix assays. J. Vis. Exp. 1–5.

Schwabe, T., Neuert, H., and Clandinin, T.R. (2013). A network of cadherin-mediated interactions polarizes growth cones to determine targeting specificity. Cell *154*, 351–364.

Serafini, T., Colamarino, S. a, Leonardo, E.D., Wang, H., Beddington, R., Skarnes, W.C., and Tessier-Lavigne, M. (1996). Netrin-1 is required for commissural axon guidance in the developing vertebrate nervous system. Cell *87*, 1001–1014.

Shen, X., Ruan, X., and Zhao, H. (2012). Stimulation of Midbrain Dopaminergic Structures Modifies Firing Rates of Rat Lateral Habenula Neurons. PLoS One *7*, e34323.

Shumake, J., Ilango, A., Scheich, H., Wetzel, W., and Ohl, F.W. (2010). Differential neuromodulation of acquisition and retrieval of avoidance learning by the lateral habenula and ventral tegmental area. J. Neurosci. *30*, 5876–5883.

Stamatakis, A.M., Jennings, J.H., Ung, R.L., Blair, G.A., Weinberg, R.J., Neve, R.L., Boyce, F., Mattis, J., Ramakrishnan, C., Deisseroth, K., et al. (2013). A Unique Population of Ventral Tegmental Area Neurons Inhibits the Lateral Habenula to Promote Reward. Neuron *80*, 1039–1053.

Sweeney, L.B., Couto, A., Chou, Y.-H., Berdnik, D., Dickson, B.J., Luo, L., and Komiyama, T. (2007). Temporal target restriction of olfactory receptor neurons by Semaphorin-1a/PlexinA-mediated axon-axon interactions. Neuron *53*, 185–200.

Takeuchi, H., Inokuchi, K., Aoki, M., Suto, F., Tsuboi, A., Matsuda, I., Suzuki, M., Aiba, A., Serizawa, S., Yoshihara, Y., et al. (2010). Sequential arrival and graded secretion of Sema3F by olfactory neuron axons specify map topography at the bulb. Cell *141*, 1056–1067.

Tessier-Lavigne, M., and Goodman, C.S. (1996). The molecular biology of axon guidance. Science *274*, 1123–1133.

Timofeev, K., Joly, W., Hadjieconomou, D., and Salecker, I. (2012). Localized netrins act as positional cues to control layer-specific targeting of photoreceptor axons in Drosophila. Neuron *75*, 80–93.

Veenvliet, J. V., Dos Santos, M.T.M., Kouwenhoven, W.M., von Oerthel, L., Lim, J.L., van der Linden, A.J.A., Koerkamp, M.J.A.G., Holstege, F.C.P., Smidt, M.P. (2013). Specification of dopaminergic subsets involves interplay of En1 and Pitx3. Development *140*, 4116–4116.

Wang, L., and Marquardt, T. (2013). What axons tell each other: axon-axon signaling in nerve and circuit assembly. Curr. Opin. Neurobiol. *23*, 974-982.

Wang, L., Klein, R., Zheng, B., and Marquardt, T. (2011). Anatomical coupling of sensory and motor nerve trajectory via axon tracking. Neuron *71*, 263–277.

Williams, M.E., de Wit, J., and Ghosh, A. (2010). Molecular mechanisms of synaptic specificity in developing neural circuits. Neuron *68*, 9–18.

Xiao, T., Staub, W., Robles, E., Gosse, N.J., Cole, G.J., and Baier, H. (2011). Assembly of lamina-specific neuronal connections by slit bound to type IV collagen. Cell *146*, 164–176.

Zhao, S., Maxwell, S., Jimenez-Beristain, A., Vives, J., Kuehner, E., Zhao, J., O'Brien, C., de Felipe, C., Semina, E., and Li, M. (2004). Generation of embryonic stem cells and transgenic mice expressing green fluorescence protein in midbrain dopaminergic neurons. Eur. J. Neurosci. *19*, 1133–1140.

Zhukareva, V., and Levitt, P. (1995). The limbic system-associated membrane protein (LAMP) selectively mediates interactions with specific central neuron populations. Development *121*, 1161–1172.

Chapter 3

Supplemental Information

SUPPLEMENTAL FIGURES

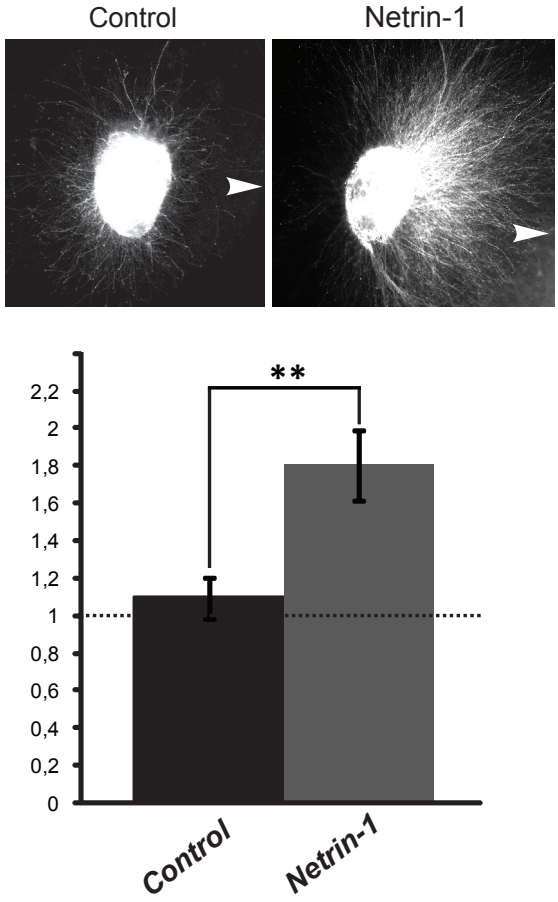

Figure S1. Netrin-1 is an Attractant for Dopaminergic Axons of the Ventral Tegmental Area (VTA), Related to Figure 1.

(**A**) Collagen matrix assays combining E14.5 VTA and control or Netrin-1 expressing HEK 293 cells. Dopaminergic axons are attracted towards Netrin-1 expressing cells, but not control cells. Arrowheads indicate position of adjacent HEK 293 cell aggregates.

(**B**) Average P/D ratio for control and Netrin-1 conditions. P/D ratios, 1.09, n = 14, and 1.80, n = 14, respectively, ** $P < 0.01$. Error bars indicate SEM.

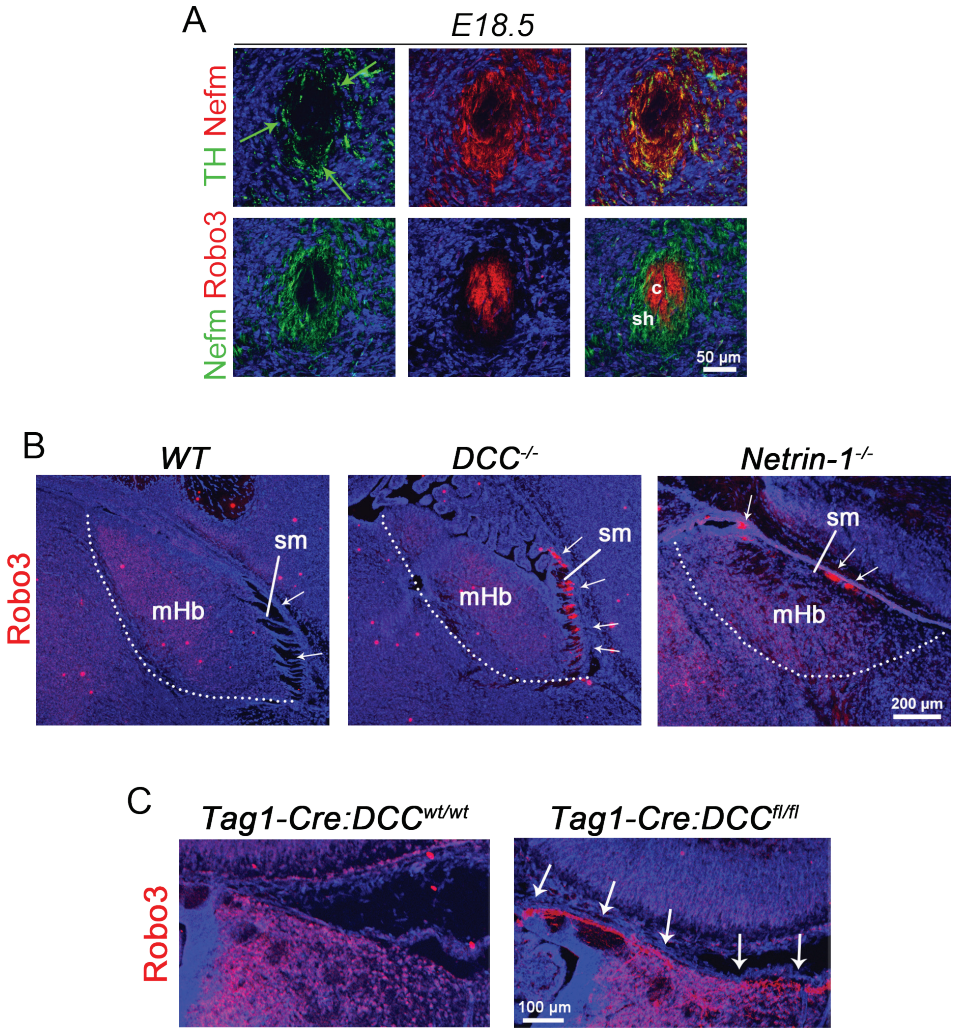

Figure S2. Markers Allow For Specific Visualization of the Core and Sheath Domains of the Fasciculus Retroflexus (FR), Related to Figure 3.

(**A**) Immunohistochemistry for tyrosine hydroxylase (TH), neurofilament medium polypeptide (Nefm) and/or Robo3 on coronal sections of the FR. Nefm is specific for the sheath and shows that dopaminergic axons (green arrows) are confined to this subdomain of the FR. The core is stained by Robo3. Double staining of Robo3 and Nefm reveals the complete segregation of the core and sheath domain.

(**B,C**) Immunohistochemistry for Robo3 in the habenula. In *DCC*$^{-/-}$ and *Netrin-1*$^{-/-}$ mice (**B**) and in *Tag1-Cre:DCC*$^{fl/fl}$ mice (**C**) Robo3-positive axons are found at the dorsal roof of the habenula. c, core; mHb, medial habenula; sh, sheath; sm, stria medullaris.

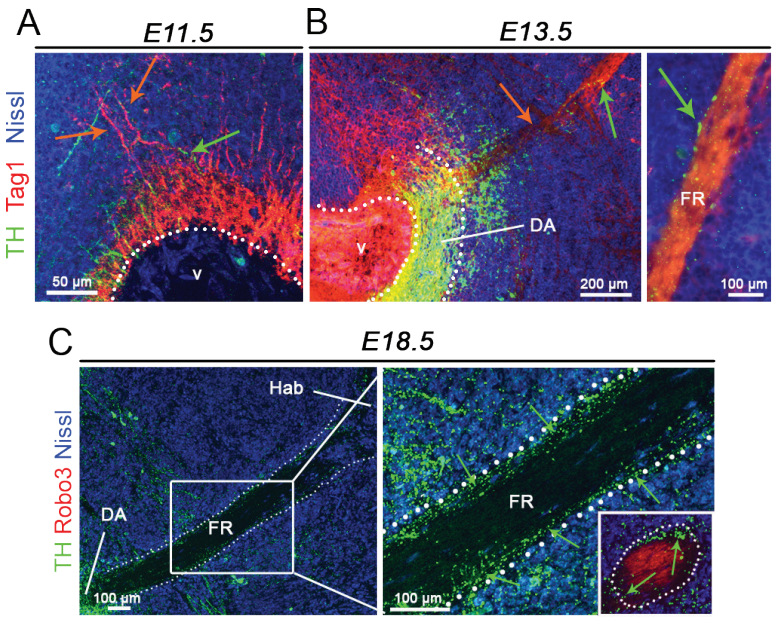

Figure S3. Development of Reciprocal Habenular and Dopaminergic Projections, Related to Figure 4.

(**A-C**) Immunohistochemistry for tyrosine hydroxylase (TH), Tag1 and/or Robo3 on sagittal sections of the fasciculus retroflexus (FR). At E11.5, Tag1-positive axons from the habenula arrive at the dopaminergic midbrain (red arrows). Dopaminergic neurons extend axons but these do not yet progress towards the habenula (green arrow) (**A**). At E13.5, a bundle of fasciculated axons from the habenula (red arrow) extends into the dopaminergic midbrain. A few dopaminergic axons (green arrow) grow along this bundle and are restricted to the outer part of the FR (**B**). At E18.5, dopaminergic axons (green arrows) are restricted to the outer part of the FR (**C**). Inset shows a coronal cross section of the FR. DA, dopamine neuron pool; Hab, habenula; v, ventricle.

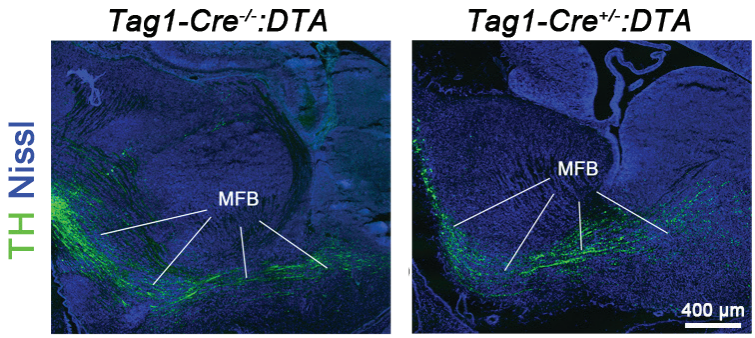

Figure S4. Dopaminergic Projections to the Forebrain Are Intact in *Tag1-Cre*$^{+/-}$*:DTA* Mice, Related to Figure 4.

Immunohistochemistry for tyrosine hydroxylase (TH) on sagittal sections of the forebrain. Dopaminergic axons projecting to the forebrain run through the MFB and are intact in *Tag1-Cre*$^{+/-}$*:DTA* mice. MFB, medial forebrain bundle.

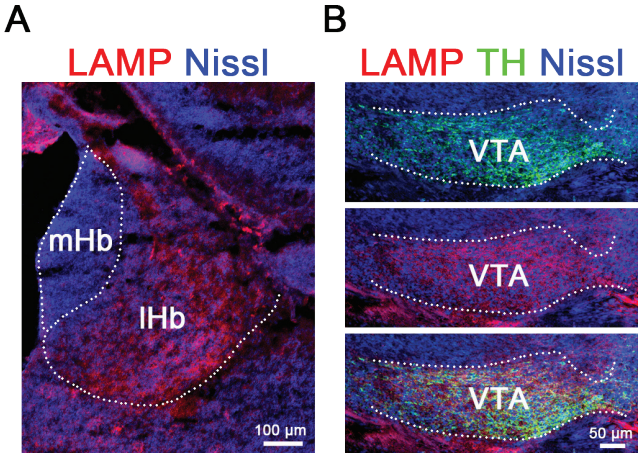

Figure S5. LAMP Protein is Expressed in the Lateral Habenula (lHb) and Ventral Tegmental Area (VTA), Related to Figure 7.

(**A-B**) Immunohistochemistry for limbic-system associated membrane protein (LAMP) and/or tyrosine hydroxylase (TH) on coronal sections. At E18.5, LAMP is specifically expressed in the lHb (**A**) and in dopaminergic neurons in the VTA (**B**). mHb, medial habenula.

	Symbol (Entrez)	Protein
mHb	ALCAM	Activated leukocyte cell adhesion molecule
	Amigo2	Adhesion molecule with Ig like domain 2
	Cntn2	Contactin-2
	Crk	Adapter molecule crk
	DCC	Deleted in colorectal carcinoma
	Nrp2	Neuropilin 2
	Plxnb2	Plexin-B2
lHb	Gap43	Neuromodulin
	Gpc2	Glypican-2
	NCAM1	Neural cell adhesion molecule 1
	Nefm	Neurofilament medium polypeptide
	Nlgn2	Neuroligin-2
	Nlgn3	Neuroligin-3
	NrCAM	Neuronal cell adhesion molecule

Table S1. Related to Figure 1.

List of cell adhesion and axon guidance molecules detected or enriched in either the mHb or lHb.

	Symbol (Entrez)	Protein
Whole FR	ALCAM	Activated leukocyte cell adhesion molecule
	Cdh13	Cadherin 13
	Negr1	Neuronal growth regulator 1
	Nfasc	Neurofascin
	Nrp2	Neuropilin 2
	Robo1	Roundabout homolog 1 (*Drosophila*)
Core	DCC	Deleted in colorectal carcinoma
	Gpc2	Glypican 2 (cerebroglycan)
	L1CAM	L1 cell adhesion molecule
	NCAM1	Neural cell adhesion molecule 1
	NrCAM	Neuron-glia-CAM-related cell adhesion molecule
	Robo3	Roundabout homolog 3 (*Drosophila*)
Sheath	CHL1	Cell adhesion molecule with homology to L1CAM
	LAMP	Limbic system-associated membrane protein

Table S2. Related to Figure 5.

List of cell adhesion and axon guidance molecules detected in the FR. Expression and localization was confirmed by immunohistochemistry, as shown in main Figure 5.

SUPPLEMENTAL EXPERIMENTAL PROCEDURES

MOUSE LINES

All animal use and care were in accordance with institutional guidelines. The morning on which a vaginal plug was detected was considered embryonic day 0.5 (E0.5). C57BL/6 mice were obtained from Charles River. *DTA* and *Rosa26-eYFP* mice were obtained from the Jackson Lab. *En1-Cre* mice were a kind gift of Wolfgang Wurst (Helmholtz Zentrum München) and kindly provided by Alain Chédotal (INSERM). *Pitx3-GFP* mice were a kind gift of Meng Li (MRC Clinical Science Center) and kindly provided by Marten Smidt (University of Amsterdam). *DCC* conditional mutant mice were a kind gift of Anton Berns (Netherlands Cancer Institute) and kindly provided by Cecilia Flores (McGill University). *DCC*$^{-/-}$ (Fazeli et al., 1997) and *Netrin1* hypomorph mice (Serafini et al., 1996) were originally obtained from the laboratory of Marc Tessier-Lavigne (Rockefeller University) and then bred at the University of Queensland under the approval of the University of Queensland Animal Ethics Committee and according to the Australian Code of Practice for the Care and Use of Animals for Scientific Purposes. *DCC* and *Netrin1* knockout mice were backcrossed for over 10 generations onto a C57Bl/6 background.

GENERATION OF *TAG1-CRE* MICE

The *Tag1*(Tg)Cre line was generated using BAC technology (Bacterial Artificial Chromosome) as described previously (Fogarty et al., 2007; Kessaris et al., 2006; Lee et al., 2001). Briefly, 3 clones containing the entire murine *Tag1* gene and upstream and downstream genomic sequences were selected from a BAC library (Ensemble CytoView). In parallel, a plasmid was constructed containing a transgene that included Cre-recombinase flanked by sequences homologous to sequences upstream (9565-9796 bp) and downstream (9861-10159) of exon 2 of the *Tag1* gene that contains the ATG. A polyA-frt-kanamycin-frt cassette was also included in the vector. The appropriate BAC clone and the plasmid were introduced into EL250 cells, colonies were tested for homologous recombination (by which exon 2 sequences were replaced by Cre-recombinase) using restriction digestion and Southern blotting with a probe for the 5' homology region of the *Tag1* gene. Finally, the recombined transgene was isolated and generation of transgenic mice by pronuclear injection of the modified BAC was as described previously (Kessaris et al., 2006). Mice were genotyped using

primers to detect a 550bp Cre fragment (5'-TGAGTGCTTTAGCTCTACAGC-3' and 5'-GACACAGCATTGGAGTCAGA-3'). To examine the spatiotemporal patterns of Cre recombination in the *Tag1-Cre* mice, *Tag1-Cre* mice were crossed with *Rosa26-eYFP* mice, in which a *YFP* cDNA is preceded by a lox-STOP-lox cassette (Srinivas et al., 2001).

IMMUNOHISTOCHEMISTRY

After cervical dislocation, brains were fixed in 4% paraformaldehyde (PFA) in PBS after which they were cryoprotected in 30% sucrose in PBS. Cryostat sections were cut at 16-18 µm, mounted on Superfrost Plus slides (Thermo Fisher Scientific), air-dried, and stored at -20°C. Sections were blocked with 1% BSA in PBS containing 0.4% Triton X-100 for 30 min at room temperature (RT). Subsequent incubation with primary antibodies in blocking buffer was done overnight at 4°C. Sections were washed extensively in PBS and incubated with secondary antibodies conjugated to Alexa Fluor-488, 555 and 680 from appropriate species. After several washes in PBS, sections were counterstained with fluorescent Nissl (Neurotrace; Invitrogen; 1:500), washed in PBS and mounted in FluorSave reagent (Merck Millipore). Staining was visualized on a Zeiss Axioskop A1 epifluorescent microscope or by confocal laser-scanning microscopy (Olympus FV1000). Average fluorescence intensity was measured using the histogram function in Adobe Photoshop. Background was determined in areas without staining and subtracted from images after which the mean signal intensity was measured. Primary antibodies used were:
mouse anti-Nefm (clone 2H3; 1:30), rabbit anti-TH (Millipore; 1:1000), goat anti-Robo3 (R&D Systems; 1:50), mouse anti-Tag1 (DSHB; 1:50), chicken anti-GFP (Abcam; 1:500), mouse anti-DCC (Calbiochem; 1:500), rabbit anti-DCC (a kind gift from Dr. Helen M. Cooper (Queensland Brain Institute; 1:500), goat anti-Neurofascin (Santa Cruz; 1:50), goat anti-ALCAM (R&D Systems, 1:50), anti-Cadherin 13 (Santa-Cruz, 1:50), goat anti-Neurotractin (Santa Cruz; 1:50), goat anti-Robo1 (R&D Systems; 1:50), goat anti-Glypican 2 (R&D Systems, 1:50), rabbit anti-NrCAM (Abcam, 1:50), mouse anti-NCAM (R&D Systems, 1:50), goat anti-L1 (R&D Systems, 1:100), goat anti-CHL1 (R&D Systems, 1:100), mouse anti-LAMP (DSHB; 1:50), goat anti-Neuropilin-2 (R&D Systems, 1:100).

LASER CAPTURE MICRODISSECTION

Fresh frozen sections of E16.5 mouse brains were sagittally cut (16 µm) and mounted on MembraneSlides 1.0 PEN (Zeiss). Sections were dried within the cryostat chamber to prevent protein degradation and were stored at -80°C until use. Before the laser dissection procedure, sections were incubated in ice-cold 70% ethanol for 2 min and stained for 1 min with 1% (w/v) cresyl violet in 50% ethanol. Next, sections were washed shortly in ice-cold 70% ethanol and 100% ethanol and subsequently air-dried. Laser capture microdissection was performed on a PALM laser microscope system (Zeiss). Dissected tissue was collected in lysis buffer (20 mM Tris pH7.5, 15 0mM NaCl, 10% glycerol, 1% NP-40) containing protease inhibitor cocktail (Complete; Roche). After the procedure, LDS sample buffer (NuPAGE) and 2-mercaptoethanol was added and samples were stored at -80°C. Samples were subjected to SDS-PAGE and stained using GelCode Blue Stain reagent (Thermo Scientific). Gels were sent for mass spectrometry analysis at the Erasmus Proteomics Center (Rotterdam).

RNA *IN SITU* HYBRIDIZATION

cDNA was made from whole mouse brain RNA using a one-step RT-PCR kit (Qiagen), according to supplied protocol and using the following primers:

DCC, 5'-CCCAGTCCAAGGTTACAGATTG-3' and
5'-GGAGGTGTCCAACTCATGATG-3';
Netrin-1, 5'-GATGTGCCAAAGGCTACCAG-3' and
5'-TTCTTGCACTTGCCCTTCTTC-3';.

cDNA was cloned into pGEM-T Easy (Promega) and transcribed using either SP6 or T7 RNA polymerase (Roche) and digoxigenin-labeled nucleotide mix (Roche) to produce digoxigenin-labeled cRNA probes. Brain sections were from prepared on a cryostat from brains frozen on dry-ice. Sections were cut at 16 µm and stored at -80°C. After hybdrization of probes, digoxigenin was detected using anti-digoxigenin FAB fragments conjugated to alkaline phosphatase (Roche; 1:3000) and stained with NBT/BCIP (Roche). Sections were counterstained with fluorescent Nissl (Neurotrace; Invitrogen; 1:500), mounted using FluorSave reagent and visualized on a Zeiss Axioscope A1.

EXPLANT CULTURES

E14.5 mouse embryos were collected in ice-cold L15. Appropriate brain regions were dissected in L15 with 5% FCS and explants were cut to a diameter of approximately 350 μm. For cocultures, explants and/or transfected HEK 293 cells were placed together in a collagen hill at a distance of approximately 300 μm and were cultured in Neurobasal containing HEPES, B27, β-mercaptoethanol, glutamine and penicillin/streptomycin. For blocking experiments, sodium azide was removed from IgG control (Millipore) and anti-DCC blocking antibodies (Calbiochem) using Slide-A-Lyzer 10K dialysis cassettes (Thermo Scientific). Antibodies were added at a final concentration of 10 μg/ml. After 72 h in culture, explants were fixed in 4% PFA and stained using appropriate antibodies. Quantification of cocultures was done by measuring the 20 longest neurites in both the proximal and distal quadrants. Using average values the proximal/distal (P/D) ratio was determined for each explant. For growth on LAMP substrate, coverslips were coated with either poly-D-lysine (PDL) for control or PDL and 10 μg/mL of recombinant mouse LAMP (Sino Biological). Average axon length was determined after 72 h in culture.

ORGANOTYPIC SLICE CULTURES

For organotypic slice culture experiments, E12.5 mouse brains were dissected and cut along the midline to produce two sagittal hemisections. Brain slices were cultured on Millicell cell culture inserts (PTFE, 0.4 μm, Millipore) for three days in 1.6 ml slice culture medium consisting of Basal Medium Eagle (Sigma) and supplemented with cHBSS, glucose, glutamine and penicillin/streptomycin, as described previously (Polleux and Ghosh, 2002). For blocking of axon outgrowth, membrane blocking filters (Nuclepore Track-Etched 8 μm, Whatman) were cut to a size roughly covering the complete ventral side of the habenula and were placed at 0 days in vitro (DIV) where they remained for the entire culture period. For removal of GPI-linked proteins, PI-PLC (Sigma) was dissolved according to manufacturer's protocol and added at 0, 1 and 2 DIV to a final concentration of 1 U/ml. Control slices were incubated with the same volume of vehicle. Blocking experiments were performed by adding LAMP blocking antibodies (R&D Systems) to a final concentration of 30 μg/ml at 0, 1 and 2 DIV. After 3 DIV slices were fixed in 4% PFA for 1 h and washed in PBS. Slices were blocked in PBS-T (PBS containing 1% Triton-X100) and 10% fetal calf serum (FCS) for 3 h at RT. Slices were stained with primary antibodies

overnight in blocking buffer at 4°C and subsequently washed 6 times for 1 h in PBS-T with 1% FCS at RT. Next, slices were incubated with secondary antibodies overnight at 4°C after which they were washed several times in PBS, mounted on microscope slides with ProLong Gold antifade reagent (Invitrogen) and visualized on an Olympus FV1000 confocal laser-scanning microscope. For quantification of axon growth, three bins of equal size were drawn along the axon bundle and average fluorescence intensity in each bin was determined, as described above.

SIRNA KNOCKDOWN PROCEDURE

HEK 293 human embryonic kidney cells were plated onto poly-D-lysine coated coverslips. For transfection, 1.75 µl of Lipofectamine 2000 was diluted in 25 µl Opti-MEM (Gibco). Separately, 15 pmol siRNA together with 0.5 µg of DNA encoding LAMP (LAMP-pIRES-hrGFP-1a) (Hashimoto et al., 2009) was added to 25 µl Opti-MEM. Both Opti-MEM dilutions were mixed and allowed to incubate for 10 min after which they were directly added to each well. After 72 h cells were fixed in 4% PFA, briefly washed in PBS, and incubated for 30 min in blocking buffer containing 1% BSA in PBS and 0.4% Triton X-100. Cells were incubated with appropriate primary antibodies in blocking buffer overnight at 4°C. Cells were washed in PBS and incubated for 1 h with appropriate secondary antibodies at RT. After washing in PBS, nuclei were counterstained with DAPI (Sigma) after which the coverslips were mounted in Prolong Gold antifade reagent (Invitrogen).

EX VIVO ELECTROPORATION

Mouse embryos were collected at E13.5 and the third ventricle was injected, as described (Quina et al., 2009), with siRNA (25 µM) and/or DNA (GFP or LAMP-pIRES-hrGFP-1a; 1 µg/µl) diluted in 0.05% Fast Green Dye (Sigma) using a PLI-100 Pico-injector (Harvard Apparatus). Brains were electroporated using an ECM 830 Electro-Square-Porator (Harvard Apparatus) set to three unipolar pulses at 30 V (100-ms interval and length) and using gold-plated Genepaddles (Fisher Scientific). Brains were dissected and prepared for slice culture assay as described above. Slices were grown for 3 DIV after which they were fixed, stained and visualized on a confocal laser-scanning microscope (Olympus FV1000). For LAMP knockdown experiments, axon growth in each electroporated slice was quantified by drawing three bins of equal size along the axon bundle and subsequently determining average fluorescence

intensity in each bin, as described above. LAMP overexpression experiments were quantified by counting the number of TH-positive axons that inappropriately innervated the mHb, as determined by double immunohistochemistry for TH and Robo3. Only those slices were considered where a sufficient amount of GFP-positive cells was found in the habenula and where no abnormal growth of Robo3-positive axons was observed.

SUPPLEMENTAL REFERENCES

Fazeli, A., Dickinson, S., Hermiston, M., Tighe, R., Steen, R., Small, C., Stoeckli, E., Keino-Masu, K., Masu, M., Rayburn, H., et al. (1997). Phenotype of mice lacking functional Deleted in colorectal cancer (Dcc) gene. Nature *386*, 796–804.

Fogarty, M., Grist, M., Gelman, D., Marín, O., Pachnis, V., and Kessaris, N. (2007). Spatial genetic patterning of the embryonic neuroepithelium generates GABAergic interneuron diversity in the adult cortex. J. Neurosci. *27*, 10935–10946.

Hashimoto, T., Maekawa, S., and Miyata, S. (2009). IgLON cell adhesion molecules regulate synaptogenesis in hippocampal neurons. Cell Biochem. Funct. *27*, 496–498.

Kessaris, N., Fogarty, M., Iannarelli, P., Grist, M., Wegner, M., and Richardson, W.D. (2006). Competing waves of oligodendrocytes in the forebrain and postnatal elimination of an embryonic lineage. Nat. Neurosci. *9*, 173–179.

Lee, E.C., Yu, D., Martinez de Velasco, J., Tessarollo, L., Swing, D. A., Court, D.L., Jenkins, N. A., and Copeland, N.G. (2001). A highly efficient Escherichia coli-based chromosome engineering system adapted for recombinogenic targeting and subcloning of BAC DNA. Genomics *73*, 56–65.

Polleux, F., and Ghosh, A. (2002). The Slice Overlay Assay: A Versatile Tool to Study the Influence of Extracellular Signals on Neuronal Development. Sci. Signal., pl9.

Quina, L. A., Wang, S., Ng, L., and Turner, E.E. (2009). Brn3a and Nurr1 mediate a gene regulatory pathway for habenula development. J. Neurosci. *29*, 14309–14322.

Srinivas, S., Watanabe, T., Lin, C.S., William, C.M., Tanabe, Y., Jessell, T.M., and Costantini, F. (2001). Cre reporter strains produced by targeted insertion of EYFP and ECFP into the ROSA26 locus. BMC Dev. Biol. *1*, 4.

'I think animal testing is a terrible idea. They get all nervous and give silly answers.'

-A bit of Fry and Laurie

Chapter 4

Unc5C haploinsufficient phenotype: striking similarities with the *DCC* haploinsufficiency model

Meagan L. Auger[1], Ewoud R. E. Schmidt[2], Colleen Manitt[1], Greg Dal-Bo[1], R. Jeroen Pasterkamp[2], and Cecilia Flores[1]

[1]Department of Psychiatry and of Neurology and Neurosurgery, McGill University, Douglas Menthal Health University Institute, 6875 LaSalle Boulevard, Verdun, Quebec, Canada, H4H1R3
[2]Department of Neuroscience and Pharmacology, University Medical Center Utrecht, Universiteitsweg 100, 3584 CG, Utrecht, the Netherlands

European Journal of Neuroscience, 2013; 38(6): 2853-63

ABSTRACT

DCC and UNC5 homologues (UNC5H) are guidance cue receptors highly expressed by mesocorticolimbic dopamine neurons. We have shown that *dcc* heterozygous mice exhibit increased dopamine, but not norepinephrine, innervation and function in medial prefrontal cortex. Concomitantly, *dcc* heterozygotes show blunted mesolimbic dopamine release and behavioral responses to stimulant drugs. These changes appear only in adulthood. Recently, we found an adolescent emergence of UNC5H expression by dopamine neurons and co-expression of DCC and UNC5H by single dopamine cells. Here, we demonstrate selective expression of *unc5* homologue *c* mRNA by dopamine neurons in adulthood. We show that *unc5c* haploinsufficiency results in diminished amphetamine-induced locomotion in male and female mice. This phenotype is identical to that produced by *dcc* haploinsufficiency and is observed after adolescence. Notably, and similar to *dcc* haploinsufficiency, *unc5c* haploinsufficiency leads to dramatic increases in tyrosine hydroxylase expression in the medial prefrontal cortex, but not in the nucleus accumbens. In contrast, medial prefrontal cortex dopamine-β-hydroxylase expression is not altered. We confirmed that UNC5C protein is reduced in the ventral tegmental area of *unc5c* heterozygous mice, but that DCC expression in this region remains unchanged. UNC5C receptors may also play a role in dopamine function and influence sensitivity to behavioral effects of stimulant drugs of abuse, at least upon first exposure. The striking similarities between the *dcc*– and the *unc5c*– haploinsufficient phenotypes raise the possibility that functions mediated by DCC/UNC5C complexes may be at play.

INTRODUCTION

Netrin-1 is a developmental cue that directs axons and dendrites towards their appropriate targets ("long-range" function) and participates in events that occur following pathfinding ("short-range" function), including synaptogenesis and axonal sprouting (Manitt & Kennedy, 2002; Barallobre *et al.*, 2005; Colon-Ramos *et al.*, 2007; Hutchins & Kalil, 2008; Poon *et al.,* 2008; Chao *et al.*, 2009; Manitt *et al.*, 2009). DCC (Deleted in Colorectal Cancer) and the UNC-5 homologues (UNC5H, A-D) are netrin-1 receptors that mediate attraction and repulsion, respectively (Hong *et al.*, 1999; Bouchard *et al.*, 2004; Muramatsu *et al.*, 2010). However, DCC/UNC5H receptor complexes can also mediate netrin-1-induced repulsion (Keleman & Dickson, 2001).

We and others have shown that DCC receptors are discretely and highly expressed by dopamine (DA) neurons in the ventral tegmental area (VTA) from embryonic life to adulthood in rodents (Osborne *et al.*, 2005; Grant *et al.*, 2007; Yetnikoff *et al.*, 2007; Manitt *et al.*, 2010). Our group has accumulated substantial evidence showing that DCC receptors are critically implicated in the development of the mesocorticolimbic DA system (Flores, 2011). Briefly, we have shown that adult *dcc* haploinsufficient mice have blunted locomotor responses to amphetamine and cocaine and resistance to drug-induced deficits in sensorimotor gating. These phenotypes do not depend on genetic background and are observed in both male and female mice (Flores *et al.*, 2005; Grant *et al.*, 2007; Flores, 2011). Correspondingly,

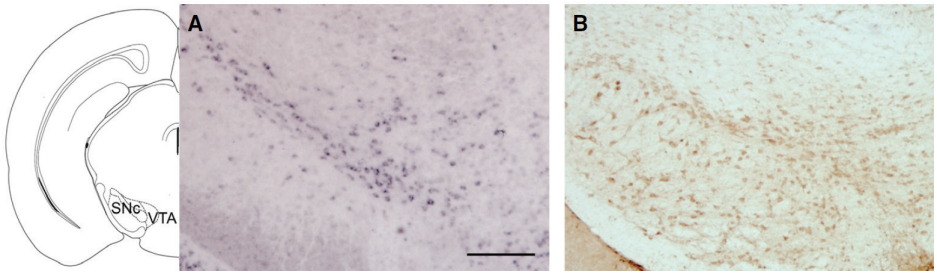

Figure 1. *Unc5c* mRNA is Expressed in the Ventral Tegmental Area of the Adult Mouse Brain.
Micrographs of coronal midbrain hemisections of adult wild-type male mice. In both pictures, dorsal is on top, lateral is on the left and medial is on the right. (**A**) Low magnification image showing *unc5c* mRNA expression within the ventral tegmental area (VTA) and substantia nigra pars compacta (SNc). (**B**) UNC5H protein expression in the VTA and SNc; note that the pattern of labeling is nearly identical to that detected in **A**. Sections correspond to plate 55 of the Mouse Brain Atlas (Franklin & Paxinos, 2007). Scale bar: 250 μm.

dcc heterozygotes exhibit reduced amphetamine-induced DA release in the NAcc, but have exaggerated extracellular concentrations of DA, but not norepinephrine, in the mPFC. This is observed both at baseline and following exposure to amphetamine (Grant *et al.*, 2007). These behavioral and neurochemical traits are opposite to those observed in putative developmental animal models of schizophrenia (Tseng *et al.*, 2009; Boksa, 2010), in the disease itself (Lieberman *et al.*, 1987; Breier *et al.*, 1997; Akil *et al.,* 1999; Meyer-Lindenberg *et al.*, 2002; Abi-Dargham *et al.*, 2009; Howes *et al.*, 2012), or following repeated exposure to stimulant drugs (Vezina, 2004; Evans *et al.*, 2006; Leyton, 2007). In fact, we have demonstrated an association between variation in the human *DCC* gene and schizophrenia (Grant *et al.,* 2012). Strikingly, the *dcc* "protective" phenotype emerges only after adolescence (Grant *et al.*, 2009; Yetnikoff *et al.*, 2011; Yetnikoff *et al.,* 2013) and is tightly associated with a selective increase in DA connectivity in the mPFC (Manitt *et al.*, 2011).

Although mesocorticolimbic DA neurons express DCC throughout life, they only begin to co-express UNC5H receptors during the adolescent period (Manitt *et al.*, 2010). Moreover, the emergence of UNC5H expression within DA neurons in the VTA marks a drastic switch in the DCC:UNC5H ratio in this region, leading to a predominant, but not exclusive, UNC5H expression from adolescence onwards (Manitt *et al.*, 2010). UNC5H receptors may therefore contribute to the

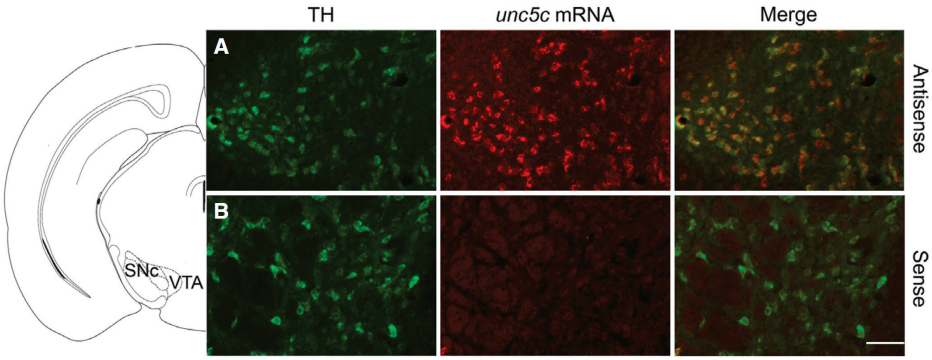

Figure 2. *Unc5c* mRNA Is Expressed By Ventral Tegmental Area DA Neurons.

Micrographs of coronal midbrain hemisections of adult wild-type male mice. In (**A**), dorsal is on top, medial is on the left and lateral is on the right. In (**B**), dorsal is on top, medial is on the right, and lateral is on the left. (**A**) High magnification images showing that *unc5c* mRNA (red) is expressed by most TH-positive neurons (green) in the ventral tegmental area (VTA). (**B**) No mRNA expression (red) is detected using the mRNA sense probe. Sections correspond to plate 55 of the Mouse Brain Atlas (Franklin & Paxinos, 2007). Scale bar: 50 μm.

adolescent maturation of the DA circuitry, either alone or as DCC/ UNC5H receptor complexes. As such, one would expect that *unc5* homologue receptor haploinsufficiency would also lead to DA-related phenotypes in adulthood. We have previously found that only *unc5* homologue *c* (*unc5c*) mRNA, and to a lesser extent *unc5d,* are expressed within the VTA of adult rodents (Manitt *et al.*, 2010). Thus, the goal of this study was to begin to determine whether *unc5c* heterozygous mice exhibit behavioral and molecular indicators of altered DA function. We chose to study *unc5c* haploinsufficiency to make comparisons to our previous studies in *dcc* heterozygotes. To this end, we employed experimental protocols identical to those used in our *dcc* haploinsufficiency studies. Indeed, netrin-1 receptor haploinsufficiency models recapitulate naturally occurring variations in gene expression in humans (Srour *et al.*, 2010; Grant *et al.*, 2012).

RESULTS

ADULT MIDBRAIN DOPAMINE NEURONS EXPRESS *UNC5C* MRNA

As shown in Figure 1a, there is robust and selective expression of *unc5c* mRNA in both the VTA and substantia nigra pars compacta of adult mice. Furthermore, the pattern of expression appears to be specific to a subset of neurons within these regions. The labeling within the substantia nigra pars reticulata is sparse, suggesting that DA

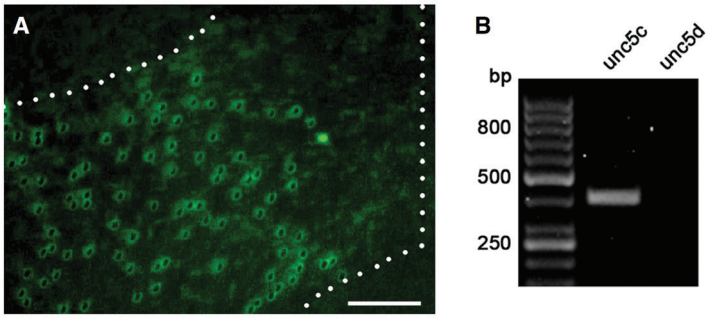

Figure 3. *Unc5c*, But Not *Unc5d*, mRNA Is Expressed By DA Neurons In the Ventral Tegmental Area of the Adult Mouse.

(**A**) Micrograph of a coronal midbrain hemisection from an adult *Pitx3-GFP* mouse. The ventral tegmental area is delineated with white dots. GFP-positive DA neurons were laser-dissected from the delineated area, and mRNA from these neurons was subjected to RT-PCR using primers specific to *unc5c* and *unc5d*. Scale bar: 150 µm. (**B**) RT-PCR products after gel electrophoresis. Note that only *unc5c*, and not *unc5d*, mRNA was amplified from adult DA neurons from the ventral tegmental area (VTA). bp; base pairs.

cells express the *unc5c* homologue. Interestingly, the patterns of *unc5c* mRNA and UNC5H protein expression in the adult VTA are very similar (Figure 1b), indicating that the UNC5H antiserum does detect UNC5 homologue C within the VTA.

To further verify whether adult midbrain DA neurons express *unc5c* mRNA, we conducted dual *unc5c* in situ hybridization-TH immunohistochemistry experiments on brain sections of adult wild-type male mouse. These experiments revealed that neurons that express *unc5c* mRNA co-express TH. This is the case for both VTA (Figure 2) and substantia nigra pars compacta (data not shown). Most, if not all, TH-positive neurons appear to express *unc5c* mRNA within the VTA, but there are *unc5c* mRNA positive neurons that are non-dopaminergic. No signal was detected when sense probes were used, confirming the specificity of the *unc5c* antisense probe (Figure 2).

In a previous study we performed RT-PCR experiments on whole tissue punches of the VTA of adult rodents and found that both *unc5c* and *unc5d* homologues were expressed in this region. To further investigate *unc5* homologue expression within VTA DA neurons specifically, we laser-dissected VTA DA neurons of adult *Pitx3-GFP* transgenic mice and conducted RT-PCR using primers specific to *unc5c* and *unc5d* mRNA. We found that adult VTA DA neurons express significant levels of *unc5c*, but not *unc5d* mRNA (Figure 3). Previous studies have shown similar functional and neuroanatomical characteristics between DA neurons of *Pitx3-GFP* mice and DA neurons of wild-type mice and of other transgenic lines (Dougalis *et al.*, 2012). The fact that *unc5c* mRNA is expressed in DA neurons of both *Pitx3-GFP* and wild-type mice in adulthood is consistent with these reports.

BLUNTED BEHAVIORAL RESPONSE TO AMPHETAMINE IN ADULT *UNC5C* HETEROZYGOUS MICE

As shown in Figure 4, adult male *unc5c* heterozygous (n=8) and their wild-type littermate (n=14) mice show similar locomotor activity at baseline (Figure 4a) or following an i.p. injection of saline (Figure 4b). However, male *unc5c* heterozygous mice exhibit significantly reduced locomotion in response to an i.p. injection of amphetamine (2.5 mg/kg) in comparison to their wild-type controls (Figure 4c). A repeated measures ANOVA revealed no main effect of genotype ($F_{1,20} = 1.61$, $P = 0.21$), but a significant genotype × time interaction ($F_{17,340} = 4.25$, $P < 0.0001$). We have shown previously that *dcc* haploinsufficiency also leads to blunted amphetamine-

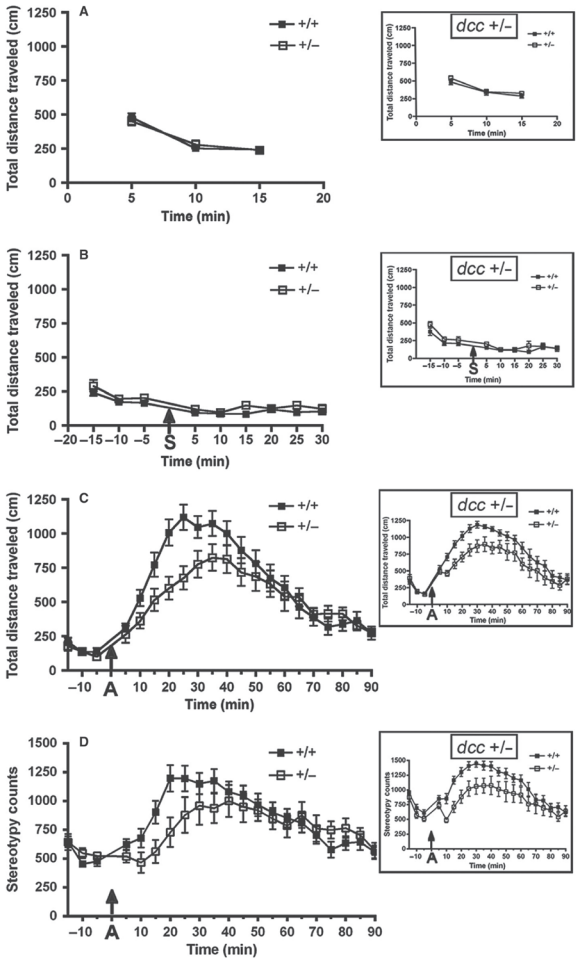

Figure 4. Blunted Amphetamine-induced Locomotion In Adult Male *Unc5c* Heterozygous Mice.

Data points represent the total distance traveled in centimeters (mean ± SEM). The injection time point is indicated by an arrow. (**A**) No difference was observed between *unc5c* heterozygous (+/-) and wild-type (+/+) mice during habituation. (**B**) No difference was observed between groups following an injection of 0.9% saline, 15 min after habituation. (**C**) Male +/- mice display a blunted response to a single injection of amphetamine (2.5 mg/kg i.p.) compared to male +/+ mice. Post hoc analysis revealed significantly less amphetamine-induced locomotion in *unc5c* +/- male mice compared to +/+ controls at the following times, post-drug injection: t = 15 min: p = 0.0386; t = 20 min: p = 0.0038; t = 25 min: p = 0.0024. (**D**) Adult male *unc5c* +/- mice show diminished amphetamine-induced stereotypy in comparison to +/+ controls. Data from adult male *dcc* +/- mice presented in the insets were adapted from Grant *et al.,* 2007. A repeated measures ANOVA on amphetamine-induced stereotypy of these previous data revealed both a main effect of genotype ($F_{1, 19} = 8.50$, $P = 0.0089$) and a significant genotype x time interaction ($F_{17, 323} = 3.34$, $P < 0.0001$). Note that the phenotypes of adult male *unc5c* +/- and *dcc* +/- mice are almost identical. A, amphetamine injection; S, saline injection

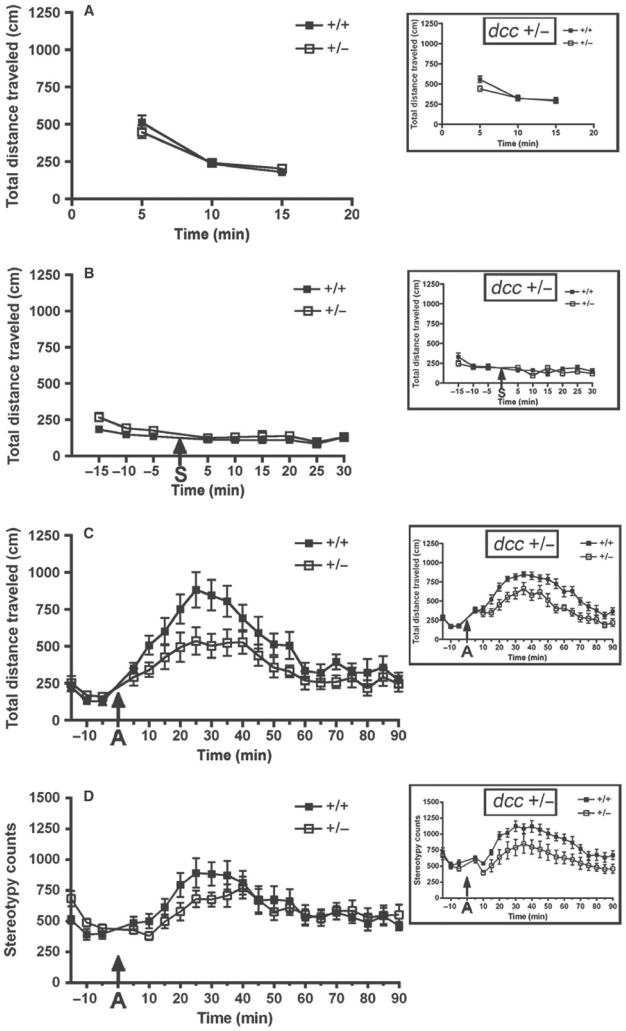

Figure 5. Blunted Amphetamine-induced Locomotion In Adult Female *Unc5c* Heterozygous Mice.
Data points represent the total distance traveled in centimeters (mean ± SEM). The injection time point is indicated by an arrow. (**A**) No difference was observed between *unc5c* heterozygous (+/-) and wild-type (+/+) mice during habituation. (**B**) No difference was observed between groups following an injection of 0.9% saline, 15 min after habituation. (**C**) Female *unc5c* +/- mice display a blunted response to a single injection of amphetamine (2.2 mg/kg i.p.) compared to female +/+ mice. (**D**) No differences in amphetamine-induced stereotypy were observed between *unc5c* +/- mice and +/+ controls. Data from adult female *dcc* +/- mice presented in the insets were adapted from Grant *et al.*, 2007. A repeated measures ANOVA on amphetamine-induced stereotypy of these previous data revealed a main effect of genotype ($F_{1,18} = 6.04$, $P = 0.024$), but a non-significant genotype × time interaction ($F_{17,306} = 1.12$, $P = 0.33$). Note that the phenotypes of adult female *unc5c* +/- and *dcc* +/- mice are almost identical. A, amphetamine injection; S, saline injection

induced locomotion in adulthood. The time course and magnitude of the reduced behavioral responding to amphetamine is remarkably similar between adult male *unc5c* heterozygous and adult male *dcc* heterozygous mice (see Figure 4 inset).

As shown in Figure 5, both adult female and male *unc5c* heterozygous mice show blunted amphetamine-induced locomotion in comparison to their corresponding littermate controls. There are no differences in locomotor activity between adult female *unc5c* heterozygous (n=8) and female wild-type mice (n=9) during habituation (Figure 5a) or after an injection of saline (Figure 5b). However, single exposure to amphetamine (2.2 mg/kg) elicits significantly blunted locomotor activity in female *unc5c* heterozygous mice versus their wild-type counterparts (Figure 5c). A repeated measures ANOVA revealed a main effect of genotype ($F_{1,15} = 4.14$, $P = 0.05$), but a non-significant genotype × time interaction ($F_{17,225} = 1.5$, $P = 0.08$). The time course and magnitude of the reduced behavioral responding to AMPH is remarkably similar between adult *unc5c* heterozygous female mice and *dcc* heterozygous female mice (Figure 5 inset).

We also examined amphetamine-induced stereotypy in order to ensure that the locomotor phenotype of *unc5c* heterozygotes was not a consequence of increased stereotypy. In adult males, a repeated measures ANOVA revealed no main effect of genotype ($F_{1,20} = 0.66$, $P = 0.42$). However there is a significant genotype × time interaction ($F_{17,340} = 3.94$, $P < 0.0001$), with *unc5c* heterozygous mice showing less amphetamine-induced stereotypy than their control littermates during the first part of the test (Figure 4d). In adult female mice, no differences in stereotypy counts were observed between genotypes (Figure 5d). A repeated measures ANOVA revealed no main effect of genotype ($F_{1,15} = 0.41$, $P = 0.52$) and a non-significant genotype × time interaction ($F_{17,255} = 1.41$, $P = 0.13$).

THE BEHAVIORAL PHENOTYPE OF *UNC5C* HETEROZYGOUS MICE IS NOT EVIDENT BEFORE ADOLESCENCE

We found no differences in locomotor activity between male juvenile *unc5c* heterozygous mice (n=7) and their corresponding male wild-type littermates (n=11) at baseline (Figure 6a) or after an i.p. injection of saline (Figure 6b). However, in contrast to adults, male juvenile *unc5c* heterozygous and wild-type mice show identical locomotor activity in response to a single injection of 2.5 mg/kg of amphetamine (Figure 6c; repeated measures ANOVA: no significant main effect of genotype ($F_{1,16}$

= 0.19, P = 0.66) and a non significant genotype × time interaction ($F_{17,272}$ = 0.44, P = 0.97).

Similarly, juvenile female unc5c heterozygous (n=12) and female wild-type littermate (n=9) mice show indistinguishable behavioral responses at baseline (Figure 6d), following an i.p. injection of saline (Figure 6e), or after a single injection of 2.2. mg/kg of amphetamine (Figure 6f; repeated measures ANOVA: no significant main effect of genotype ($F_{1,19}$ = 0.76, P = 0.39) and a non significant genotype × time interaction ($F_{17,323}$ = 1.08, P = 0.36). The post-adolescence expression of the behavioral phenotype of *unc5c* heterozygous mice parallels our previous findings with *dcc* heterozygous mice (Grant *et al.*, 2009; Yetnikoff *et al.*, 2011), which exhibit blunted behavioral responses to amphetamine only in adulthood (Grant *et al.*, 2009; Yetnikoff *et al.*, 2010)

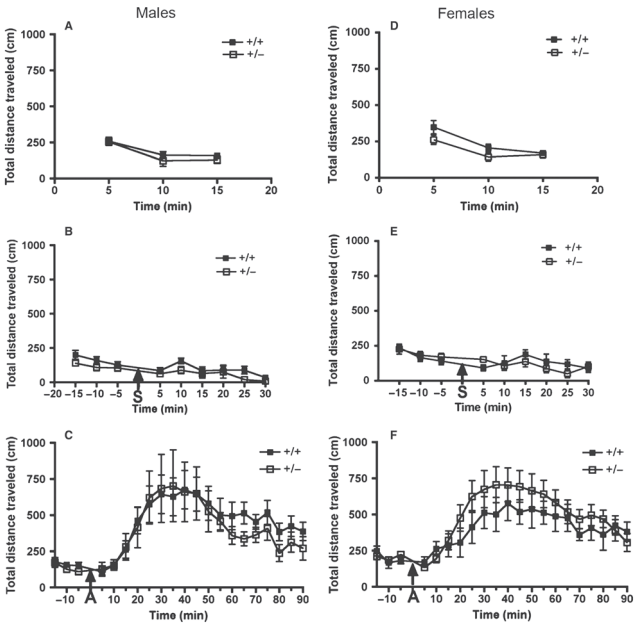

Figure 6. Juvenile Male And Female *Unc5c* Heterozygous Mice Show No Differences In Amphetamine-induced Locomotion Compared to Wild-type Littermates.

Data points represent the total distance traveled in centimeters (mean ± SEM). The injection time point is indicated by an arrow. (**A, D**) During habituation, no differences in locomotion were observed between juvenile male *unc5c* heterozygous (+/-) and wild-type (+/+) controls, or between juvenile female *unc5c* +/- and +/+ mice. (**B, E**) No difference in locomotion was observed between groups following an injection of 0.9% saline. (**C, F**) Both juvenile male and female *unc5c* +/- mice display identical behavioral responses relative to their respective +/+ control groups following a single injection of amphetamine (2.5 mg/kg i.p.). A, amphetamine injection; S, saline injection.

Both male and female juvenile *unc5c* heterozygous mice show nearly identical amphetamine-induced stereotypy in comparison to their corresponding male or female wild-type littermates (data not shown). For juvenile males, a repeated measures ANOVA revealed no main effect of genotype ($F_{1, 16}$= 0.16, P = 0.68) and a non-significant genotype × time interaction ($F_{17,272}$ = 0.33, P = 0.99). Likewise, for juvenile females a repeated measures ANOVA showed no main effect of genotype ($F_{1, 19}$ = 0.21, P = 0.64) and a non-significant interaction of genotype × time ($F_{17, 323}$ = 0.87, P = 0.59).

UNC5C HETEROZYGOUS MICE EXHIBIT A SELECTIVE INCREASE IN TH PROTEIN EXPRESSION IN THE MPFC, BUT NOT IN THE NACC

To assess whether the behavioral changes in *unc5c* heterozygous mice are accompanied by changes in DA function, we examined the expression of TH in the mPFC and NAcc of adult *unc5c* heterozygotes and wild-type controls using Western blot. *unc5c* heterozygous mice show a large and significant increase (2.3 fold) in TH expression in the mPFC in comparison to control groups (Figure 7A; t_{11} = 2.251 P = 0.04). In the NAcc, however, the levels of TH expression are comparable between genotypes (Figure 7A; t_{12} = 0.621 P = 0.54). *dcc* heterozygous mice also exhibit increased TH expression in the mPFC, but not in the NAcc (Flores *et al.*, 2005).

The mPFC receives both DA and noradrenergic innervation. Thus, to determine whether the changes in TH observed in *unc5c* heterozygotes reflect changes in DA terminals, we examined mPFC expression of DBH, the enzyme responsible for converting DA to norepinephrine. Similar to what we reported previously in adult *dcc* haploinsufficient mice (Flores *et al.*, 2005), we found no differences in DBH expression between *unc5c* heterozygous mice and wild-type controls (Figure 7A, inset; t_9 = 0.944 P = 0.36).

UNC5C HETEROZYGOUS MICE HAVE REDUCED UNC5C PROTEIN EXPRESSION IN THE VTA, BUT NO CHANGES IN *DCC* EXPRESSION

To determine whether UNC5C protein expression is altered in adult *unc5c* heterozygous mice, we conducted western blot analysis in bilateral punches of the VTA of *unc5c* heterozygous and wild-type mice using the same UNC5H antiserum as in Figure 1. We found a significant reduction in UNC5H immunoreactivity in *unc5c* heterozygous mice in comparison to wild-type controls (Figure 7B; t_{12} = 2.179 P = 0.01). This finding, together with the fact that only *unc5c* and *unc5d* mRNA are

expressed within the VTA, indicates that *unc5c* haploinsufficiency leads to reduction of UNC5C protein expression.

In contrast, we found no changes in DCC expression in the VTA of adult *unc5c* heterozygous mice, indicating that reductions in UNC5C expression within this region are not associated with corresponding compensatory changes in DCC expression (Figure 7B; t_{15} = 2.179 P = 0.4). Likewise, there are no compensatory changes in UNC5C expression in the VTA of adult *dcc* heterozygous mice (Grant *et al.*, 2007).

DISCUSSION

In this study, we first demonstrate, using two different strategies, that DA neurons in the VTA express, selectively, *unc5c* mRNA in the adult mouse. We then show that haploinsufficiency of *unc5c* results in reduced UNC5C protein expression and diminished sensitivity to the effects of a single injection of amphetamine on locomotor activity. This behavioral phenotype is observed in both male and female *unc5c* haploinsufficient mice and, remarkably, becomes evident in adulthood. Furthermore, adult *unc5c* haploinsufficient mice exhibit dramatic increases in TH, but not DBH expression in the mPFC selectively; TH levels in the NAcc are not different between *unc5c* heterozygous and wild-type mice. Importantly, there are no compensatory changes in DCC expression in the VTA of *unc5c* heterozygotes. These behavioral and DA phenotypes are remarkably similar to the ones exhibited by mice that develop with *dcc* haploinsufficiency (Flores, 2011). Thus, our findings raise the intriguing possibility that reduced UNC5C expression, similar to *dcc* heterozygosity, may lead to alterations in adult mPFC DA function. In turn, reduced UNC5C function may confer diminished sensitivity to the behavioral effects of stimulant drugs.

DOPAMINE NEURONS OF THE VTA EXPRESS *UNC5 HOMOLOGUE C* EXCLUSIVELY

In a previous study, we assessed UNC5H expression within mesocorticolimbic DA neurons in rodents from embryonic life to adulthood. We found robust UNC5H immunofluorescence in VTA DA neurons, but only from adolescence onwards (Manitt *et al.*, 2010). The antiserum we used was raised against UNC5C, but it detects recombinant UNC5A and UNC5B proteins too (Tong *et al.*, 2001; Manitt

et al., 2004). We then conducted RT-PCR on tissue punches of the VTA of adult mice using primers specific to mRNA of *unc5a-d* homologues. We found a robust amplification of *unc5c* cDNA, but also a faint *unc5d* band (Manitt *et al.*, 2010). In the present study, we now show, using in situ hybridization, that *unc5c* mRNA is expressed by most, if not all, adult VTA DA neurons. Furthermore, our laser dissection experiments revealed that the *unc5c,* but not *unc5d,* transcript is expressed by DA neurons of the VTA. *unc5d* mRNA expression in the VTA is exclusive to non-dopaminergic VTA neurons.

In this study we found that the patterns of *unc5c* mRNA and UNC5H protein expression within the VTA are almost identical; confirming that the UNC5H antiserum we have used in all our studies detects UNC5C protein in this region (Grant *et al.*, 2007; Yetnikoff *et al.*, 2007; Manitt *et al.*, 2010). Within this context, the

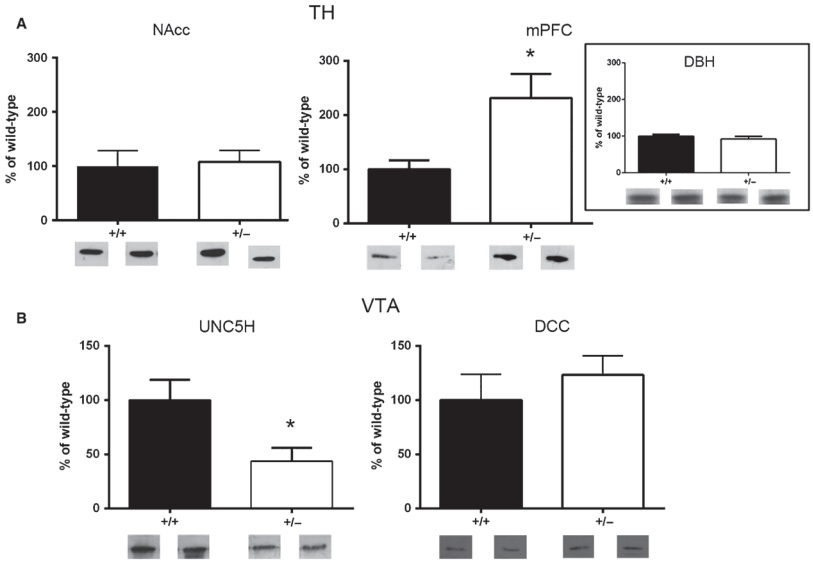

Figure 7. Increased Medial Prefrontal Cortex Tyrosine Hydroxylase Expression and Reduced Ventral Tegmental Area UNC5C Protein Expression In Adult Unc5c Heterozygous Mice.

Optical density data were converted to percent of the wild-type (+/+) group (100%). All data are presented as the mean ± SEM. (**A**) There is increased tyrosine hydroxylase (TH) protein expression in the medial prefrontal cortex (mPFC) of *unc5c* heterozygous (+/-) mice in comparison to +/+ controls, but no changes in TH expression within the nucleus accumbens (NAcc). Furthermore, expression of dopamine-β-hydroxylase (DBH) in the mPFC of +/- mice is unaltered relative to +/+ controls (inset). (**B**) There is reduced UNC5H protein in the ventral tegmental area (VTA) of *unc5c* +/- mice in comparison to +/+ controls, but no differences in DCC expression. Representative examples of western blots for *unc5c* +/- and +/+ groups are shown below the graphs. n = 4-9 mice per group.

significant reduction in UNC5H immunoreactivity we observed in the VTA of *unc5c* heterozygous mice relative to controls indicates that *unc5c* haploinsuffiency leads to reduced UNC5C protein expression.

A POTENTIAL ROLE FOR DCC/UNC5C RECEPTOR COMPLEXES IN DOPAMINE FUNCTION

We have shown previously that *dcc* heterozygous mice display blunted behavioral responses to amphetamine, including reduced drug-induced locomotion. This phenotype, which is associated with blunted amphetamine-induced DA release in the NAcc, is observed in adult, but not juvenile or adolescent mice (Grant *et al.*, 2007; Grant *et al.*, 2009; Yetnikoff *et al.*, 2010; Yetnikoff *et al.*, 2011). Similarly, here we show that *unc5c* heterozygous mice exhibit diminished amphetamine-induced locomotion and that this phenotype becomes evident in adulthood. Importantly, there are no compensatory changes in DCC or UNC5C expression in either *unc5c* or *dcc* mice (Grant *et al.*, 2007), indicating that reduction in DCC or UNC5C, alone, leads to the same age-dependent behavioral phenotype. This is intriguing considering that DCC and UNC5C receptors have been shown to mediate opposite responses during axonal guidance (Hong *et al.*, 1999; Keleman & Dickson, 2001). Notably, however, it has also been shown that certain functions, such as netrin-1-induced repulsion, can be mediated by both UNC5H alone and by DCC/UNC5H receptor complexes (Hong *et al.*, 1999; Keleman & Dickson, 2001).

Because from adolescence onwards single VTA DA neurons co-express DCC and UNC5C (Manitt *et al.*, 2010), it is possible that DCC/UNC5C receptor complexes play a role in the function of DA neurons, but only starting in adolescence. As such, a reduction in levels of these complexes caused by either *dcc* or *unc5c* haploinsufficiency, could potentially explain why both *dcc* and *unc5c* heterozygous mice show identical phenotypes and at the same developmental periods. Alternatively, both DCC and UNC5C receptors may modify the function of DA neurons, but via separate and perhaps independent mechanisms. To shed light into this issue, we are now beginning to conduct experiments aimed at determining the presence of DCC/UNC5C complexes within adult DA neurons. These studies will begin to address whether DCC/UNC5C receptor complexes are likely to participate in the critical effects of DCC on the adolescent maturation of the mesocortical DA circuitry (Manitt *et al.*, 2011).

It is important to note that, in addition to regulating neuronal connectivity, UNC5 homologues are also known to induce apoptosis (Llambi *et al.*, 2001; Williams *et al.*, 2006). Thus, our future investigations will also examine whether reduced UNC5C expression produces differences in DA cell number (Flores *et al.*, 2005).

PHENOTYPES IN *UNC5C* HETEROZYGOUS MICE: DOPAMINE OR OTHER TRANSMITTERS?

Previous work has shown *unc5c* mRNA expression within norepinephrine neurons in the locus coeruleus during embryonic development (Shi *et al.*, 2008). Moreover, changes in norepinephrine function, within the mPFC, have been shown to contribute to amphetamine-induced locomotion (Blanc *et al.*, 1994; Ventura *et al.*, 2003). Therefore, one could argue that the behavioral phenotype of adult *unc5c* mice may result from alterations in norepinephrine function. However, *unc5c* haploinsufficient mice show *a)* exaggerated levels of TH, but not DBH expression in the mPFC in adulthood and *b)* nearly identical phenotypes to those observed in *dcc* haploinsufficient mice, which is a model of altered DA development and function (Flores 2011; Manitt *et al.*, 2011). Thus, we propose that the behavioral changes observed in adult *unc5c* haploinsufficient mice are related to alterations in DA function specifically. Future stereological studies will address whether enhanced mPFC TH immunoreactivity in *unc5c* mutants results from an increase in the span of the DA innervation within this region, similar to what we observed in adult *dcc* heterozygotes (Manitt *et al.*, 2011). Nonetheless, we are currently examining the contributions of other neurotransmitter systems, including serotonin and glutamate, to the development of phenotypic traits of *unc5c* heterozygous mice.

CONCLUSIONS

UNC5C is a protein implicated in orchestrating assembly of neural circuits during development. Here we show that reduced expression of UNC5C leads to increased TH, but not DBH expression in the mPFC selectively and to blunted behavioral responses to stimulant drugs in adulthood. This novel finding raises the possibility that, like *dcc* haploinsufficiency, *unc5c* haploinsufficiency may confer resilience to the development of dopamine and behavioral abnormalities associated with schizophrenia and other psychiatric disorders (Flores, 2011; Grant *et al.*, 2012). These effects may be mediated by disruption in the function of DCC/UNC5C receptor complex during adolescence.

MATERIALS AND METHODS

ANIMALS

Mice heterozygous for a null mutation in the *unc5c* gene (B6.cg-*unc5c*$^{rcmTg(Ucp)1.23Kz/Slac}$) were obtained from Dr. S. Ackerman (The Jackson Laboratory; Ackerman *et al.*, 1997). The C57BL6 background was maintained by crossing *unc5c* heterozygous males with female C57BL6 wild-type mice. Mice were kept on a 12h light/dark cycle with *ad-libitum* access to water and food. All behavioral testing was conducted during the light phase of the cycle. Mice were weaned at postnatal day 21 (PND 21 ± 1) and housed with same-sex littermates. Different cohorts of *unc5c* heterozygotes and wild-type littermates were used for each experiment. Each cohort had mice from a minimum of 5 litters. In all the behavioral experiments we used both male and female mice. We conducted behavioral tests in separate groups of juvenile (postnatal day; PND 21 ± 1) and adult (PND 75 ± 15) mice, these ages are based on our previous developmental studies (Grant *et al.*, 2009; Manitt *et al.*, 2010; Yetnikoff *et al.*, 2011). The neuroanatomical experiments were conducted on C57BL6 wild-type male mice bred in our animal colony. All experiments were performed in accordance with the guidelines of Canadian Council of Animal Care. The experimental procedures were approved by the McGill University / Douglas Mental Health University Institute Animal Care Committee.

GENOTYPING

Mice were genotyped using primers against the mutant allele and the wild-type *unc5c* allele:

Mutant, 5'-CAGGAGAAGATACATTTAACCAC-3' and
5'-GACAGAAGAGCATAGCATTCAC-3';

Wild-type, 5'-CACTCTATGGAAATGGCTGAAT-3' and
5'-GTCCTCCAATCCAAGAACTG-3'.

DRUGS

d-amphetamine sulphate salt was dissolved in sterile 0.9% saline on the day of the experiment and injected i.p.

ANTIBODIES

The UNC5H antiserum was provided generously by Dr. Pawson (University of Toronto). This antibody was raised against a GST fusion protein containing the region between the ZU-5 and the death domain of UNC5C (residue 605-877). The region of UNC5C used to generate this antiserum shares high amino acid identity with the corresponding region of other mammalian UNC5 homologues. The specificity of the antiserum for UNC5C has previously been demonstrated with immunoprecipitation, western blot and immunostaining of HEK-293 cells transfected with *unc5c* cDNA. However, the antiserum also detects recombinant UNC5A and UNC5B by western blot (Manitt *et al.*, 2004). Our western blot experiments with tissue punches of rodent midbrain and forebrain regions indicate that this antiserum detects a single band of 135 kDa (Manitt *et al.*, 2010). The monoclonal DCC antibody (BD Pharmingen, Missisauga, ON Canada, Cat: 554223, Clone G97-449) was raised in mouse against the intracellular domain of recombinant human DCC. The antibody detects a single band of 185 kDa on western blots, consistent with the molecular weight of DCC (manufacturer's technical information). We have demonstrated the specificity of this DCC antibody previously by performing western blots on tissue lysates from newborn *dcc* knockout mice (Manitt *et al.*, 2010). The tyrosine hydroxylase (TH) antibody (Chemicon, Temecula, CA USA) was raised in rabbit against SDS-denatured TH from rat pheochromocytoma. It detects a single band of 60 kDa on western blot (manufacturer's technical information). The antibody labels DA cell bodies and terminals in wild-type mice, but not mice lacking TH protein. The monoclonal dopamine beta-hydroxylase (DBH) antibody (MediMabs, Montreal, QC Canada, Cat No.: MM-0008-P) was raised in mouse against rat DBH protein. This antibody detects two bands of 70 and 75 kDa that correspond to soluble and membrane-bound forms of the enzyme, respectively (manufacturer's technical information).

IN SITU HYBRIDIZATION

Adult wild-type mice were killed by decapitation and their brains were quickly dissected and flash-frozen in 2-methylbutane. Brains were sliced into 16 µm coronal sections using a cryostat and mounted onto Superfrost slides. Sense and antisense digoxigenin-labeled riboprobes against 582 bp of the cytoplasmic domain of the *unc5c* transcript were transcribed from a linearized plasmid provided by Dr. S. Ackerman (The Jackson Laboratory). SP6 and T7 RNA polymerases (Promega, Madison WI,

USA) were used to transcribe sense and antisense probes, respectively. Slices were fixed with 4% paraformaldehyde, underwent acetylation with triethanolamine and acetic anhydride, and were dehydrated in increasing concentrations of ethanol; these steps were conducted in RNAse-free conditions. Probes were then hybridized to the slices (200 ng/slide) for 18h at 56°C. After hybridization, slides were stringently washed in 4X SSC and 50X formamide for 30 min at 60°C, treated with RNAse A for 1 hr at 37°C and washed in decreasing concentrations of SSC. Sections were then processed for *unc5c* mRNA expression alone or for *unc5c* mRNA/TH co-expression. For mRNA detection alone, sections were incubated overnight with an anti-DIG antibody coupled to alkaline phosphatase (1:1000, Roche, Indianapolis IN, USA) and developed with NBT/BCIP solution for 10-20 hours. For the fluorescent co-labeling experiments, sections were incubated overnight with both an anti-DIG antibody coupled to horseradish peroxidase (1:1000, Roche, Indianapolis IN, USA) and an anti-TH antibody raised in rabbit (1:500, Chemicon, Temecula CA, USA). The following day, sections were incubated with tyramide coupled to Cy3, according to the manufacturer's instructions (Perkin Elmer, Waltham MA, USA) to reveal mRNA expression. Following this step, sections were incubated for 30 min with a goat anti-rabbit secondary antibody coupled to Alexa 488 (1:500) to reveal TH immunofluorescence.

IMMUNOHISTOCHEMISTRY

Adult male mice were anesthetized with an overdose of sodium pentobarbital (>75 mg/kg, i.p.) and were perfused intracardially with 0.9% saline, followed by a fixative solution (4% PFA in 0.1 m phosphate buffer, pH 7.5). Brains were sectioned at 35 µm on a vibratome. Free-floating sections were used immediately for immunohistochemical processing. Endogenous peroxidase was quenched with a solution of 0.3% hydrogen peroxide and 0.3% heat-inactivated goat serum in PBS, for 30 min. After a 1 hour incubation in blocking solution (2% bovine serum albumin, 0.2% Tween 20 in PBS at room temperature), sections were incubated in rabbit UNC5H antiserum (1:5000) for 48–72 h at 4˚C. Immunostaining was visualized with a peroxidase-conjugated donkey anti-rabbit secondary antibody and DAB kit (Vector Labs, Burlingame CA, USA).

LASER DISSECTION OF DA NEURONS AND UNC5 HOMOLOGUE RT-PCR

To assess *unc5c* and *unc5d* mRNA expression in adult DA neurons selectively, we used adult C57BL6 *Pitx3-GFP* mice (Zhao *et al.*, 2004). Adult *Pitx3-GFP* mice were deeply anesthetized and perfused intracardially with PBS, followed by a fixative solution (1% PFA in PBS) and by 20% sucrose in PBS. Brains were dissected, flash frozen, and stored at -80°C until use (Khodosevich *et al.*, 2007; Fenstermaker *et al.*, 2010). Coronal cryosections were cut (10µm) and mounted on MembraneSlides 1.0 PEN (Zeiss). Laser microdissection was performed on a PALM laser microscope system (Zeiss, Oberkochen, Germany). For each animal, approximately 1200 cells were isolated and laser catapulted into AdhesiveCap 200 opaque tubes (Zeiss, Oberkochen, Germany). RNA was then isolated immediately using a Qiagen RNeasy FFPE kit. Samples were incubated with Proteinase K overnight at 55°C for complete digestion and higher RNA yields. RNA was eluted in 20 µl of RNAse-free water and 2 µl were used for subsequent RT-PCR reactions using the one-step RT-PCR kit (Qiagen, Hilden, Germany). The following primers were used:

unc5c, 5'-ACCTGCGCCTGTCTATTCAT-3' and
5'-GGGCCAGCATCCTCCAGTCA-3';

unc5d, 5'-GCCTGTCACGTGCTGCTTGA-3' and 5'-
TCGTGTGTGTCCTCCCAATC-3'.

RT-PCR amplification was conducted at the following temperatures and times: 50°C for 30 min; 95°C for 15 min; 94°C for 1 min, 56°C for 1 min, 72°C for 1 min for 42 cycles; 72°C for 10 min. PCR products were separated on a 1.5% agarose-ethidium bromide gel. Both primer pairs yielded positive signals following RT-PCR on embryonic whole brain mRNA.

LOCOMOTOR ACTIVITY

Locomotor activity was quantified using an infrared activity-monitor apparatus modified for use with mice (AccuScan Instruments, Columbus, OH USA), as previously done in our laboratory (Grant *et al.*, 2007; Grant *et al.*, 2009; Yetnikoff *et al.*, 2010). Data are expressed as total distance traveled in cm in a given period of time. Stereotypy was measured as the number of repeated breaks of one or more photocell

beams when the animal is not locomoting, but engaging in repetitive movements (Yetnikoff *et al.*, 2011). Although this automated system cannot distinguish between head bobbing, sniffing, grooming, and other stereotypic movements, other research groups have validated that the measure reflects total stereotypy (Pierce & Kalivas, 2007). *Procedure:* On day 1, mice were placed in the activity boxes and their locomotion was recorded for 15 min. On the day 2, mice were placed in the activity boxes for a 15-min habituation period and their locomotor activity was then measured for 30 min following an i.p. injection of 0.9% saline. On day 3, following a 15 min period of habituation, mice were given an i.p. injection of amphetamine and their locomotor was measured for 90 min. At both ages, male mice were given a dose of 2.5 mg/kg and female mice were given a dose of 2.2 mg/kg. The experimental procedure and doses of amphetamine are identical to those used in our previous studies with *dcc* heterozygous mice (Grant *et al.*, 2007; Grant *et al.*, 2009) The doses of amphetamine given to males and female mice were adjusted in order to produce equivalent concentrations of drug in the brain (Castner *et al.*, 1993; Becker *et al.*, 2001).

WESTERN BLOTTING

Western blot experiments were conducted as previously (Grant *et al.*, 2007; Grant *et al.*, 2009; Yetnikoff *et al.*, 2011). Briefly, brains of adult wild-type and *unc5c* heterozygous mice were flash-frozen in 2-methylbutane and sectioned into 800 µm slices. Bilateral tissue punches were taken from the VTA, nucleus accumbens (NAcc), including the core and shell, and mPFC, including cingulate areas 1 and 2, using a 0.5-mm diameter punch. Sections corresponded to Plates 15 and 55 of the Paxinos and Franklin's mouse brain atlas (Franklin & Paxinos, 2007). Protein samples (25 µg) were separated using SDS-PAGE and transferred to a nitrocellulose membrane, which was incubated with rabbit anti-TH antibody (1:5000), mouse anti-DBH antibody (1:100), the rabbit anti-UNC5H antiserum (1:4000), or mouse anti-DCC antibody (1:1000). Immunoreactivity was visualized following incubation with horseradish peroxidase-conjugated secondary antibodies using a chemiluminescence reagent (Perkin Elmer, Waltham MA, USA). Protein expression was normalized to total protein loaded in each lane as determined by ponceau-S staining (Sigma Aldrich, St. Louis, MO USA; Romero-Calvo *et al.*, 2010; Yetnikoff *et al.*, 2011; Argento *et al.*, 2012).

STATISTICAL ANALYSIS

Locomotor Activity: Differences in total distance traveled between *unc5c* heterozygous and wild-type mice were analyzed using two-way repeated measures ANOVAs with genotype as the between-group variable, and time (min) as the within-group variable. Post-hoc analyses of significant interactions were decomposed using ANOVA tests for simple effects. Student's *t*-tests for independent samples were used to analyze differences in stereotypy counts between groups.

Western Blot analysis: Raw data (optical density of scanned immunoblots) were normalized to Ponceau-S staining to correct for differences in loading. Differences in protein expression between *unc5c* heterozygous and wild-type mice were analyzed on the normalized data using Student's *t*-tests for independent samples.

ACKNOWLEDGEMENTS

We would like to thank Dr S. Ackerman (Jackson Laboratory) for providing the original *unc5c* heterozygous breeders and the in situ hybridization probe, Dr T. Pawson (University of Toronto) for the UNC5H antiserum, and Dr. L. Yetnikoff for critical reading of the manuscript. The *Pitx3-GFP* mice were provided by Dr. Meng Li (Imperial College London, UK). The Natural Sciences and Engineering Research Council of Canada, the Canadian Institutes for Health Research, the Fonds de la Recherché en Santé du Québec, and the Netherlands Organization for Scientific Research Top Talent Program, FP7 funded this work. The authors have no conflicts of interest to report.

REFERENCES

Abi-Dargham, A., van de Giessen, E., Slifstein, M., Kegeles, L.S. & Laruelle, M. (2009) Baseline and amphetamine-stimulated dopamine activity are related in drug-naive schizophrenic subjects. Biol. Psychiatry, 65, 1091-1093.

Ackerman, S.L., Kozak, L.P., Przyborski, S.A., Rund, L.A., Boyer, B.B. & Knowles, B.B. (1997) The mouse rostral cerebellar malformation gene encodes an UNC-5-like protein. Nature, 386, 838-842.

Akil, M., Pierri, J.N., Whitehead, R.E., Edgar, C.L., Mohila, C., Sampson, A.R. & Lewis, D.A. (1999) Lamina-specific alterations in the dopamine innervation of the prefrontal cortex in schizophrenic subjects. Am. J. Psychiatry, 156, 1580-1589.

Argento, J.K., Arvanitogiannis, A. & Flores, C. (2012) Juvenile exposure to methylphenidate reduces cocaine reward and alters netrin-1 receptor expression in adulthood. Behav. Brain Res., 229, 202-207.

Barallobre, M.J., Pascual, M., Del Rio, J.A. & Soriano, E. (2005) The Netrin family of guidance factors: emphasis on Netrin-1 signalling. Brain Res. Brain Res. Rev., 49, 22-47.

Becker, J.B., Molenda, H. & Hummer, D.L. (2001) Gender differences in the behavioral responses to cocaine and amphetamine. Implications for mechanisms mediating gender differences in drug abuse. Ann. N.Y. Acad. Sci., 937, 172-187.

Blanc, G., Trovero, F., Vezina, P., Herve, D., Godeheu, A.M., Glowinski, J. & Tassin, J.P. (1994) Blockade of prefronto-cortical alpha 1-adrenergic receptors prevents locomotor hyperactivity induced by subcortical D-amphetamine injection. Eur. J. Neurosci, 6, 293-298.

Boksa, P. (2010) Effects of prenatal infection on brain development and behavior: a review of findings from animal models. Brain Behav. Immun., 24, 881-897.

Bouchard, J.F., Moore, S.W., Tritsch, N.X., Roux, P.P., Shekarabi, M., Barker, P.A. & Kennedy, T.E. (2004) Protein kinase A activation promotes plasma membrane insertion of DCC from an intracellular pool: A novel mechanism regulating commissural axon extension. J. Neurosci., 24, 3040-3050.

Breier, A., Su, T.P., Saunders, R., Carson, R.E., Kolachana, B.S., de Bartolomeis, A., Weinberger, D.R., Weisenfeld, N., Malhotra, A.K., Eckelman, W.C. & Pickar, D. (1997) Schizophrenia is associated with elevated amphetamine-induced synaptic dopamine concentrations: evidence from a novel positron emission tomography method. Proc. Nat. Acad. Sci. U.S.A., 94, 2569-2574.

Castner, S.A., Xiao, L. & Becker, J.B. (1993) Sex differences in striatal dopamine: in vivo microdialysis and behavioral studies. Brain Res., 610, 127-134.

Chao, D.L., Ma, L. & Shen, K. (2009) Transient cell-cell interactions in neural circuit formation. Nat Rev Neurosci, 10, 262-271.

Colon-Ramos, D.A., Margeta, M.A. & Shen, K. (2007) Glia promote local synaptogenesis through UNC-6 (netrin) signaling in C. elegans. Science, 318, 103-106.

Dougalis, A.G., Matthews, G.A.C., Bishop, M.W., Brischoux, F., Kobayashi, K & Ungless, M.A. (2012) Functional properties of dopamine neurons and co-expression of vasoactive intestinal polypeptide in the dorsal raphe nucleus and ventro-lateral periaqueductal grey. Eur. J. Neurosci. 36, 3322-3332.

Evans, A.H., Pavese, N., Lawrence, A.D., Tai, Y.F., Appel, S., Doder, M., Brooks, D.J., Lees, A.J. & Piccini, P. (2006) Compulsive drug use linked to sensitized ventral striatal dopamine transmission. Ann. Neurol., 59, 852-858.

Fenstermaker, A.G., Prasad, A.A., Bechara, A., Adolfs, Y., Tissir, F., Goffinet, A., Zou, Y. & Pasterkamp, R.J. (2010) Wnt/planar cell polarity signaling controls the anterior-posterior organization of monoaminergic axons in the brainstem. J. Neurosci., 30, 16053-16064.

Flores, C. (2011) Role of netrin-1 in the organization and function of the mesocorticolimbic dopamine system. J. Psychiatry Neurosci., 36, 296-310.

Flores, C., Manitt, C., Rodaros, D., Thompson, K.M., Rajabi, H., Luk, K.C., Tritsch, N.X., Sadikot, A.F., Stewart, J. & Kennedy, T.E. (2005) Netrin receptor deficient mice exhibit functional reorganization of dopaminergic systems and do not sensitize to amphetamine. Mol. Psychiatry, 10, 606-612.

Franklin, K.B.J. & Paxinos, G. (2007). The mouse brain in stereotaxic co-ordinates. Amsterdam: Elsevier.

Grant, A., Fathalli, F., Rouleau, G., Joober, R. & Flores, C. (2012) Association between schizophrenia and genetic variation in DCC: A case-control study. Schiz. Res., 137, 26-31.

Grant, A., Hoops, D., Labelle-Dumais, C., Prevost, M., Rajabi, H., Kolb, B., Stewart, J., Arvanitogiannis, A. & Flores, C. (2007) Netrin-1 receptor-deficient mice show enhanced mesocortical dopamine transmission and blunted behavioural responses to amphetamine. Eur. J. Neurosci., 26, 3215-3228.

Grant, A., Speed, Z., Labelle-Dumais, C. & Flores, C. (2009) Post-pubertal emergence of a dopamine phenotype in netrin-1 receptor-deficient mice. Eur. J. Neurosci., 30, 1318-1328.

Hong, K., Hinck, L., Nishiyama, M., Poo, M.M., Tessier-Lavigne, M. & Stein, E. (1999) A ligand-gated association between cytoplasmic domains of UNC5 and DCC family receptors converts netrin-induced growth cone attraction to repulsion. Cell, 97, 927-941.

Howes, O.D., Kambeitz, J., Kim, E., Stahl, D., Slifstein, M., Abi-Dargham, A. & Kapur, S. (2012) The Nature of Dopamine Dysfunction in Schizophrenia and What This Means for Treatment: Meta-analysis of Imaging Studies. Arch. Gen. Psychiatry. 69, 776-786.

Hutchins, B.I. & Kalil, K. (2008) Differential outgrowth of axons and their branches is regulated by localized calcium transients. J. Neurosci, 28, 143-153.

Keleman, K. & Dickson, B.J. (2001) Short- and long-range repulsion by the Drosophila Unc5 netrin receptor. Neuron, 32, 605-617.

Khodosevich, K., Inta, D., Seeburg, P.H. & Monyer, H. (2007) Gene expression analysis of in vivo fluorescent cells. PloS one, 2, e1151.

Leyton, M. (2007) Conditioned and sensitized responses to stimulant drugs in humans. Prog. Neuropsychopharmacol. Biol. Psychiatry, 31, 1601-1613.

Lieberman, J.A., Kane, J.M. & Alvir, J. (1987) Provocative tests with psychostimulant drugs in schizophrenia. Psychopharmacol., 91, 415-433.

Llambi, F., Causeret, F., Bloch-Gallego, E. & Mehlen, P. (2001) Netrin-1 acts as a survival factor via its receptors UNC5H and DCC. EMBO J., 20, 2715-2722.

Manitt, C. & Kennedy, T.E. (2002) Where the rubber meets the road: netrin expression and function in developing and adult nervous systems. Prog. Brain Res., 137, 425-442.

Manitt, C., Labelle-Dumais, C., Eng, C., Grant, A., Mimee, A., Stroh, T. & Flores, C. (2010) Peri-pubertal emergence of UNC-5 homologue expression by dopamine neurons in rodents. PloS one, 5, e11463.

Manitt, C., Mimee, A., Eng, C., Pokinko, M., Stroh, T., Cooper, H.M., Kolb, B. & Flores, C. (2011) The netrin receptor DCC is required in the pubertal organization of mesocortical dopamine circuitry. J. Neurosci., 31, 8381-8394.

Manitt, C., Nikolakopoulou, A.M., Almario, D.R., Nguyen, S.A. & Cohen-Cory, S. (2009) Netrin participates in the development of retinotectal synaptic connectivity by modulating axon arborization and synapse formation in the developing brain. J. Neurosci, 29, 11065-11077.

Manitt, C., Thompson, K.M. & Kennedy, T.E. (2004) Developmental shift in expression of netrin receptors in the rat spinal cord: predominance of UNC-5 homologues in adulthood. J. Neurosci Res., 77, 690-700.

Meyer-Lindenberg, A., Miletich, R.S., Kohn, P.D., Esposito, G., Carson, R.E., Quarantelli, M., Weinberger, D.R. & Berman, K.F. (2002) Reduced prefrontal activity predicts exaggerated striatal dopaminergic function in schizophrenia. Nature Neurosci., 5, 267-271.

Muramatsu, R., Nakahara, S., Ichikawa, J., Watanabe, K., Matsuki, N. & Koyama, R. (2010) The ratio of 'deleted in colorectal cancer' to 'uncoordinated-5A' netrin-1 receptors on the growth cone regulates mossy fibre directionality. Brain, 133, 60-75.

Osborne, P.B., Halliday, G.M., Cooper, H.M. & Keast, J.R. (2005) Localization of immunoreactivity for deleted in colorectal cancer (DCC), the receptor for the guidance factor netrin-1, in ventral tier dopamine projection pathways in adult rodents. Neuroscience, 131, 671-681.

Pierce, R.C. & Kalivas, P.W. (2007) Locomotor behavior. Current protocols in neuroscience / editorial board, Jacqueline N. Crawley et al., Chapter 8, Unit 8.1.

Poon, V.Y., Klassen, M.P. & Shen, K. (2008) UNC-6/netrin and its receptor UNC-5 locally exclude presynaptic components from dendrites. Nature, 455, 669-673.

Romero-Calvo, I., Ocon, B., Martinez-Moya, P., Suarez, M.D., Zarzuelo, A., Martinez-Augustin, O. & de Medina, F.S. (2010) Reversible Ponceau staining as a loading control alternative to actin in Western blots. Anal. Biochem., 401, 318-320.

Shi, M., Guo, C., Dai, J.X. & Ding, Y.Q. (2008) DCC is required for the tangential migration of noradrenergic neurons in locus coeruleus of mouse brain. Mol. and Cell. Neurosci, 39, 529-538.

Srour, M., Riviere, J.B., Pham, J.M., Dube, M.P., Girard, S., Morin, S., Dion, P.A., Asselin, G., Rochefort, D., Hince, P., Diab, S., Sharafaddinzadeh, N., Chouinard, S., Theoret, H., Charron, F. & Rouleau, G.A. (2010) Mutations in DCC cause congenital mirror movements. Science, 328, 592.

Tong, J., Killeen, M., Steven, R., Binns, K.L., Culotti, J. & Pawson, T. (2001) Netrin stimulates tyrosine phosphorylation of the UNC-5 family of netrin receptors and induces Shp2 binding to the RCM cytodomain. J Biol Chem, 276, 40917-40925.

Tseng, K.Y., Chambers, R.A. & Lipska, B.K. (2009) The neonatal ventral hippocampal lesion as a heuristic neurodevelopmental model of schizophrenia. Behav. Brain Res., 204, 295-305.

Ventura, R., Cabib, S., Alcaro, A., Orsini, C. & Puglisi-Allegra, S. (2003) Norepinephrine in the prefrontal cortex is critical for amphetamine-induced reward and mesoaccumbens dopamine release. J. Neurosci, 23, 1879-1885.

Vezina, P. (2004) Sensitization of midbrain dopamine neuron reactivity and the self-administration of psychomotor stimulant drugs. Neurosci. Biobehav. Rev., 27, 827-839.

Williams, M.E., Lu, X., McKenna, W.L., Washington, R., Boyette, A., Strickland, P., Dillon, A., Kaprielian, Z., Tessier-Lavigne, M. & Hinck, L. (2006) UNC5A promotes neuronal apoptosis during spinal cord development independent of netrin-1. Nature Neurosci., 9, 996-998.

Yetnikoff, L., Almey, A., Arvanitogiannis, A. & Flores, C. (2011) Abolition of the behavioral phenotype of adult netrin-1 receptor deficient mice by exposure to amphetamine during the juvenile period. Psychopharmacology (Berl.), 217, 505-514.

Yetnikoff, L., Eng, C., Benning, S. & Flores, C. (2010) Netrin-1 receptor in the ventral tegmental area is required for sensitization to amphetamine. Eur. J. Neurosci., 31, 1292-1302.

Yetnikoff, L., Labelle-Dumais, C. & Flores, C. (2007) Regulation of netrin-1 receptors by amphetamine in the adult brain. Neurosci., 150, 764-773.

Yetnikoff, L., Pokinko, M., Arvanitogiannis, A. & Flores, C. (2013) Adolescence: a time of transition for the phenotype of dcc heterozygous mice. Psychopharmacol. (Berl.) In Press.

Zhao, S., Maxwell, S., Jimenez-Beristain, A., Vives, J., Kuehner, E., Zhao, J., O'Brien, C., de Felipe, C., Semina, E. & Li, M. (2004) Generation of embryonic stem cells and transgenic mice expressing green fluorescence protein in midbrain dopaminergic neurons. Eur. J. Neurosci., 19, 1133-1140.

'Only as an aesthetic product can the world be justified to all eternity.'

- Friedrich Nietzsche

Chapter 5

Transgenic Strategy for Analyzing Midbrain Dopamine Neuron Diversity

Ewoud R. E. Schmidt. Sara Brignani, Jitte Groothuis, Marieke Martens, and R. Jeroen Pasterkamp

Department of Translational Neuroscience, Brain Center Rudolf Magnus, University Medical Center Utrecht, Universiteitsweg 100, 3584 CG, Utrecht, the Netherlands

ABSTRACT

The mesodiencephalic dopamine (mdDA) system is composed of a heterogeneous group of dopamine neurons which control cognitive and motor behavior. However, the molecular mechanisms underlying development and function of different neuronal subsets in the mdDA system remain largely unknown. To address these questions we designed a genetic strategy, called *Pitx3-ITC*, which relies on subset-specific Cre or Flp expression for labeling two mdDA subsets in a single mouse. In addition, we generated *Nrp2-FlpO* and *Gucy2c-Cre* mice which, in combination with *Pitx3-ITC* mice, sparsely label mdDA neurons. Initial characterization of these mice reveals previously unknown axonal organization of mdDA subsets, as well as characteristic, but poorly understood, connectivity patterns at both the pre- and postsynaptic level. The ability to differentially label two mdDA subsets in a single mouse and to visualize mdDA neurons at a single-cell level, offers a unique opportunity for studying the function and development of the mdDA system.

INTRODUCTION

A key feature of the central nervous system (CNS) is its organization into distinct brain areas. These functionally distinct brain regions are composed of heterogeneous groups of neurons necessary to accommodate different aspects of behavior. For example, retinal ganglion cells (RGCs) of the mouse retina are grouped together in the ganglion cell layer. Although they share the same functionality as being output neurons of the retina, approximately 20 different RGC subtypes have been identified (Kim et al., 2010). Each RGC type encodes a different aspect of visual information, such as movement or luminosity, which is determined by differences in their synaptic input (Masland, 2012). Similar organizational features are present in other parts of the CNS, such as the cortex, striatum, and olfactory system (Ding et al., 2012; Molyneaux et al., 2007; Sakano, 2010). The functional properties of brain regions are largely determined by the organization of their neuronal subsets and the precise pattern of pre- and postsynaptic connectivity. Hence, understanding how neuronal subsets develop and how subset-specific connectivity is established is crucial for unraveling the complex workings of the brain. However, our knowledge on the molecular mechanisms controlling subset-specific wiring is rather limited.

A striking example of a brain region where heterogeneity is crucial for coordinating complex physiological and cognitive functions is the mesodiencephalic dopamine (mdDA) system. The mdDA system consists of dopamine neurons grouped together in the ventral midbrain and plays a critical role in voluntary movement and motivational control. As such, it has been implicated in both neurological and neuropsychiatric diseases such as Parkinson's disease, depression, schizophrenia, and drug addiction (Björklund and Dunnett, 2007a; Bromberg-Martin et al., 2010; Dunlop and Nemeroff, 2007; Iversen and Iversen, 2007; Sesack and Carr, 2002; Sulzer, 2007). Although neurons within the mdDA system share the same neurotransmitter phenotype, heterogeneity is apparent in both its structure and connectivity. Midbrain dopamine neurons are organized into distinct anatomical groups of neurons, the substantia nigra (SNc) and ventral tegmental area (VTA), which give rise to different patterns of connectivity. Axons from the SNc form the mesostriatal pathway, which extensively innervates the dorsal striatum and is involved in control of voluntary movement. The VTA projects to the ventromedial striatum and medial prefrontal cortex, giving rise to the mesocorticolimbic pathway, and plays an important role in

regulating emotion and reward (Björklund and Dunnett, 2007b; Van den Heuvel and Pasterkamp, 2008). The heterogeneous nature of the system is also apparent in different neurological and psychiatric disorders, such as Parkinson's disease where neurons in the SNc selectively degenerate, leading to severe deficits in motor control (Sulzer, 2007). Insights into the heterogeneity of the mdDA system, including the ongoing identification and characterization of new DA neuronal subtypes (Chung et al., 2005; Greene et al., 2005; Simeone et al., 2011), has provided a valuable framework for investigating how this brain region controls cognitive and motor behaviors (Ikemoto, 2007; Roeper, 2013). However, the mechanisms underlying development of these neuronal subsets are still poorly understood (Van den Heuvel and Pasterkamp, 2008; Smidt and Burbach, 2007).

Studies on the development of mdDA subsets have been hampered by the lack of tools to selectively identify and label these neurons. Progress has been made by studying transgenic mouse lines, *e.g. CCK-Cre* and *Otx2-Cre* mice, in which specific subsets are targeted (Fossat et al., 2006; Di Salvio et al., 2010a; Taniguchi et al., 2011; Veenvliet et al., 2013). However, expression in these lines is not confined to mdDA neurons, making experiments such as axon tract tracing cumbersome. Furthermore, these lines label single mdDA subsets, preventing studies on how development of subsets is differentially regulated and whether interaction between different subsets is required for proper development. This has precluded in-depth studies on the formation of the mdDA system, including migration, subset-specific axon pathfinding and dendritic development. The latter being even more challenging, since it requires sparse subset-specific labeling of neurons for proper visualization of individual dendrites.

To address these issues, we designed a genetic strategy, called ITC (IFP/tdTomato/Citrine), which combines the widely used Cre/*lox* and Flp/*frt* recombination system with selective expression of different fluorescent proteins. This approach enables Cre-dependent expression of tdTomato or Flp-dependent expression of Citrine in mdDA neurons and allows for specific labeling of two mdDA subsets in a single mouse. Furthermore, in our attempt to develop subset-specific Cre and Flp lines, we generated mice which label mdDA neurons in a highly sparse manner, enabling the in-depth study of features such as dendritic development and axonal arborization. Taken together, the ITC strategy offers a unique approach towards unraveling the complex cellular and molecular mechanisms underlying mdDA subset development.

RESULTS

STRATEGY FOR SUBSET-SPECIFIC LABELING OF MDDA NEURONS

The Cre/*loxP* and Flp/*frt* systems have been widely used in mammals to drive expression of fluorescent markers into specific cell types (Branda and Dymecki, 2004). We devised an approach which combines these two systems to enable specific labeling of neuronal subsets with different fluorescent proteins in one mouse. Figure 1A illustrates the design of this construct, termed ITC (IFP/tdTomato/Citrine), which incorporates two *loxP* sites, two *frt* sites and three genes encoding three

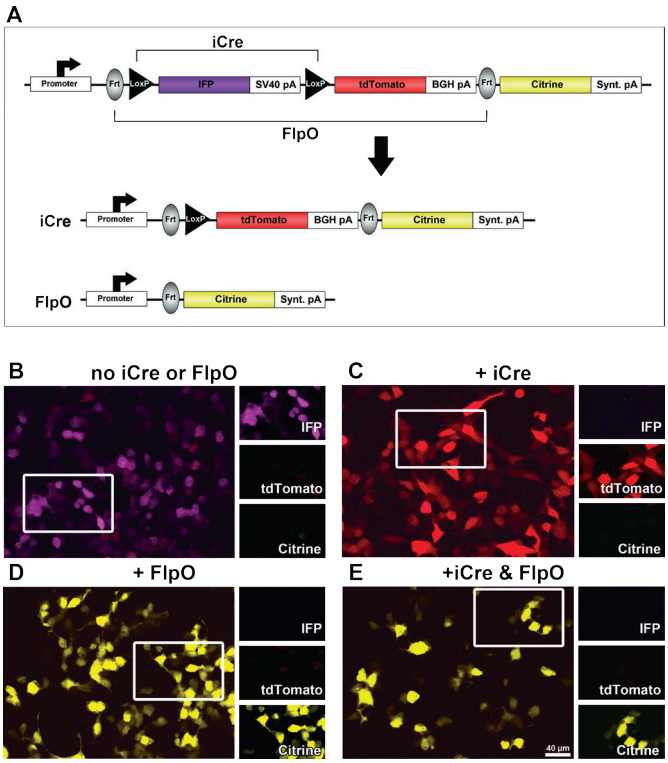

Figure 1. Cre/Flp Dependent Expression of Specific Fluorophore.

(**A**) Schematic of ITC. Without the presence of Cre or Flp, expression of IFP is induced, while the *SV40 pA* signal prevents expression of downstream tdTomato. Recombination of *loxP* sites by Cre results in removal of IFP and activation of tdTomato. Alternatively, recombination of *frt* sites by Flp removes both IFP and tdTomato resulting in expression of Citrine.

(**B**-**D**) HEK 293 cells were transfected with *CMV-ITC* and express IFP, but not tdTomato or Citrine (**B**). Co-transfection with iCre results in expression of tdTomato (**C**), while co-transfection with FlpO results in expression of Citrine (**D**). Combined expression of ITC, iCre and FlpO results in expression of Citrine (**E**). Boxed areas are shown as separate channels at the right.

different fluorescent proteins. Each gene is followed by a unique stop codon which prevents expression of the next gene located downstream. The first gene, encoding Infrared Fluorescent Protein (*IFP*; Shu et al., 2009), is expressed in all cells where the promoter is active. IFP is flanked by two *loxP* sites, while IFP and tdTomato (Shaner et al., 2004) together are flanked by two *frt* sites. Cre-mediated recombination of the *loxP* sites leads to excision of IFP and in turn activates tdTomato, while Flp-mediated recombination of *frt* sites leads to excision of both IFP and tdTomato and subsequently activates Citrine (Griesbeck et al., 2001). Since Flp-mediated recombination removes IFP and tdTomato, the presence of both Cre and Flp does not result in double labeling of cells.

Transfection of the ITC construct in HEK 293 cells resulted in expression of IFP without expression of tdTomato or Citrine (Figure 1B). Cells that were co-transfected with both improved Cre (iCre; Shimshek et al., 2002) and ITC showed no expression of IFP and instead cells expressed tdTomato (Figure 1C). Cells co-transfected with ITC and a codon optimized version of Flp (FlpO; Raymond and Soriano, 2007) also did not express IFP but showed expression of Citrine (Figure 1D). As expected from the configuration of *loxP* and *frt* sites in the ITC construct, combining Flp and Cre resulted in expression of Citrine only, without expression of IFP or tdTomato (Figure 1E).

Thus, differential labeling of cells from a single construct can be achieved, with the fluorescent label being determined by either Cre or Flp. Furthermore, double labeling of cells is prevented due to the arrangement of *loxP* and *frt* sites, with Flp ultimately determining Citrine expression.

CRE/FLP-DEPENDENT LABELING OF MDDA NEURONS *IN VIVO*

Our ITC strategy relies on expression of ITC specifically in mdDA neurons. Within the CNS, mdDA neurons can be recognized specifically by the expression of *Pitx3*. This transcription factor is important for proper development of mdDA neurons and is first detected at E11.5, correlating with the first appearance of these neurons (Smidt et al., 1997). Because of this early and specific localization, we selected the *Pitx3* promoter for driving expression of ITC in mdDA neurons.

Pitx3-ITC mice were generated using a BAC mediated transgenesis approach (Gong et al., 2002). As expected, *Pitx3-ITC* mice did not express tdTomato or Citrine. However, we were unable to detect IFP expression (not shown). Since

expression levels *in vivo* may be much lower than observed in HEK 293 cells, our inability to detect IFP might be due to limitations of our confocal setup as excitation by our 635 nm laser only results in approximately 50% emission intensity. In addition, IFP fluorescence relies on the incorporation of biliverdine (BV) into the fluorophore. Although the endogenous concentration of BV is sufficient to induce fluorescence, intravenous injections of BV can increase this fluorescence by about fivefold and may reveal IFP expression in our *Pitx3-ITC* mice (Shu et al., 2009). To determine whether we could obtain Cre-induced expression of tdTomato or Flp-induced expression of Citrine in mdDA neurons, we crossed *Pitx3-ITC* mice with *EIIa-Cre* (Lakso and Pichel, 1996) or *ACTB-FlpE* mice (Rodríguez et al., 2000). Both lines express their transgene under control of a ubiquitous promoter, resulting in complete germline excision of *loxP* or *frt* flanked sequences. This enabled us to identify which cells express the ITC transgene as well as determine the ability of Cre and Flp to induce expression of tdTomato or Citrine. Dopamine neurons were identified by immunohistochemistry for tyrosine hydroxylase (TH), the rate-limiting enzyme in dopamine synthesis. Analysis of adult animals positive for both ITC and FlpE showed expression of Citrine in 3 out of 4 lines, which was limited to a subset of mdDA neurons (Figure 2A, B). Most SNc neurons were positive for Citrine, while only the ventrolateral portion of the VTA showed expression of Citrine. This pattern of expression was similar in all lines, with the exception of line #4, in which labeling was more confined to the SNc with almost no positive neurons present within the VTA (not shown). As expected, crossing of *Pitx3-ITC* and *EIIa-Cre* mice resulted in expression of tdTomato in the same set of neurons as observed following *ACTB-FlpE* crosses (Figure 2A, C). Because of this identical expression pattern, subsequent analysis of *Pitx3-ITC* mice was done using *ACTB-FlpE:Pitx3-ITC* mice. The lateral distribution of labeled mdDA neurons was also observed during embryonic (E16.5) and postnatal (P5) development (Figure 2D). A small number of labeled neurons were detected medially at E16.5. This number decreased over time, with only a few labeled neurons present at P5 (Figure 2E). Although most other brain areas were devoid of Citrine, few non-dopaminergic neurons were detected caudally of the VTA and in layer V/VI of the cortex (Figure 2F, G). No expression of *Pitx3* has been reported in these regions, although a previous report on the generation of a *Pitx3-Cre* knock-in animals described the same groups of neurons to be positive for their transgene (Smidt et al., 2012). These neurons may belong to an as of yet

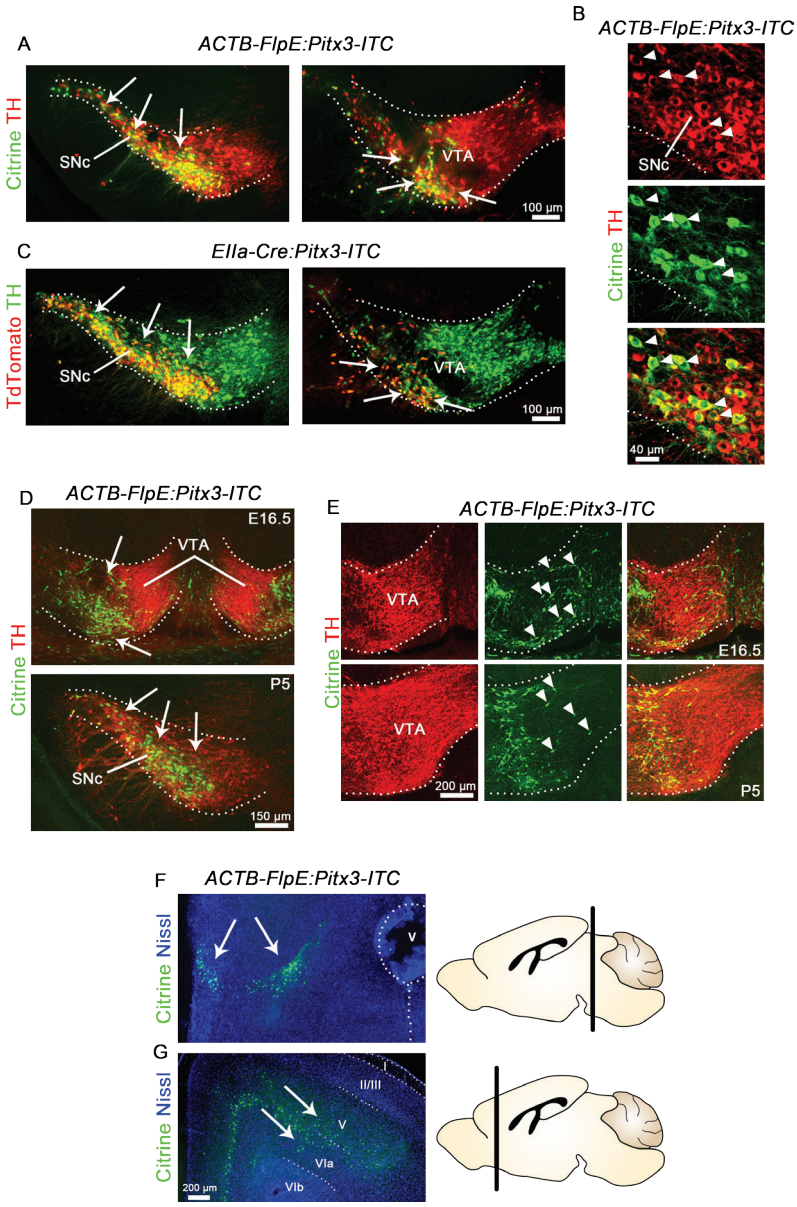

Figure 2. *Pitx3-ITC* Mice Label a Subset of Mesodiencephalic (mdDA) Neurons.

(**A-C**) Immunohistochemistry for tdTomato, Citrine, and tyrosine hydroxylase (TH) on adult *ACTB-FlpE:Pitx3-ITC* (**A, B**) and *EIIa-Cre:Pitx3-ITC* (**C**) coronal brain sections. Neurons are labeled within the substantia nigra pars compacta (SNc) and lateral part of the ventral tegmental area (VTA) (white arrows; **A, B**) and labeling is specific for TH-positive neurons (arrowheads; **B**).

(**D** and **E**) Immunohistochemistry for Citrine and TH on coronal sections of E16.5 and P5 *ACTB-FlpE:Pitx3-*

unidentified group of *Pitx3* expressing neurons, or may indicate that an unknown regulatory element in one of the first exons, which gets disturbed in both *Pitx3-ITC* and *Pitx3-Cre* mice, normally suppresses expression of *Pitx3* in these neurons.

Thus, our ITC strategy allows for Cre-dependent tdTomato or Flp-dependent Citrine expression specifically in the SNc and ventrolateral VTA neurons at developmental stages and during adulthood.

ANALYSIS OF MDDA SUBSET DEVELOPMENT USING *PITX3-ITC* MICE

Since *Pitx3-ITC* mice show expression of ITC in many but not all dopamine neurons of the mdDA system, we characterized which of the known targets innervated by these neurons contain Citrine-positive fibers. A prominent target of SNc neurons is the dorsal striatum, where axons extensively branch to make numerous synaptic contacts (Matsuda et al., 2009; Prensa and Parent, 2001). In *ACTB-FlpO:Pitx3-ITC* mice we observed a dense innervation of the dorsal striatum by Citrine-positive fibers (Figure 3A). Using TH immunohistochemistry we confirmed all these fibers to be dopaminergic (Figure 3D), indicating that these projections were originating from the mdDA system and did not stem from the small population of non-dopaminergic neurons in the cortex or hindbrain. Similar innervation patterns were found in *EIIa-Cre:Pitx3-ITC* animals (Figure 3C), confirming the ability of ITC expressing axons to switch between Citrine or tdTomato expression depending on the presence of Cre or Flp. Besides a diffuse and widespread innervation of Citrine-positive fibers, we also observed patches of more intense clustering of fibers (Figure 3A, A", B, B'). This type of innervation has been described as an important feature of the compartmentalized makeup and connectivity pattern of the striatum (Snyder-Keller, 1991; Voorn et al., 1988). In the ventral striatum less prominent innervation of Citrine-positive fibers was observed, as expected from the minimal amount of VTA neurons that express ITC. Still, similar patches of innervation were found in both the nucleus accumbens (Figure 3B, B') and the olfactory tubercle, though in this latter structure the patches were visibly smaller (Figure 3B, B"). Subset-specific wiring of the mdDA system

ITC coronal brain sections. Labeled neurons are present within the developing SNc (white arrows, **D**) and VTA (arrowheads, **E**).

(**F** and **G**) Immunohistochemistry for Citrine and counterstained with Nissl on adult *ACTB-FlpE:Pitx3-ITC* coronal brain sections. A small group of Citrine-positive neurons is detected in the hindbrain (white arrows; **F**) and layer V/VI of the cortex (white arrows; **G**). Position of sections is indicated in the adjacent mouse brain schematic.

begins around E16.5, when mdDA axons are innervating the dorsal and ventral striatum (Torigoe et al., 2013). However, the molecular mechanisms underlying the development of this subset-specific connectivity are still poorly understood. To assess whether we could study the development of mdDA connectivity with our *Pitx3-ITC* mice, we analyzed the expression of ITC during embryonic and postnatal development. At E16.5, Citrine-positive fibers innervated the striatum, though the patch-like innervation pattern observed at adult stages was not yet established (Figure 3D). At P5, this innervation was increased and a patch-like pattern was clearly observed throughout the striatum (Figure 3E).

Dopaminergic projections traveling towards the forebrain collectively run through the MFB. Recent studies have begun to unravel how organization of axon bundles is essential for proper wiring of neuronal networks. To assess whether *Pitx3-ITC* mice are useful for studying these mechanisms in the development of the mdDA system, we analyzed the distribution of Citrine-positive axons in the MFB. The MFB could clearly be recognized as a grouping of TH immunoreactive fibers running through the ventral forebrain. Analyzing Citrine-positive fibers within the MFB showed that approximately half of all TH-positive axons were also Citrine-positive. Remarkably, instead of being dispersed throughout the MFB, these fibers were grouped together in the dorsal portion of the MFB (Figure 3G), a feature we could detect at earlier embryonic stages (Figure 3H, unpublished data). This novel insight may indicate that organizational properties play an important role in subset-specific wiring of the mdDA system.

Together, these results show that *Pitx3-ITC* mice label a large subset of mdDA neurons and that their projections can be visualized with different fluorophores in several of the known target areas of the mdDA system, allowing for the studies on different developmental aspects of mdDA neuronal connectivity.

Figure 3. *Pitx3-ITC* Neurons Project to the Dorsal and Ventral Striatum.

(**A** and **B**) Immunohistochemistry for Citrine and tyrosine hydroxylase (TH) on adult *ACTB-FlpE:Pitx3-ITC* coronal brain sections. The dorsal striatum (dS) is strongly innervated by Citrine-positive fibers (**A**), which show both a diffuse (**A'**) and patch-like (arrowheads; **A**, **A"**) innervation pattern. Within the ventral striatum, the nucleus accumbens (NAc) and olfactory tubercle (OT) (**B**) contain dopaminergic fibers mainly organized as patches (**B'**, **B"**). Boxed areas are shown at higher magnification at the right.

(**C**) Immunohistochemistry for tdTomato and TH on adult *EIIa-Cre:Pitx3-ITC* coronal brain sections. The dorsal striatum is strongly innervated by tdTomato-positive fibers, which show both diffuse and patch-like (white arrow) innervation patterns.

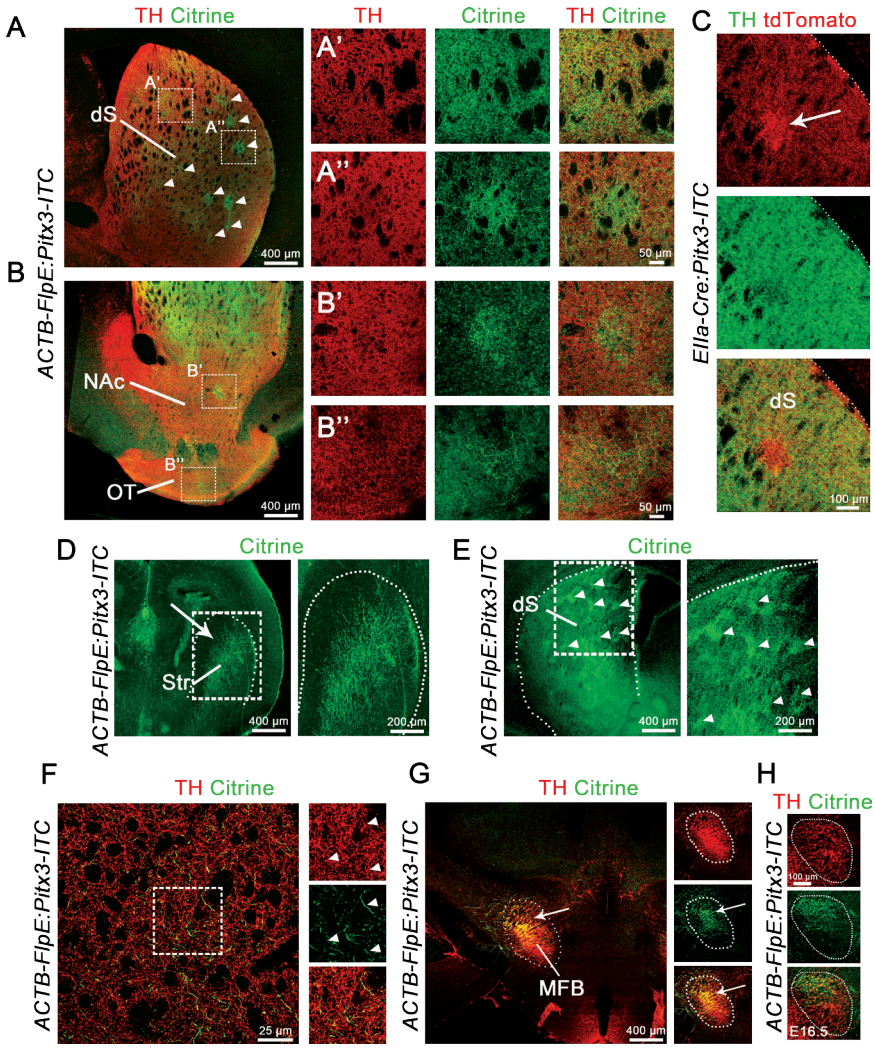

(**D** and **E**) Immunohistochemistry for Citrine on *ACTB-FlpE:Pitx3-ITC* coronal brain sections. Innervation of the striatum (Str) is detected at E16.5 (**D**) and increased at P5 (**E**). At P5, numerous patches were observed (arrowheads). Boxed areas are shown at higher magnification at the right.

(**F**) Single confocal slice of the dorsal striatum of a *ACTB-FlpE:Pitx3-ITC* mouse stained for Citrine and TH. Citrine-positive fibers stain for TH (arrowheads), confirming their dopaminergic identity.

(**G** and **H**) Immunohistochemistry for Citrine and TH on adult *ACTB-FlpE:Pitx3-ITC* coronal brain sections. Approximately 50% of all TH-positive axons within the medial forebrain bundle (MFB; indicated by dashed line) are Citrine-positive and cluster together in the dorsal part of the MFB (white arrow; **G**). This type of organization is similarly observed at E16.5 (**H**).

MARKERS FOR SUBSETS OF DOPAMINERGIC NEURONS

Over the past several years extensive studies have been performed to characterize mdDA neuronal subsets, and several Cre lines have been generated that target molecular subsets such as *Otx2*-positive or *CCK*-positive mdDA neurons within the VTA (Fossat et al., 2006; Di Salvio et al., 2010a; Taniguchi et al., 2011; Veenvliet et al., 2013). Although these lines are suitable for labeling subsets within our *Pitx3-ITC* mice, there is still a lack of SNc specific Cre lines, while in general not many Flp lines have been generated. In order to obtain more flexibility in choosing which subsets to label in our *Pitx3-ITC* mouse, we set out to identify new molecular markers for subsets of mdDA neurons.

With the development of the Anatomic Gene Expression Atlas (AGEA, http://www.brain-map.org; Ng et al., 2007) it is possible to identify genes that are expressed within a specific region of interest. An AGEA analysis of the SNc or VTA (Figure 4A, B) resulted in a large number of genes expressed in and around these areas. A short list was made based on expression within either the SNc or VTA, paying attention to how well the expression pattern described a subset of mdDA neurons. Importantly, results from AGEA are based on expression patterns in the adult mouse brain. To understand whether these genes display similar patterns of expression during early development, we analyzed their expression at E13.5 and E16.5 using *in situ* hybridization. Based on these results we selected two candidates, guanylate cyclase 2c (*Gucy2c*) and Neuropilin-2 (*Nrp2*), which showed specific expression in the SNc or VTA, respectively (Figure 4C).

Gucy2c was predominantly expressed within the SNc. At E13.5 expression was detected in the lateral part of the dopaminergic midbrain, as shown by the expression pattern of *Pitx3* in adjacent sections (Figure 4C). At E16.5, most of the SNc expressed *Gucy2c*, while no expression was observed within the VTA (Figure 4D). In contrast, *Nrp2* was specifically expressed within the VTA, as has been reported previously (Torigoe et al., 2013). A medial population of *Nrp2* expressing cells was detected at E13.5 (Figure 4C), while at E16.5 a subpopulation of cells in the ventromedial part of the VTA expressed *Nrp2* (Figure 4D).

Thus, *Gucy2c* and *Nrp2* define two different subsets within the SNc and VTA, respectively. Expression remains stable within these subsets during development, making them suitable candidates to drive expression of Cre and Flp within subsets of the mdDA system for studies on neural development.

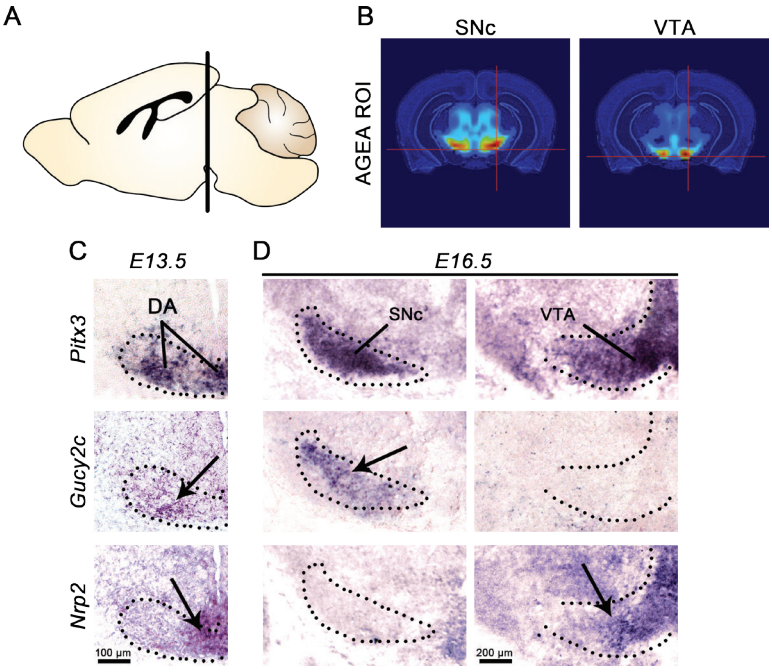

Figure 4. *Gucy2c* and *Nrp2* Mark Different Mesodiencephalic (mdDA) Subsets.

(**A** and **B**) Using the Anatomic Gene Expression Atlas (AGEA) explorer and Gene Finder search tool of the Allen Brain Atlas a region of interest was selected for either the ventral tegmental area (VTA) or substantia nigra pars compacta (SNc). Coronal planes shown in (**B**) correspond with the plane indicated in the schematic sagittal section in (**A**). Color coding in (**B**) shows the correlation between the transciptome profile of the selected voxel and the adjacent voxels (as described in Ng et al., 2009).

(**C** and **D**) In situ hybridization for *Gucy2c* and *Nrp2* at E13.5 (**C**) and E16.5 (**D**). Expression of *Gucy2c* is selective for the SNc, while *Nrp2* is specifically expressed in the VTA. DA, dopaminergic midbrain.

GENERATION AND ANALYSIS OF *NRP2-FLPO* AND *GUCY2C-CRE* MICE

Similar to *Pitx3-ITC* mice, *Nrp2-FlpO* and *Gucy2c-Cre* mice were generated using a BAC mediated transgenesis approach (Gong et al., 2002). In order to analyze the Cre recombinase excision patterns, *Gucy2c-Cre* animals were crossed with *lox-STOP-lox-YFP* animals. As expected, dopaminergic neurons in the SNc were labeled, but to our surprise this labeling was very sparse (Figure 5A). Labeled neurons were primarily located in the ventral SNc and the lateral part of the VTA (Figure 5A, F). Of the 5 lines we generated, 3 lines showed this sparse labeling with comparable cell numbers and distribution, while in the 2 remaining lines no labeling of neurons was detected. Crossing *Gucy2-Cre* and *Pitx3-ITC* mice resulted in similar sparse

labeling of neurons in the SNc (Figure 5B). Unfortunately, no *frt*-STOP-*frt* reporter animals were available to us for analysis of *Nrp2-FlpO* mice. Since our main interest was to use these mice to label subset of neurons in the *Pitx3-ITC* mice, we instead used *Pitx3-ITC* animals for analyzing the *Nrp2-FlpO* lines. In *Nrp2-FlpO:Pitx3-ITC* mice we found sparse labeling of neurons in the SNc and VTA (Figure 5C, F). Sparse labeling in these animals can be explained by the notion that *Nrp2-FlpO* animals were designed to express FlpO in VTA neurons. Since most VTA neurons are negative for ITC in *Pitx3-ITC* mice, we can only label a few SNc neurons that are expressing FlpO in *Nrp2-FlpO* animals. This view was supported by that fact that similar results were obtained when crossing *Pitx3-ITC* and *CCK-Cre* mice, which express Cre primarily in VTA neurons and sparsely in SNc neurons (Figure 5D). Crossing *CCK-Cre* mice with *Pitx3-ITC* mice induced sparse labeling of neurons with tdTomato in the SNc (Figure 5E). Although we observed sparse labeling of neurons in all these lines, comparison of their distribution suggested that they belong to different, and perhaps overlapping, subsets of mdDA neurons (Figure 5F).

DEVELOPMENT OF MDDA CONNECTIVITY AT THE SINGLE-CELL LEVEL

Subsets of mdDA neurons show differences in connectivity at both the pre- and postsynaptic level. This includes differences in target selection and innervation, but also the position of their dendritic fields and the extent of arborization within their targets. However, the cellular and molecular mechanisms underlying the development of these differences remain unknown, largely due to a lack of tools which allow for identification of axons and dendrites at a single-cell level. In order to assess whether single-labeling of neurons in *Pitx3-ITC* mice can address these problems, we characterized the cellular properties of labeled neurons in these animals.

Figure 5. *Gucy2c-Cre* and *Nrp2-FlpO* Mice Label Single Mesodiencephalic (mdDA) Neurons in *Pitx3-ITC* Mice.

(**A**) Immunohistochemistry for tyrosine hydroxylase (TH) and YFP on coronal sections of adult *Gucy2c-Cre:lox-YFP* mice. Single mdDA neurons are labeled (white arrows) which co-stain with TH, indicating their dopaminergic origin. Boxed area is shown as separate channels below. SNc, substantia nigra pars compacta; VTA, ventral tegmental area.

(**B**,**C**) Immunohistochemistry for TH, tdTomato, and Citrine on coronal brain sections of adult mice. In both *Gucy2c-Cre:Pitx3-ITC* (**B**) and *Nrp2-FlpO:Pitx3-ITC* (**C**) mice single mdDA neurons are labeled (white arrows). Their dopaminergic identity is confirmed by co-staining with TH (arrowheads). Boxed area is shown as separate channels below.

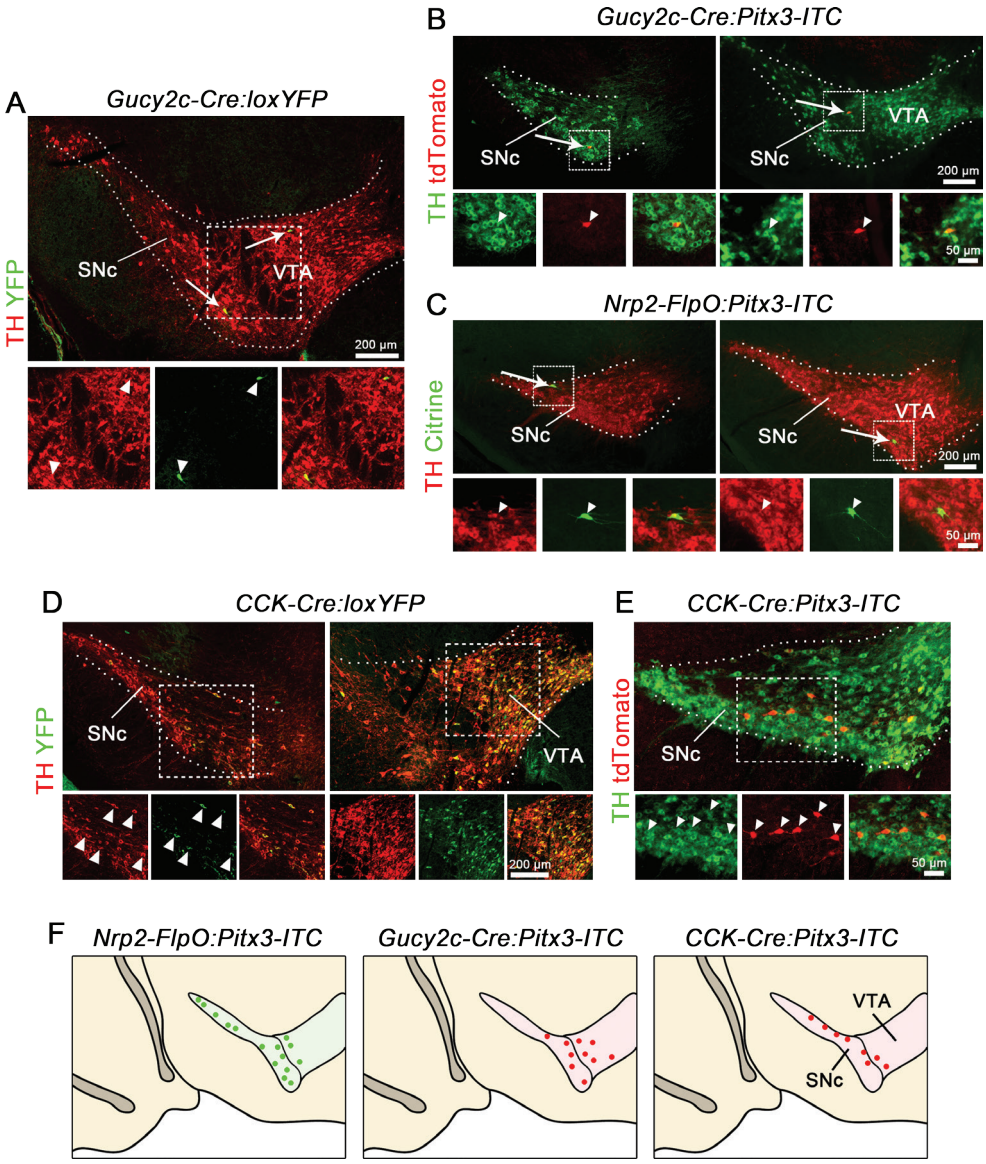

(**D** and **E**) Immunohistochemistry for TH, tdTomato and YFP on coronal brain sections of adult *CCK-Cre* mice. In *CCK-Cre:loxYFP* mice most VTA neurons are labeled, while SNc neurons are labeled sparsely (arrowheads; **D**). Similar sparse labeling of SNc neurons is observed in *CCK-Cre:Pitx3-ITC* mice (arrowheads; **E**). Boxed area is shown as separate channels below.

(**F**) Schematic of a coronal section of the mdDA system depicting the distribution of single-labeled cells in *Nrp2-FlpO*, *Gucy2-Cre* and *CCK-Cre* mice crossed with *Pitx3-ITC* mice.

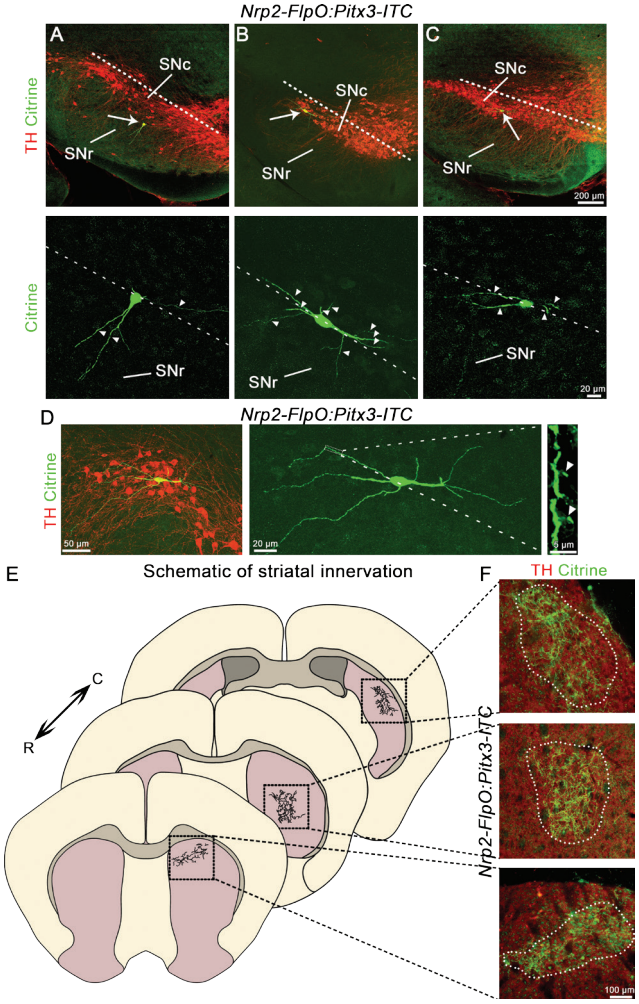

Figure 6. Labeling of Single Mesodiencephalic (mdDA) Neurons Reveals Characteristic Dendritic Projections and Axonal Arborizations.

(**A**-**C**) Immunohistochemistry for tyrosine hydroxylase (TH) and Citrine. Single-labeled mdDA neurons indicated by white arrows are shown at high magnification below. Pyramidal shaped neurons primarily target their dendrite into the substantia nigra pars reticulata (SNr) with only a single projection confined within the substantia nigra pars compacta (SNc; arrowheads; A). Dashed line indicates orientation of the SNc. Fusiform shaped neurons (**B**, **C**) either have dendritic projections (arrowheads) in both the SNr and SNc (**B**) or align all their dendrites with the SNc without projections into the SNr (**C**).

(**D**) High magnification of sections stained for TH and Citrine reveals spine-like protrusions (arrowheads) on dendrites of labeled mdDA neurons in *Nrp2-FlpO:Pitx3-ITC* mice.

(**E** and **F**) Schematic of single-axon projection fields in the dorsal striatum along the rostrocaudal axis of adult *Nrp2-FlpO:Pitx3-ITC* mice (**E**). Corresponding coronal brain sections stained for TH and Citrine are shown in (**F**). R, rostral; C, caudal.

Nrp2-FlpO mice labeled single neurons throughout the ITC-positive population, as compared to the more restricted group of neurons being labeled using *Gucy2c-Cre* or *CCK-Cre* mice (Figure 2, Figure 5F). Therefore, analysis of individually labeled mdDA neurons was done using *Nrp2-FlpO:Pitx3-ITC* mice. Single-labeled neurons were primarily located within the SNc and lateral VTA. We could clearly identify three types of neurons based on their morphology. In the ventral SNc, pyramidal shaped neurons were observed which extended their dendrites primarily within the substantia nigra pars reticulata (SNr), with occasional extensions parallel with and into the SNc (Figure 6A). Neurons located more dorsally within the SNc had a fusiform appearance and extended their dendrites both within the SNc and SNr (Figure 6B). A third type of neuron had a similar fusiform shape, but restricted its dendrites within the SNc without extensions into the SNr (Figure 6C). This corresponds with earlier studies which used Golgi staining to show that the dendritic field of neurons within the dorsal SNc is aligned horizontally, parallel to the SNc, while neurons within the ventral portion of the SNc project their dendrites both within the SNc as well as perpendicularly into the SNr (Fallon et al., 1978; Juraska et al., 1977). High-magnification imaging of dendrites revealed spine-like protrusions (Figure 6D), indicating the ability of Citrine to fill the entire dendrite, a feature that is crucial for studying dendritic development.

MdDA neurons projecting to the dorsal striatum are known to extensively arborize within their target areas (Matsuda et al., 2009; Prensa and Parent, 2001), but the mechanisms underlying this type of target innervation are poorly understood. Single-labeling of neurons in our *Pitx3-ITC* mice presents a unique opportunity to study this distinct feature. In *Nrp2-FlpO:Pitx3-ITC* mice Citrine-positive fibers were primarily detected throughout the dorsal striatum at different levels along the rostrocaudal axis (Figure 6E). Citrine-positive fibers formed localized and dense patches, confirming the distinct and highly arborized innervation pattern of mdDA neurons in the dorsal striatum (Figure 6E, F). These patches were consistent in size and density, which may indicate that each patch is composed of a single axon and not of coincidental overlapping projection fields of multiple mdDA neurons.

Together, these results show how single-cell labeling of mdDA neurons in *Pitx3-ITC* mice, using either *Nrp2-FlpO* or *Gucy2c-Cre* animals, enables studies on different development aspects of mdDA connectivity at both the pre- and postsynaptic level.

DISCUSSION

Brain regions within the CNS are often composed of a heterogeneous population of neurons. This is apparent within the mdDA system, where heterogeneity is crucial for coordinating cognitive and motor behaviors. Although the functional properties of the mdDA system are largely determined by how these different types of neurons are connected, their development and patterns of connectivity remain poorly understood. Here we present a transgenic approach, called *Pitx3-ITC*, which allows for the differential labeling of two non-overlapping neuronal subsets within the SNc and lateral VTA of the mdDA system. Furthermore, in our attempt to develop subset-specific Cre and Flp lines we have generated *Nrp2-FlpO* and *Gucy2c-Cre* mice which sparsely label mdDA neurons in *Pitx3-ITC* mice. Together, these mice offer a unique tool for unraveling the molecular mechanisms underlying the development of subset-specific connectivity patterns at both the pre- and postsynaptic level.

DIFFERENTIAL LABELING OF MDDA SUBSETS

Development of a heterogeneous group of neurons is a complex task and requires a high degree of coordination between different subsets within given a brain region. Neurons need to migrate to their distinct anatomical location, extend their dendritic fields into the appropriate domains and project their axons over long distances for proper target innervation. Studies into the molecular mechanisms controlling these processes in mdDA subsets have shown to be challenging, especially when set in the context of mdDA development as a whole, where possible interactions between subsets need to be taken into account. For example, during early development mdDA neurons migrate together to form the SNc and VTA. Interactions with radial glia are crucial for the first step in migration, but how these neurons acquire their final positional information remains unknown (Kawano et al., 1995). One possible mechanism is that interactions between mdDA subsets signals the position of these neurons and ensures proper organization of the mdDA system. For example, SNc neurons that have arrived at their final position in the lateral part of the mdDA system may interact with VTA neurons and prevent their migration into this area. This view is supported by the notion that expression of the chemorepellent Semaphorin7A (Sema7A) and PlexinC1 defines two different mdDA subsets (Pasterkamp et al., 2007). Sema7A expressing neurons are located in the SNc, while neurons expressing PlexinC1 are located in the VTA. In addition, the role of Sema7A-PlexinC1

signaling in controlling cell migration has been described for different systems and cell types, although its role in mdDA development remains unknown (Jongbloets et al., 2013). Labeling different mdDA subsets in *Pitx3-ITC* mice will provide the opportunity to study the cellular and molecular mechanisms that control this process of migration. Interestingly, at E16.5 a large number of Citrine-positive neurons were detected within the developing VTA of *ACTB-FlpE:Pitx3-ITC* mice. The number of cells decreased at P5, while at adult stages they were no longer observed. A possible explanation for this observation is the ongoing migration of mdDA neurons from the midline area towards the SNc. At E16.5 many of these neurons still reside within the VTA, but as their migration progresses they leave the VTA and migrate into the SNc. An alternative explanation would be that these neurons remain in the VTA, but lose their expression of Citrine at later stages of development. Future studies will need to determine whether indeed these cells are migrating towards the SNc, or whether they remain within the VTA and lose their expression of Citrine over time. Furthermore, it is important to note that analysis of *Pitx3-ITC* mice at earlier developmental stages will be necessary to assess whether neurons are labeled throughout the entire process of migration. Still, the data we present here show stable expression of ITC at different developmental stages and, together with the use of the *Pitx3* promoter, predicts that mdDA neurons will also be labeled during earlier stages of development.

At the axonal level, interactions between subsets may be important for establishing proper mdDA connectivity. Our data show that mdDA neurons located in the SNc and lateral part of the VTA extend their axons in the dorsal part of the MFB and primarily project to the dorsal and ventral striatum. This organization may be an important mechanism for shaping mdDA connectivity as has been described for other neuronal systems (Imai et al., 2009; Lokmane et al., 2013). For example, the position of mdDA axons within the MFB may confer guidance information and direct axons to their appropriate target areas. This position may be determined by axon-axon interactions between different mdDA axons in MFB. However, whether organization of mdDA axons in the MFB plays a role in targeting of forebrain areas remains currently unresolved.

The ITC strategy we propose allows for the differential labeling of two mdDA subsets in a single mouse. This offers a unique approach for studying subset-specific development, by visualizing the migration, axon pathfinding and dendritic

development of specific subsets. Further, it allows for studying possible interactions between subsets and characterization of their molecular profiles. Future studies will benefit from the differential labeling of mdDA neurons, as it provides an opportunity of visualizing differential responses to candidate molecules in a single *ex vivo* or *in vitro* setup, or testing whether manipulations *in vivo* have differential effects on these mdDA subsets.

LABELING OF MDDA NEURONS IN *PITX3-ITC* MICE

Our strategy to specifically label mdDA subsets benefits from the *Pitx3* promoter to target expression of ITC to mdDA neurons. Although all midbrain dopamine neurons express *Pitx3* at the adult stage (Maxwell et al., 2005), our *Pitx3-ITC* mice show expression of the ITC transgene only in the SNc and lateral part of the VTA. Some variation between different lines was found, but approximately the same subset was labeled in all lines. It remains unclear how to explain the lack of labeling of medial VTA neurons, although the inherent variability of BAC transgenesis and the possible lack of regulatory elements from the used BAC clone may account for this. Interestingly, there are striking similarities between the lack of ITC expression in VTA neurons and the reported expression pattern of the classical mdDA subset marker G-protein-gated inwardly rectifying K^+ channel subunit 2 (*Girk2*) (Schein et al., 1998; Thompson et al., 2005), raising the possibility that mechanisms restricting *Girk2* to these neuronal subsets might similarly restrict expression of ITC.

With a large portion of the mdDA neurons expressing ITC, our strategy offers a unique approach in differentially labeling of mdDA subsets within the SNc and lateral VTA. Different types of mdDA neurons have been described within the SNc and lateral VTA, based on their anatomical position, morphology or molecular signature. For example, most neurons within the SNc express *Girk2*, while a small population of neurons located dorsally, also known as the substantia nigra pars lateralis (SNl), shows no expression of *Girk2* but instead expresses *Calbindin* (Liang et al., 1996; Schein et al., 1998; Thompson et al., 2005). Similarly, the lateral VTA contains different types of dopamine neurons which express varying combinations of *Ahd2*, *Otx2* and *Girk2* (Di Salvio et al., 2010a, 2010b; Simeone et al., 2011). In addition, as described in previous studies (Fallon et al., 1978; Juraska et al., 1977), and supported by our own data (Figure 6A-D), there is a clear distinction between ventral SNc neurons, which are pyramidal shaped and extend their dendrites within

the SNr, and dorsal SNc neurons which display a fusiform shape and either retain their dendrites within the SNc or have prominent extensions in both the SNc and SNr. Tracing studies have revealed how different subsets exist in the SNc and lateral VTA based on their connectivity pattern, with some of these subsets being dispersed throughout the entire mdDA system (Björklund and Dunnett, 2007b; Lammel et al., 2008; Matsuda et al., 2009; Prensa and Parent, 2001). Using Cre or Flp lines specific for these groups of neurons together with our *Pitx3-ITC* mice will provide a powerful approach in studying the development of different mdDA subsets.

DISTINCT FEATURES OF CONNECTIVITY WITHIN THE MDDA SYSTEM

In our *Pitx3-ITC* mice prominent innervation of the dorsal and ventral striatum was observed (Figure 3). Co-staining for TH revealed that axons targeting the striatum are dopaminergic and uncovered a remarkable innervation pattern within the dorsal and ventral striatum. In between the more diffuse pattern of labeled axons, more intense patches of innervation were found. This type of compartmentalized innervation of the striatum has been reported previously. It was shown that these patches of dopaminergic axons overlapped with high-density regions of opiate receptors (Graybiel, 1984; Herkenham et al., 1984; Voorn et al., 1988). In these studies, dopaminergic patches were clearly recognized during embryonic and early postnatal development. In contrast, at adult stages these patches were barely observable, probably due to increased dopaminergic innervation of the surrounding striatal matrix. In our *Pitx3-ITC* mice we could identify many patches, even at adult stages, most likely because parts of the extensive dopaminergic projections in the striatal matrix that usually occlude these patches are not present in our *Pitx3-ITC* mice. Both the development and function of these patches remain unknown. Being able to visualize these during structural development as well as during adulthood provides a unique opportunity to establish how these patches develop and how they function within the mdDA system.

Axons originating in the mdDA system reach the forebrain through the MFB, after which they segregate to innervate their targets. Interestingly, instead of being dispersed throughout the MFB, ITC expressing axons are grouped together within the dorsal portion of the MFB. It is becoming increasingly clear that axon-axon interactions and the organization of axon tracts is critical during the wiring of the nervous system (Wang and Marquardt, 2013). These mechanisms have not been

described for the mdDA system, but may play an important role in the formation of subset-specific connectivity. For example, subsets of axons may be sorted within the MFB such that their position within this tract mediates pathfinding towards their appropriate targets, as has been described for other neuronal systems (Imai et al., 2009; Lokmane et al., 2013; Wang and Marquardt, 2013).

SINGLE-CELL LABELING OF MDDA NEURONS

Our current understanding of the development of mdDA circuitry is still limited and mainly derives from studies focused on axon pathfinding and target innervation. Still, much remains unknown about the molecular mechanisms underlying the formation of subset-specific connectivity patterns. Besides their different target areas, mdDA subsets show differences in the extent of arborization within these targets as well as the complexity and extension of their dendrites (Fallon et al., 1978; Juraska et al., 1977; Matsuda et al., 2009; Prensa and Parent, 2001). These features are difficult to study without consistent visualization of single-cell morphology.

In our attempt to develop SNc- and VTA-specific Cre and Flp lines, respectively, we generated mice in which mdDA neurons are sparsely labeled. Many of these cells were located within the SNc, where different subtypes could be recognized. Pyramidal shaped neurons located ventrally, extended their dendrites within both the SNc and SNr, while dorsally located SNc neurons retained their dendrites within the SNc. Although dendritic patterning is an important aspect in wiring of neuronal networks, the functional implications and molecular determinants of mdDA dendritic organization remain unknown. In addition, single-labeled neurons were found to project their axons mainly towards the dorsal striatum, where they extensively arborized to cover a relatively large projection area (Figure 6E, F), confirming earlier reports which used different types of tracing technique to characterize the full morphology of single SNc neurons and the notion that a single SNc neuron may give rise of up to 150,000 presynaptic terminals (Matsuda et al., 2009; Prensa and Parent, 2001; Sulzer, 2007).

Labeling of single mdDA neurons in *Pitx3-ITC* mice enables in-depth studies of different developmental processes, such as identifying which molecular mechanisms control subset-specific dendritic patterning and how synaptic specificity is acquired in the striatum. Furthermore, visualization of dendritic structures and projection fields of a single axon allows for studies on whether the structure and morphology

is regulated in response to certain behavioral paradigms and pharmacological treatments known to influence dopaminergic functioning. This will provide insight into the functional properties of this stereotypic patterning and arborization.

In summary, our *Pitx3-ITC* strategy presents a unique and novel tool for studying mdDA subset development and overcomes many of the difficulties involved in studying the development and function of this complex neuronal system. Together with subset-specific or single-cell specific Cre and Flp lines, such as *Nrp2-FlpO* or *Gucy2c-Cre* mice, this approach enables in-depth studies of different developmental and functional aspects of the mdDA system.

MATERIALS AND METHODS

DNA CONSTRUCTS

The ITC construct was assembled using conventional cloning techniques. First, Citrine was cloned into the psiCheck2 vector (Promega) which contains a Synthetic poly(A) sequence. Next, primers containing an *frt* site were used to clone Citrine and the Synthetic poly(A) sequence into pcDNA3.1 (Invitrogen). TdTomato together with a bGH poly(A) sequence was subsequently cloned upstream of Citrine. Next, IFP with a SV40 poly(A) sequence was cloned upstream of tdTomato using primers containing *loxP* and frt sequences generating ITC. For expression of iCre and FlpO in HEK 293 cells, CMV-iCre and CMV-FlpO expression vectors were generated by cloning iCre (a kind gift from Rolf Sprengel (Max Planck Institute, Heidelberg)) and FlpO into pcDNA3.1 (Invitrogen).

CELL CULTURE AND TRANSFECTION

HEK 293 human embryonic kidney cells were transfected using Lipofectamine 2000 (Invitrogen) according to manufacturer's protocol. Briefly, 1.75µl of Lipofectamine 2000 was diluted in 25µl Opti-MEM (Gibco). Separately, DNA encoding for either ITC, iCre or FlpO was added to 25µl Opti-MEM. Both Opti-MEM dilutions were mixed and allowed to incubate for 10 min after which they were directly added to each well. After 72 h cells were fixed in 4% paraformaldehyde (PFA), briefly washed in PBS and mounted in Prolong Gold antifade reagent (Invitrogen).

BAC RECOMBINATION AND MICE

All animal use and care were in accordance with institutional guidelines. Targeting constructs were assembled in pGEM-T Easy (Promega). ITC was flanked by sequences homologous to 458 bp upstream of the *Pitx3* ATG start codon in exon 2 and 450 bp downstream of exon 2, FlpO by sequences homologous to 440 bp upstream of the *Nrp2* ATG start codon in exon 1 and 447 bp downstream of exon 1, and iCre by sequences homologous to 459 bp upstream of the *Gucy2c* ATG start codon in exon 1 and 402 bp downstream of exon 1. The resulting cassettes were cloned in the pLD53 shuttle vector (Gong et al., 2002) and used for introducing ITC into *Pitx3* BAC clone RP23-125F3 (CHORI), FlpO into *Nrp2* BAC clone RP24-238H6 (CHORI) and iCre into *Gucy2c* BAC clone RP23-93A18 (CHORI).

Recombination was verified by PCR and enzymatic digestion of the recombined BAC clones. In order to generate transgenic mice, purified DNA was microinjected into fertilized eggs obtained by mating (C57BL/6 X SJL)F1 or C57BL/6 female mice with (C57BL/6 X SJL)F1 male mice. Pronuclear microinjection was performed as described (Nagy et al., 2003). Mice were genotyped by PCR on genomic DNA using the following primers:

Pitx3-ITC, 5'-CTGACGCCACTGGAGAGATG-3' and
5'-TGGTGGCAGACAATCAGTCC-3';

Nrp2-FlpO, 5'-GCAGGTTCAGCGACATCAAG-3' and
5'-GGTAGGGGGCGTTCTTCTTC-3';

Gucy2c-Cre, 5'-CCCGGGGCCACCATGGT-3' and
5'-GACACAGCATTGGAGTCAGA-3'.

TISSUE TREATMENT

Timed-pregnant mice were killed by means of cervical dislocation. The morning of which a vaginal plug was detected was considered embryonic day 0.5 (E0.5). Tissue preparation was done as previously described (Kolk et al., 2009). For *in situ* hybridization experiments, brains were directly frozen and sections were cut on a cryostat. For immunohistochemistry, brains were fixed in 4% PFA in PBS after which they were cryoprotected in 30% sucrose in PBS. Cryostat sections were cut at 16-18 μm, mounted on Superfrost Plus slides (Thermo Fisher Scientific), air-dried, and stored at -20°C for immunohistochemistry sections and -80°C for *in situ* hybridization sections. For immunohistochemistry, mice were transcardially perfused with 4% PFA. Brains were isolated and postfixed overnight at 4°C in 4% PFA. Fixed brains were vibratome sectioned in the coronal plane at 50 μm.

IMMUNOHISTOCHEMISTRY

Sections were blocked with 10% FCS in PBS containing 1% Triton X-100 for 3 h at room temperature (RT). Subsequent incubation with primary antibodies in blocking buffer was done overnight at 4°C. Sections were washed extensively in PBS and incubated with secondary antibodies conjugated to Alexa Fluor-488, 555 and 680

from appropriate species overnight at 4°C. After several washes in PBS, sections were either counterstained with fluorescent DAPI (4',6'-diamidino-2-phenylindole; 0.1 mg/ml in PBS; Invitrogen) and washed in PBS, or directly mounted in FluorSave reagent (Merck Millipore). Staining was visualized on a Zeiss Axioskop A1 epifluorescent microscope or by confocal laser-scanning microscopy (Olympus FV1000). Primary antibodies used were rabbit anti-TH (Millipore; 1:1000), mouse anti-TH (Millipore; 1:750), rabbit anti-GFP (Millipore; 1:500), chicken anti-GFP (Abcam; 1:500), rabbit anti-tdTomato (Rockland; 1:500).

RNA *IN SITU* HYBRIDIZATION

Nonradioactive *in situ* hybridization was performed as described previously (Kolk et al., 2009; Pasterkamp et al., 2007). cDNA was made from whole mouse brain RNA using a one-step RT-PCR kit (Qiagen), according to supplied protocol and using the following primers:

Gucy2c, 5'-CATAGGGACCTTTGAGTTGGAG-3' and
5'-GTTTGAGACCAGCTTGGGATAC-3';

Nrp2, 5'-AGGACACGAAGTGAGAAGCC-3' and
5'-TTGCAGTCGTGTTTCTCGATTTC-3';

TH, 5'-CAGCTTGCACTATGCCCACC-3' and
5'-GAATTCCACAGTGAACCAG-3'.

cDNA was cloned into pGEM-T Easy (Promega) and transcribed using either SP6 or T7 RNA polymerase (Roche) and digoxigenin-labeled nucleotide mix (Roche) to produce digoxigenin-labeled cRNA probes. Digoxigenin was detected using anti-digoxigenin FAB fragments conjugated to alkaline phosphatase (Roche; 1:3000) and stained with NBT/BCIP (Roche). Sections were counterstained with fluorescent Nissl (Neurotrace; Invitrogen; 1:500), mounted using FluorSave reagent and visualized on a Zeiss Axioscope 2.

ACKNOWLEDGEMENTS

We thank members of the Pasterkamp laboratory for assistance and helpful discussions throughout the course of this project. We thank Rolf Sprengel for sharing the iCre construct and we are grateful to Nathaniel Heintz and Shiaoching Gong for sharing the pLD53 construct and for technical advice on BAC transgenesis. We thank Roger Tsien for sharing the tdTomato, Citrine, and IFP constructs. We are grateful to Roman Giger for his support in coordinating the generation of BAC transgenic mice. We acknowledge Galina Gavrilina, Keith Childs, and Wanda Filipiak for preparation of transgenic mice at the Transgenic Animal Model Core of the University of Michigan's Biomedical Research Core Facilities. This study is supported by grants from the Netherlands Organization for Scientific Research (TopTalent; to E.R.E.S.), the European Union (mdDANeurodev, FP/2007-2011, Grant 222999), Dutch Top Institute Pharma Project T5-207, and the International Parkinson Foundation (to R.J.P.).

REFERENCES

Björklund, A., and Dunnett, S.B. (2007a). Fifty years of dopamine research. Trends Neurosci. *30*, 185–187.

Björklund, A., and Dunnett, S.B. (2007b). Dopamine neuron systems in the brain: an update. Trends Neurosci. *30*, 194–202.

Branda, C., and Dymecki, S. (2004). Talking about a revolution: The impact of site-specific recombinases on genetic analyses in mice. Dev. Cell *6*, 7–28.

Bromberg-Martin, E.S., Matsumoto, M., and Hikosaka, O. (2010). Dopamine in motivational control: rewarding, aversive, and alerting. Neuron *68*, 815–834.

Chung, C.Y., Seo, H., Sonntag, K.C., Brooks, A., Lin, L., and Isacson, O. (2005). Cell type-specific gene expression of midbrain dopaminergic neurons reveals molecules involved in their vulnerability and protection. Hum. Mol. Genet. *14*, 1709–1725.

Ding, J.B., Oh, W.-J., Sabatini, B.L., and Gu, C. (2012). Semaphorin 3E-Plexin-D1 signaling controls pathway-specific synapse formation in the striatum. Nat. Neurosci. *15*, 215–223.

Dunlop, B.W., and Nemeroff, C.B. (2007). The role of dopamine in the pathophysiology of depression. Arch. Gen. Psychiatry *64*, 327–337.

Fallon, J., Riley, J., and Moore, R. (1978). Substantia nigra dopamine neurons: separate populations project to neostriatum and allocortex. Neurosci. Lett. *7*, 157-162

Fossat, N., Chatelain, G., Brun, G., and Lamonerie, T. (2006). Temporal and spatial delineation of mouse Otx2 functions by conditional self-knockout. EMBO Rep. *7*, 824–830.

Gong, S., Yang, X.W., Li, C., and Heintz, N. (2002). Highly efficient modification of bacterial artificial chromosomes (BACs) using novel shuttle vectors containing the R6Kgamma origin of replication. Genome Res. *12*, 1992–1998.

Graybiel, A. M. (1984). Correspondence between the dopamine islands and striosomes of the mammalian striatum. Neuroscience *13*, 1157–1187.

Greene, J.G., Dingledine, R., and Greenamyre, J.T. (2005). Gene expression profiling of rat midbrain dopamine neurons: implications for selective vulnerability in parkinsonism. Neurobiol. Dis. *18*, 19–31.

Griesbeck, O., Baird, G.S., Campbell, R.E., Zacharias, D. A., and Tsien, R.Y. (2001). Reducing the environmental sensitivity of yellow fluorescent protein. Mechanism and applications. J. Biol. Chem. *276*, 29188–29194.

Herkenham, M., Edley, S.M., and Stuart, J. (1984). Cell clusters in the nucleus accumbens of the rat, and the mosaic relationship of opiate receptors, acetylcholinesterase and subcortical afferent terminations. Neuroscience *11*, 561–593.

Van den Heuvel, D.M.A, and Pasterkamp, R.J. (2008). Getting connected in the dopamine system. Prog. Neurobiol. *85*, 75–93.

Ikemoto, S. (2007). Dopamine reward circuitry: two projection systems from the ventral midbrain to the nucleus accumbens-olfactory tubercle complex. Brain Res. Rev. *56*, 27–78.

Imai, T., Yamazaki, T., Kobayakawa, R., Kobayakawa, K., Abe, T., Suzuki, M., and Sakano, H. (2009). Pre-target axon sorting establishes the neural map topography. Science *325*, 585–590.

Iversen, S.D., and Iversen, L.L. (2007). Dopamine: 50 years in perspective. Trends Neurosci. *30*, 188–193.

Jongbloets, B.C., Ramakers, G.M.J., and Pasterkamp, R.J. (2013). Semaphorin7A and its receptors: pleiotropic regulators of immune cell function, bone homeostasis, and neural development. Semin. Cell Dev. Biol. *24*, 129–138.

Juraska, J.M., Wilson, C.J., and Groves, P.M. (1977). The substantia nigra of the rat: a Golgi study. J. Comp. Neurol. *172*, 585–600.

Kawano, H., Ohyama, K., Kawamura, K., and Nagatsu, I. (1995). Migration of dopaminergic neurons in the embryonic mesencephalon of mice. Brain Res. Dev. Brain Res. *86*, 101–113.

Kim, I.-J., Zhang, Y., Meister, M., and Sanes, J.R. (2010). Laminar restriction of retinal ganglion cell dendrites and axons: subtype-specific developmental patterns revealed with transgenic markers. J. Neurosci. *30*, 1452–1462.

Kolk, S.M., Gunput, R.-A.F., Tran, T.S., van den Heuvel, D.M.A., Prasad, A.A., Hellemons, A.J.C.G.M., Adolfs, Y., Ginty, D.D., Kolodkin, A.L., Burbach, J.P.H., et al. (2009). Semaphorin 3F is a bifunctional guidance cue for dopaminergic axons and controls their fasciculation, channeling, rostral growth, and intracortical targeting. J. Neurosci. *29*, 12542–12557.

Lakso, M., and Pichel, J. (1996). Efficient in vivo manipulation of mouse genomic sequences at the zygote stage. Proc. Natl. Acad. Sci. U. S. A. *93*, 5860–5865.

Lammel, S., Hetzel, A., Häckel, O., Jones, I., Liss, B., and Roeper, J. (2008). Unique properties of mesoprefrontal neurons within a dual mesocorticolimbic dopamine system. Neuron *57*, 760–773.

Liang, C., Sinton, C., and German, D. (1996). Midbrain dopaminergic neurons in the mouse: co-localization with Calbindin-D 28k and calretinin. Neuroscience *75*, 523–533.

Lokmane, L., Proville, R., Narboux-Nême, N., Györy, I., Keita, M., Mailhes, C., Léna, C., Gaspar, P., Grosschedl, R., and Garel, S. (2013). Sensory map transfer to the neocortex relies on pretarget ordering of thalamic axons. Curr. Biol. *23*, 810–816.

Masland, R.H. (2012). The neuronal organization of the retina. Neuron *76*, 266–280.

Matsuda, W., Furuta, T., Nakamura, K.C., Hioki, H., Fujiyama, F., Arai, R., and Kaneko, T. (2009). Single nigrostriatal dopaminergic neurons form widely spread and highly dense axonal arborizations in the neostriatum. J. Neurosci. *29*, 444–453.

Maxwell, S.L., Ho, H.-Y., Kuehner, E., Zhao, S., and Li, M. (2005). Pitx3 regulates tyrosine hydroxylase expression in the substantia nigra and identifies a subgroup of mesencephalic dopaminergic progenitor neurons during mouse development. Dev. Biol. *282*, 467–479.

Molyneaux, B.J., Arlotta, P., Menezes, J.R.L., and Macklis, J.D. (2007). Neuronal subtype specification in the cerebral cortex. Nat. Rev. Neurosci. *8*, 427–437.

Nagy, A., Gertsentein, M., Vintersten, K., and Behringer, R. (2003). Manipulating the Mouse Embryo: A Laboratory Manual (New York: Cold Spring Harbor Press).

Ng, L., Pathak, S.D., Kuan, C., Lau, C., Dong, H., Sodt, A., Dang, C., Avants, B., Yushkevich, P., Gee, J.C., et al. (2007). Neuroinformatics for genome-wide 3D gene expression mapping in the mouse brain. IEEE/ACM Trans. Comput. Biol. Bioinform. *4*, 382–393.

Ng, L., Bernard, A., Lau, C., Overly, C.C., Dong, H.-W., Kuan, C., Pathak, S., Sunkin, S.M., Dang, C., Bohland, J.W., et al. (2009). An anatomic gene expression atlas of the adult mouse brain. Nat. Neurosci. *12*, 356–362.

Pasterkamp, R.J., Kolk, S.M., Hellemons, A.J.C.G.M., and Kolodkin, A.L. (2007). Expression patterns of semaphorin7A and plexinC1 during rat neural development suggest roles in axon guidance and neuronal migration. BMC Dev. Biol. *7*, 98.

Prensa, L., and Parent, A. (2001). The nigrostriatal pathway in the rat: a single-axon study of the relationship between dorsal and ventral tier nigral neurons and the striosome/matrix striatal compartments. J. Neurosci. *21*, 7247–7260.

Raymond, C.S., and Soriano, P. (2007). High-efficiency FLP and PhiC31 site-specific recombination in mammalian cells. PLoS One *2*, e162.

Rodríguez, C.I., Buchholz, F., Galloway, J., Sequerra, R., Kasper, J., Ayala, R., Stewart, A. F., and Dymecki, S.M. (2000). High-efficiency deleter mice show that FLPe is an alternative to Cre-loxP. Nat. Genet. *25*, 139–140.

Roeper, J. (2013). Dissecting the diversity of midbrain dopamine neurons. Trends Neurosci. *36*, 336–342.

Sakano, H. (2010). Neural map formation in the mouse olfactory system. Neuron *67*, 530–542.

Di Salvio, M., Di Giovannantonio, L.G., Omodei, D., Acampora, D., and Simeone, A. (2010a). Otx2 expression is restricted to dopaminergic neurons of the ventral tegmental area in the adult brain. Int. J. Dev. Biol. *54*, 939–945.

Di Salvio, M., Di Giovannantonio, L.G., Acampora, D., Prosperi, R., Omodei, D., Prakash, N., Wurst, W., and Simeone, A. (2010b). Otx2 controls neuron subtype identity in ventral tegmental area and antagonizes vulnerability to MPTP. Nat. Neurosci. *13*, 1481–1488.

Schein, J.C., Hunter, D.D., and Roffler-Tarlov, S. (1998). Girk2 expression in the ventral midbrain, cerebellum, and olfactory bulb and its relationship to the murine mutation weaver. Dev. Biol. *204*, 432–450.

Sesack, S.R., and Carr, D.B. (2002). Selective prefrontal cortex inputs to dopamine cells: implications for schizophrenia. Physiol. Behav. *77*, 513–517.

Shaner, N.C., Campbell, R.E., Steinbach, P. A., Giepmans, B.N.G., Palmer, A.E., and Tsien, R.Y. (2004). Improved monomeric red, orange and yellow fluorescent proteins derived from Discosoma sp. red fluorescent protein. Nat. Biotechnol. *22*, 1567–1572.

Shimshek, D., Kim, J., and Hübner, M. (2002). Codon-improved Cre recombinase (iCre) expression in the mouse. Genesis *26*, 19–26.

Shu, X., Royant, A., Lin, M.Z., Aguilera, T. a, Lev-Ram, V., Steinbach, P. a, and Tsien, R.Y. (2009). Mammalian expression of infrared fluorescent proteins engineered from a bacterial phytochrome. Science *324*, 804–807.

Simeone, A., Di Salvio, M., Di Giovannantonio, L.G., Acampora, D., Omodei, D., and Tomasetti, C. (2011). The role of otx2 in adult mesencephalic-diencephalic dopaminergic neurons. Mol. Neurobiol. *43*, 107–113.

Smidt, M.P., and Burbach, J.P.H. (2007). How to make a mesodiencephalic dopaminergic neuron. Nat. Rev. Neurosci. *8*, 21–32.

Smidt, M.P., van Schaick, H.S., Lanctôt, C., Tremblay, J.J., Cox, J.J., van der Kleij, A.A., Wolterink, G., Drouin, J., and Burbach, J.P. (1997). A homeodomain gene Ptx3 has highly restricted brain expression in mesencephalic dopaminergic neurons. Proc. Natl. Acad. Sci. U. S. A. *94*, 13305–13310.

Smidt, M.P., von Oerthel, L., Hoekstra, E.J., Schellevis, R.D., and Hoekman, M.F.M. (2012). Spatial and Temporal Lineage Analysis of a Pitx3-Driven Cre-Recombinase Knock-In Mouse Model. PLoS One *7*, e42641.

Snyder-Keller, A. (1991). Development of striatal compartmentalization following pre-or postnatal dopamine depletion. J. Neurosci. *17*.

Sulzer, D. (2007). Multiple hit hypotheses for dopamine neuron loss in Parkinson's disease. Trends Neurosci. *30*, 244–250.

Taniguchi, H., He, M., Wu, P., Kim, S., Paik, R., Sugino, K., Kvitsiani, D., Kvitsani, D., Fu, Y., Lu, J., et al. (2011). A resource of Cre driver lines for genetic targeting of GABAergic neurons in cerebral cortex. Neuron *71*, 995–1013.

Thompson, L., Barraud, P., Andersson, E., Kirik, D., and Björklund, A. (2005). Identification of dopaminergic neurons of nigral and ventral tegmental area subtypes in grafts of fetal ventral mesencephalon based on cell morphology, protein expression, and efferent projections. J. Neurosci. *25*, 6467–6477.

Torigoe, M., Yamauchi, K., Tamada, A., Matsuda, I., Aiba, A., Castellani, V., and Murakami, F. (2013). Role of neuropilin-2 in the ipsilateral growth of midbrain dopaminergic axons. Eur. J. Neurosci. *37*, 1573–1583.

Veenvliet, J. V., Dos Santos, M.T.M., Kouwenhoven, W.M., von Oerthel, L., Lim, J.L., van der Linden, A.J.A., Koerkamp, M.J.A.G., Holstege, F.C.P., Smidt, M.P. (2013). Specification of dopaminergic subsets involves interplay of En1 and Pitx3. Development *140*, 4116–4116.

Voorn, P., Kalsbeek, a, Jorritsma-Byham, B., and Groenewegen, H.J. (1988). The pre- and postnatal development of the dopaminergic cell groups in the ventral mesencephalon and the dopaminergic innervation of the striatum of the rat. Neuroscience *25*, 857–887.

Wang, L., and Marquardt, T. (2013). What axons tell each other: axon-axon signaling in nerve and circuit assembly. Curr. Opin. Neurobiol. 1–9.

'If you see through everything, then everything is transparent. But a wholly transparent world is an invisible world. To 'see through' all things is the same as not to see.'

- C. S. Lewis

Chapter 6

General Discussion

The assembly of highly precise patterns of neuronal connectivity is crucial for proper functioning of the nervous system and perturbed formation of neuronal circuits may underlie various neuropsychiatric disorders. The mesodiencephalic dopamine (mdDA) system consists of dopamine neurons located primarily in the ventral midbrain and plays a critical role in control of voluntary movement and motivational behavior. Disturbances in mdDA connectivity have been implicated in various neurological and psychiatric disorders, including Parkinson's disease and schizophrenia.

Understanding how neuronal circuits are formed is crucial for unraveling complex brain functions and to gain insight into how situations of perturbed connectivity contribute to the development of neuropsychiatric disorders. Within this context, this thesis aims to unravel the mechanisms that control the formation of mdDA connectivity. Using a combination of molecular, cellular and mouse genetic approaches, we uncovered new mechanisms which control the development of mdDA circuitry. In addition, tools were presented, including a new mouse transgenic strategy, to facilitate studies of these processes *in vitro* and *in vivo*.

In the following sections, the results outlined in this thesis will be discussed within the framework of our current knowledge of the development of mdDA neuronal connectivity. In addition, suggestions will be made for future studies that will further our understanding of the development and function of the mdDA system.

WIRING THE MDDA SYSTEM: LESSONS LEARNED FROM THE MESOHABENULAR PATHWAY

For studying mechanisms that dictate the development of mdDA connectivity we focused in Chapter 3 on mdDA projections targeting the habenula. These projections are particularly well suited for studying mdDA connectivity as it concerns an easily identifiable group of axons which targets the lateral habenula (lHb), a well described and discrete subdomain (Bianco and Wilson, 2009; Hikosaka et al., 2008). In addition, recent studies have begun to unravel the important role of these projections in controlling reward related behavior and in neuropsychiatric disorders (Kowski et al., 2009; Li et al., 2011, 2013; Shen et al., 2012; Shumake et al., 2003, 2010; Stamatakis et al., 2013). However, the development of this pathway and the mechanisms controlling its formation remained unresolved.

LAMP-MEDIATED WIRING OF THE MDDA SYSTEM

An important finding reported in this thesis is the identification of the cell adhesion molecule Limbic-system Associated Membrane Protein (LAMP) as a crucial factor for controlling reciprocal axon-axon interactions between mdDA and lHb axons (Chapter 3). Expression of LAMP on lHb efferents allows mdDA axons to grow along these efferents. This positions these axons correctly for subsequent innervation of the lHb. Interestingly, LAMP is expressed in many cortical and subcortical limbic systems (Gil et al., 2002; Horton and Levitt, 1988), suggesting that it may serve to guide axons in other brain areas as well. Notably, LAMP is expressed on a subset of axons running through the striatum, as well as in the developing striatum itself (Gil et al., 2002; Horton and Levitt, 1988; Pimenta et al., 1995). These striatal axons run through the medial forebrain bundle (MFB) where they encounter mdDA axons which grow in a reciprocal direction (Chapter 5). Analogous to mdDA axons targeting the lHb, reciprocal axon-axon interactions between striatal and mdDA axons in the MFB may be important for subset-specific targeting of the striatum. In addition, LAMP expression in the striatum is graded, with high expression in the ventromedial striatum and lower expression in the dorsolateral striatum (Gil et al., 2002). Such differences in expression levels may be important for subset-specific targeting of striatal afferents, including those originating in the mdDA system. Although the expression pattern of LAMP is consistent with such a hypothesis, future studies involving localized manipulations of LAMP expression are needed to

assess whether LAMP plays a role in subset-specific targeting of mdDA axons into brain regions other than the lHb.

AXON TRACT ORGANIZATION

Ectopic expression of LAMP on medial habenula (mHb) axons in the core of the fasciculus retroflexus (FR) directly results in mistargeting of mdDA axons towards the mHb and shows that LAMP plays an important role in confining mdDA axons to the sheath of the FR. It also shows that organization of the FR into distinct subdomains is essential for proper targeting of mdDA axons towards the lHb, as it ensures that mdDA axons only interact with and follow sheath axons. Pre-target axon sorting has been shown to be important for the development of different neuronal systems (Imai et al., 2009; Lokmane et al., 2013). However, it is currently unknown whether the guidance of mdDA axons to other brain regions is controlled by pre-target axon sorting mechanisms. Characterization of our *Pitx3-ITC* mice (Chapter 5), in which neurons are labeled that are located within the lateral part of the mdDA system, reveals that mdDA axons running through the MFB show a specific organization pattern. Axonal projections of this lateral subset were confined to the dorsal part of the MFB and projected primarily to the dorsal and ventral striatum. As with mdDA axons running through the FR, mdDA axons running through the MFB intermingle with different axon populations. This, together with our results on the dependency of mdDA axons targeting the lHb, suggests that, to some extent, mdDA axon guidance is an opportunistic process where mdDA axons make use of already laid out axon tracts for guidance towards their targets. Such a mechanism may be more efficient, since it requires a much smaller set of molecules for guidance along the major part of their trajectory, with no need of molecular mechanisms controlling every required axon guidance event. However, this also comes at a cost, as the wiring of this system becomes vulnerable to disturbances in the connectivity of those axons they rely on for guidance. This supports the intriguing possibility that disorders with a clear dopaminergic phenotype may initially be caused by changes in connectivity of non-dopaminergic systems. Future studies are needed to further dissect the role of axon-axon interactions in shaping mdDA connectivity. This may provide insight into the possibility of non-dopaminergic wiring defects causing dopamine-related phenotypes.

MAJOR DEPRESSIVE DISORDER

A recent study has associated particular variations in the *LAMP* genetic sequence with Major Depressive Disorder (MDD) (Koido et al., 2012). This is striking, since hyperactivity of the lHb has similarly been implicated in MDD (Li et al., 2011, 2013; Shumake et al., 2003). Moreover, mdDA projections are thought to inhibit lHb activity and may therefore be involved in controlling reward related behavior (Kowski et al., 2009; Shen et al., 2012; Shumake et al., 2010; Stamatakis et al., 2013). Our results on the role of LAMP in targeting mdDA axons towards the lHb (Chapter 3) connects these findings, since changes in the expression or structure of LAMP are predicted to result in reduced or even a loss of dopaminergic innervation of the lHb. Consequently, the lHb would receive reduced inhibitory input leading to increased activity. It is worth noting that the initial analyses of *LAMP*$^{-/-}$ mutant mice did not reveal any gross changes in neuronal connectivity (Catania et al., 2008). Still, dopaminergic innervation of the lHb was not analyzed in these animals and a reduction or loss of mdDA projections towards the habenula may easily go unnoticed in a general analysis of neuronal connectivity. Future studies will need to establish whether and how the reported genetic variations of *LAMP* affect mdDA growth and/or targeting towards the habenula and whether this results in increased activity of the lHb causing MDD-like symptoms.

Findings: Axon-axon interactions controlled by the cell adhesion molecule LAMP play an important role in guidance of mdDA axons towards the lateral habenula (lHb) and may similarly be involved in guidance of mdDA into brain regions other than the lHb. In addition, disturbances in LAMP signaling may result in reduced dopaminergic innervation of the lHb and lead to the development of Major Depressive Disorder (MDD).

Future Research: Guidance of mdDA axons may predominantly be an opportunistic process where these axons are guided along laid out axon tracts. This calls for studies aimed at unraveling how axon-axon interactions control the wiring of mdDA circuitry. This will provide more insight into how disturbances in these mechanisms result in perturbed mdDA connectivity underlying various neuropsychiatric disorders, such as MDD.

DCC–NETRIN-1 SIGNALING CONTROLS TARGETING AND MAINTENANCE OF MDDA CONNECTIVITY

DCC–Netrin-1 signaling has previously been described as an important factor in wiring of neuronal circuits (Bielle et al., 2011; Goldman et al., 2013; Lai Wing Sun et al., 2011; Manitt et al., 2011; Poon et al., 2008; Powell et al., 2008). Results from this thesis expand these findings by identifying a new role for Netrin-1 in controlling subdomain-specific target innervation and in the formation and maintenance of functional mdDA circuitry.

A proteomics and gene expression analysis identified Netrin-1 to be selectively expressed in the lHb (Chapter 3). Here, it acts as a subdomain-specific chemoattractant controlling innervation of the lHb by mdDA axons, which express DCC. Although mdDA axons follow lHb efferents towards the lHb, they require this separate, Netrin-1 mediated, signal for innervation. Netrin-1 could be involved in uncoupling mdDA axons from lHb axons, allowing them to innervate the habenula and make appropriate synaptic contacts. During adulthood, Netrin-1 is involved in fine-tuning and maintaining the functional organization of mdDA circuitry (Chapter 4). Netrin-1 signaling can be mediated through both DCC and Unc5H (A-D) receptors, or through a multimeric DCC/Unc5H receptor complex. Interestingly, both DCC and Unc5C heterozygous mutant mice show similar phenotypes in their response to amphetamine (Chapter 4 and Flores, 2011). This effect is only present at adult stages and corresponds to the gradually increased expression of Unc5C. This suggests that this effect of Netrin-1 is mediated through the DCC/Unc5C receptor complex. A recent study has revealed how reduced expression of DCC in *DCC*$^{+/-}$ mice causes structural changes in the prefrontal cortex (PFC) at both the pre- and postsynaptic level, which may underlie the observed phenotype of these animals (Manitt et al., 2011). However, futures studies will determine whether such structural changes also occur in *Unc5C*$^{+/-}$ mice.

These results reveal different roles for Netrin-1 at distinct stages of mdDA circuit development. During formation of mdDA circuitry, Netrin-1 acts as a guidance molecule, controlling early guidance and innervation. Next, remaining Netrin-1 expression within these target areas may serve to confine mdDA axons to the lHb, as has been described for Netrin-B in the *Drosophila* visual system. Here, Netrin-B not only attracts but also confines axonal afferents, preventing their progression into

deeper layers (Timofeev et al., 2012). Finally, at adult stages, remaining Netrin-1 expression may serve to form and maintain functional circuits and control their response to external stimuli. This could include controlling the formation of synaptic contacts, as has previously been described for Netrin-1 in other systems (Goldman et al., 2013).

Future studies will need to address whether this role of Netrin-1 at different stages of development is a general mechanism for controlling formation and maintenance of mdDA circuitry. If so, it places Netrin-1 at the heart of mdDA functioning. Changes in the structure or expression of Netrin-1, or any of its downstream signaling molecules, could interfere with normal development and functioning of the mdDA system and thereby contribute to the symptomatology of various neuropsychiatric disorders. As such, Netrin-1, its transmembrane receptors, and its downstream signaling molecules, may be interesting therapeutic targets for modulating symptoms of various neuropsychiatric disorders.

Findings: During embryonic development, Netrin-1 controls the dopaminergic innervation of the lateral habenula (lHb), while during adulthood Netrin-1 is involved in maintaining functional mdDA circuitry.

Future Research: Netrin-1 serves different functions in controlling the formation of functional mdDA circuitry. Future studies will further characterize the role of Netrin-1 during different stages of mdDA development and assess whether Netrin-1 may serve as a therapeutic target for various dopaminergic-related neuropsychiatric disorders.

STRATEGIES FOR ANALYZING DEVELOPMENT OF MDDA CONNECTIVITY

Studies into how connections in the brain are established rely on the identification and manipulation of neuronal circuits and the individual neurons that form these connections. However, a lack of tools to selectively identify and label mdDA subsets has complicated such studies and as a result our current knowledge of the subsets-specific wiring of the mdDA system is still limited. Therefore, part of this thesis was aimed at developing new tools to facilitate studies into the mechanisms controlling the establishment of subset-specific connectivity patterns.

DIFFERENTIAL LABELING OF MDDA SUBSETS

The mdDA system is composed of various neuronal subsets, each of which has a distinct molecular profile and connectivity pattern (Björklund and Dunnett, 2007; Chung et al., 2005; Greene et al., 2005; Lammel et al., 2008; Roeper, 2013; Simeone et al., 2011; Veenvliet et al., 2013). In order to understand how these subset-specific connections are established, these subsets need to be identified and their development characterized. In Chapter 5 we presented a new transgenic approach, called *Pitx3-ITC*, which allows for differential labeling of two mdDA subsets in a single mouse.

Differential labeling of multiple mdDA subsets offers a unique opportunity for characterizing their molecular signature. Enriched populations of these subsets can be obtained using flow cytometry techniques, such as Fluorescence-Activated Cell Sorting (FACS). This allows for molecular profiling of mdDA subsets and the identification of candidate molecules that could control subset-specific wiring of the mdDA system. In addition, studies using *in vitro* techniques, including the three-dimensional collagen matrix assay described in Chapter 2, would greatly benefit from differential labeling of mdDA subsets. For example, the subset-specific effects of identified candidate molecules can easily be tested by co-culturing tdTomato and Citrine-labeled mdDA neurons in a single experimental setup. In this way the differential effect of presented candidate molecules or manipulation of their cognate receptors can be identified and allows for uncovering molecular determinants shaping subset-specific connectivity. Similarly, this transgenic approach facilitates *in vivo* studies by enabling the identification of subset-specific alterations at both the pre- and postsynaptic level. Mouse genetic approaches, including (conditional) knockout strategies, can be evaluated based on their effect on connectivity patterns of specific subsets. These alterations may include subtle changes in targeting of brain regions, such as the striatum, which may easily go unnoticed using classical immunohistochemistry approaches or labeling of single-subsets using GFP reporter lines.

SINGLE-CELL LABELING OF MDDA NEURONS

Diversity of mdDA neurons has mostly been considered from a molecular perspective, with different subsets expressing different molecular markers (Chung et al., 2005; Greene et al., 2005; Roeper, 2013; Simeone et al., 2011; Veenvliet et al., 2013). This has been extended by studies using advanced retrograde tracings methods which

have uncovered new subsets based on the targets they innervate (Björklund and Dunnett, 2007; Lammel et al., 2008). In contrast, little is known about the diversity of the mdDA neurons at the level of their dendritic input, although differences in the organization of dendrites were already recognized a few decades ago (Fallon et al., 1978; Juraska et al., 1977). Our analysis of *Pitx3-ITC* mice crossed with *Gucy2c-Cre* or *Nrp2-FlpO mice*, in which single mdDA neurons are labeled (Chapter 5), confirmed and expanded these previous studies by identifying differences in where mdDA neurons extend their dendritic projections. At the moment, the functional consequences and the molecular mechanisms dictating these differences remain unknown. Until now, studies on the dendritic development of mdDA neurons were complicated, since they required consistent sparse labeling of mdDA neurons. Future studies into this largely unexplored topic will be greatly facilitated by our newly generated mice.

Single-labeling of neurons also offers the opportunity of analyzing how axons, after innervation, arborize within their targets and select partner neurons for making synaptic connections. These processes are difficult to study when groups of axons are labeled, as it prevents tracking which arbor belongs to which axon. Initial analysis of single mdDA axon innervation of the striatum revealed relatively large projection fields and extensive arborization within localized domains, consistent with the notion that a single striatonigral neuron can make up to 150,000 synaptic contacts (Matsuda et al., 2009; Prensa and Parent, 2001; Sulzer, 2007). The striatum is composed of patch and surrounding matrix compartments. These are functional subdomains, with specific expression of different neurotransmitters and receptors and distinct connectivity patterns (Joel and Weiner, 2000; Mansour et al., 1995; Miura et al., 2007; Penny et al., 1986; Xu et al., 1994). We found that single mdDA axons innervate the dorsal striatum in a patch-like pattern. This pattern of innervation was also detected in *Pitx3-ITC* mice crossed with mice expressing germline-line Flp or Cre. The functional properties of mdDA axons targeting patch or matrix compartments and the molecular mechanisms controlling the formation of this specific connectivity pattern remain unresolved. The patch-like innervation pattern in *Pitx3-ITC* mice offers a unique approach for studying these processes by visualizing structural changes in these patches, in combination with mouse genetic approaches and functional challenges. For example, pruning or extension of dopaminergic patches in knockout animals or animals tested in different behavioral

paradigms may reveal the functional properties of these connections, and give insight into how this connectivity pattern is established and maintained. It is important to note that studies co-staining for patch and/or matrix specific markers will need to establish whether the dopaminergic innervation of the striatum observed in *Pitx3-ITC* mice is indeed specific for striatal patches.

BAC TRANSGENIC STRATEGY

Our strategy for differential labeling of mdDA neurons was initially aimed at the entire mdDA system because it used the *Pitx3* promoter to drive the expression of the ITC transgene (Smidt et al., 1997). However, only the lateral portion of the mdDA system, including the substantia nigra pars compacta (SNc) and lateral ventral tegmental area (VTA), showed expression of ITC. Since this expression pattern was similar for all generated lines, the most likely cause of the lack of signals in the medial VTA is the use of Bacterial Artificial Chromosomes (BACs) for generating these transgenic mice. BACs are large pieces of DNA (~200 – 300 kb) and because of their size not only contain promoter sequences for driving transgene expression, but also many of the up- and downstream regulatory elements necessary for proper expression. In contrast to a targeted knock-in approach, BACs randomly integrate into the genome after pronuclear injections. Either lack of specific regulatory elements in the BAC, or genetic influences from genomic areas surrounding the BAC could affect expression. However, the identical expression patterns observed in all generated lines does not support a role for influences by surrounding genetic sequences. Besides missing regulatory elements in the BAC, the ITC transgene is introduced into the first exon of the *Pitx3* gene located on the BAC. This disturbance of the *Pitx3* gene may contribute to the observed expression pattern of ITC, as specific elements within this exon may be crucial for proper expression of *Pitx3* in the medial VTA.

Future studies using *Pitx3-ITC* mice will focus on the development of mdDA neurons in the SNc and lateral VTA. The unique expression pattern of ITC in these mice provides novel opportunities for studying mdDA development. For example, a patch-like innervation pattern of the striatum is clearly recognized at adult stages in *Pitx3-ITC* mice. Although such patches were recognized in earlier studies using a classical immunohistochemistry approach (Graybiel, 1984; Voorn et al., 1988), massive innervation of the striatum by mdDA axons at later stages of development

prevented visualization of this patch-specific striatal innervation by mdDA axons at the adult stage. The absence of labeled projections from the medial VTA in *Pitx3-ITC* mice enables the visualization of this patch-specific innervation pattern and offers a unique approach to analyze how these connections are maintained and to investigate their function at adult stages.

Findings: *Pitx3-ITC* mice allow for differential labeling of mdDA subsets located in the substantia nigra pars compacta (SNc) and lateral ventral tegmental area (VTA). In addition, *Nrp2-FlpO* and *Gucy2c-Cre* mice crossed with *Pitx3-ITC* mice show sparse labeling of mdDA neurons, revealing distinct patterns of connectivity at the pre- and postsynaptic level.

Future Research: *Pitx3-ITC* mice, together with *Nrp2-FlpO* and *Gucy2c-Cre* mice, offer a unique approach towards studying the development of mdDA connectivity. These animals will facilitate future studies aimed at unraveling the molecular mechanisms dictating the formation of mdDA circuitry at a subset-specific level.

FINAL WORDS

Overall, this thesis provides new insights into the mechanisms controlling the development of mdDA connectivity. In particular, a novel role for LAMP-mediated axon-axon interactions in subdomain-targeting of mdDA axons was uncovered. We also revealed a new role for target derived Netrin-1, which at early developmental stages controls target entry via the DCC receptor, and at adult stages plays a role in controlling functional circuitry via the DCC/Unc5C receptor complex. In addition, we presented newly developed genetic tools to facilitate future studies aimed at unraveling how mdDA circuitry is established. Changes in the mdDA circuitry may underlie various neurological and psychiatric disorders. The findings and newly developed tools presented in this thesis will help to unravel how disturbances in the molecular mechanisms that control the formation of mdDA circuitry contribute to the symptomatology of these diseases and help develop new therapeutic strategies aimed at restoring perturbed mdDA connectivity.

REFERENCES

Bianco, I.H., and Wilson, S.W. (2009). The habenular nuclei: a conserved asymmetric relay station in the vertebrate brain. Philos. Trans. R. Soc. Lond. B. Biol. Sci. *364*, 1005–1020.

Bielle, F., Marcos-Mondéjar, P., Leyva-Díaz, E., Lokmane, L., Mire, E., Mailhes, C., Keita, M., García, N., Tessier-Lavigne, M., Garel, S., et al. (2011). Emergent growth cone responses to combinations of Slit1 and Netrin 1 in thalamocortical axon topography. Curr. Biol. *21*, 1748–1755.

Björklund, A., and Dunnett, S.B. (2007). Dopamine neuron systems in the brain: an update. Trends Neurosci. *30*, 194–202.

Catania, E.H., Pimenta, A., and Levitt, P. (2008). Genetic deletion of Lsamp causes exaggerated behavioral activation in novel environments. Behav. Brain Res. *188*, 380–390.

Chung, C.Y., Seo, H., Sonntag, K.C., Brooks, A., Lin, L., and Isacson, O. (2005). Cell type-specific gene expression of midbrain dopaminergic neurons reveals molecules involved in their vulnerability and protection. Hum. Mol. Genet. *14*, 1709–1725.

Fallon, J., Riley, J., and Moore, R. (1978). Substantia nigra dopamine neurons: separate populations project to neostriatum and allocortex. Neurosci. Lett. *7*, 157-162

Flores, C. (2011). Role of netrin-1 in the organization and function of the mesocorticolimbic dopamine system. J. Psychiatry Neurosci. *36*, 296–310.

Gil, O.D., Zhang, L., Chen, S., Ren, Y.Q., Pimenta, A., Zanazzi, G., Hillman, D., Levitt, P., and Salzer, J.L. (2002). Complementary expression and heterophilic interactions between IgLON family members neurotrimin and LAMP. J. Neurobiol. *51*, 190–204.

Goldman, J.S., Ashour, M. A., Magdesian, M.H., Tritsch, N.X., Harris, S.N., Christofi, N., Chemali, R., Stern, Y.E., Thompson-Steckel, G., Gris, P., et al. (2013). Netrin-1 Promotes Excitatory Synaptogenesis between Cortical Neurons by Initiating Synapse Assembly. J. Neurosci. *33*, 17278–17289.

Graybiel, A. M. (1984). Correspondence between the dopamine islands and striosomes of the mammalian striatum. Neuroscience *13*, 1157–1187.

Greene, J.G., Dingledine, R., and Greenamyre, J.T. (2005). Gene expression profiling of rat midbrain dopamine neurons: implications for selective vulnerability in parkinsonism. Neurobiol. Dis. *18*, 19–31.

Hikosaka, O., Sesack, S.R., Lecourtier, L., and Shepard, P.D. (2008). Habenula: crossroad between the basal ganglia and the limbic system. J. Neurosci. *28*, 11825–11829.

Horton, H.L., and Levitt, P. (1988). A unique membrane protein is expressed on early developing limbic system axons and cortical targets. J. Neurosci. *8*, 4653–4661.

Imai, T., Yamazaki, T., Kobayakawa, R., Kobayakawa, K., Abe, T., Suzuki, M., and Sakano, H. (2009). Pre-target axon sorting establishes the neural map topography. Science *325*, 585–590.

Joel, D., and Weiner, I. (2000). The connections of the dopaminergic system with the striatum in rats and primates: an analysis with respect to the functional and compartmental organization of the striatum. Neuroscience *96*, 451–474.

Juraska, J., Wilson, C., and Groves, P.M. (1977). The substantia nigra of the rat: a Golgi study. J. Comp. Neurol. *172*, 585–600.

Koido, K., Traks, T., Balõtšev, R., Eller, T., Must, A., Koks, S., Maron, E., Tõru, I., Shlik, J., Vasar, V., et al. (2012). Associations between LSAMP gene polymorphisms and major depressive disorder and panic disorder. Transl. Psychiatry *2*, e152.

Kowski, A. B., Veh, R.W., and Weiss, T. (2009). Dopaminergic activation excites rat lateral habenular neurons in vivo. Neuroscience *161*, 1154–1165.

Lai Wing Sun, K., Correia, J.P., and Kennedy, T.E. (2011). Netrins: versatile extracellular cues with diverse functions. Development *138*, 2153–2169.

Lammel, S., Hetzel, A., Häckel, O., Jones, I., Liss, B., and Roeper, J. (2008). Unique properties of mesoprefrontal neurons within a dual mesocorticolimbic dopamine system. Neuron *57*, 760–773.

Li, B., Piriz, J., Mirrione, M., Chung, C., Proulx, C.D., Schulz, D., Henn, F., and Malinow, R. (2011). Synaptic potentiation onto habenula neurons in the learned helplessness model of depression. Nature *470*, 535–539.

Li, K., Zhou, T., Liao, L., Yang, Z., Wong, C., Henn, F., Malinow, R., Yates, J.R., and Hu, H. (2013). βCaMKII in lateral habenula mediates core symptoms of depression. Science *341*, 1016–1020.

Lokmane, L., Proville, R., Narboux-Nême, N., Györy, I., Keita, M., Mailhes, C., Léna, C., Gaspar, P., Grosschedl, R., and Garel, S. (2013). Sensory map transfer to the neocortex relies on pretarget ordering of thalamic axons. Curr. Biol. *23*, 810–816.

Manitt, C., Mimee, A., Eng, C., Pokinko, M., Stroh, T., Cooper, H.M., Kolb, B., and Flores, C. (2011). The netrin receptor DCC is required in the pubertal organization of mesocortical dopamine circuitry. J. Neurosci. *31*, 8381–8394.

Mansour, A., Fox, C., Akil, H., and Watson, S. (1995). Opioid-receptor mRNA expression in the rat CNS: anatomical and functional implications. Trends Neurosci. *18*, 22-29

Matsuda, W., Furuta, T., Nakamura, K.C., Hioki, H., Fujiyama, F., Arai, R., and Kaneko, T. (2009). Single nigrostriatal dopaminergic neurons form widely spread and highly dense axonal arborizations in the neostriatum. J. Neurosci. *29*, 444–453.

Miura, M., Saino-Saito, S., Masuda, M., Kobayashi, K., and Aosaki, T. (2007). Compartment-specific modulation of GABAergic synaptic transmission by mu-opioid receptor in the mouse striatum with green fluorescent protein-expressing dopamine islands. J. Neurosci. *27*, 9721–9728.

Penny, G.R., Afsharpour, S., and Kitai, S.T. (1986). The glutamate decarboxylase-, leucine enkephalin-, methionine enkephalin- and substance P-immunoreactive neurons in the neostriatum of the rat and cat: evidence for partial population overlap. Neuroscience *17*, 1011–1045.

Pimenta, A.F., Zhukareva, V., Barbe, M.F., Reinoso, B.S., Grimley, C., Henzel, W., Fischer, I., and Levitt, P. (1995). The limbic system-associated membrane protein is an Ig superfamily member that mediates selective neuronal growth and axon targeting. Neuron *15*, 287–297.

Poon, V.Y., Klassen, M.P., and Shen, K. (2008). UNC-6/netrin and its receptor UNC-5 locally exclude presynaptic components from dendrites. Nature *455*, 669–673.

Powell, A.A.W.A., Sassa, T., Wu, Y., Tessier-Lavigne, M., and Polleux, F. (2008). Topography of thalamic projections requires attractive and repulsive functions of Netrin-1 in the ventral telencephalon. PLoS Biol. *6*, e116.

Prensa, L., and Parent, A. (2001). The nigrostriatal pathway in the rat: a single-axon study of the relationship between dorsal and ventral tier nigral neurons and the striosome/matrix striatal compartments. J. Neurosci. *21*, 7247–7260.

Roeper, J. (2013). Dissecting the diversity of midbrain dopamine neurons. Trends Neurosci. *36*, 336–342.

Shen, X., Ruan, X., and Zhao, H. (2012). Stimulation of Midbrain Dopaminergic Structures Modifies Firing Rates of Rat Lateral Habenula Neurons. PLoS One *7*, e34323.

Shumake, J., Edwards, E., and Gonzalez-Lima, F. (2003). Opposite metabolic changes in the habenula and ventral tegmental area of a genetic model of helpless behavior. Brain Res. *963*, 274–281.

Shumake, J., Ilango, A., Scheich, H., Wetzel, W., and Ohl, F.W. (2010). Differential neuromodulation of acquisition and retrieval of avoidance learning by the lateral habenula and ventral tegmental area. J. Neurosci. *30*, 5876–5883.

Simeone, A., Di Salvio, M., Di Giovannantonio, L.G., Acampora, D., Omodei, D., and Tomasetti, C. (2011). The role of otx2 in adult mesencephalic-diencephalic dopaminergic neurons. Mol. Neurobiol. *43*, 107–113.

Smidt, M.P., van Schaick, H.S., Lanctôt, C., Tremblay, J.J., Cox, J.J., van der Kleij, A.A., Wolterink, G., Drouin, J., and Burbach, J.P. (1997). A homeodomain gene Ptx3 has highly restricted brain expression in mesencephalic dopaminergic neurons. Proc. Natl. Acad. Sci. U. S. A. *94*, 13305–13310.

Stamatakis, A.M., Jennings, J.H., Ung, R.L., Blair, G.A., Weinberg, R.J., Neve, R.L., Boyce, F., Mattis, J., Ramakrishnan, C., Deisseroth, K., et al. (2013). A Unique Population of Ventral Tegmental Area Neurons Inhibits the Lateral Habenula to Promote Reward. Neuron *80*, 1039–1053.

Sulzer, D. (2007). Multiple hit hypotheses for dopamine neuron loss in Parkinson's disease. Trends Neurosci. *30*, 244–250.

Timofeev, K., Joly, W., Hadjieconomou, D., and Salecker, I. (2012). Localized netrins act as positional cues to control layer-specific targeting of photoreceptor axons in Drosophila. Neuron *75*, 80–93.

Veenvliet, J. V., Dos Santos, M.T.M., Kouwenhoven, W.M., von Oerthel, L., Lim, J.L., van der Linden, A.J.A., Koerkamp, M.J.A.G., Holstege, F.C.P., Smidt, M.P. (2013). Specification of dopaminergic subsets involves interplay of En1 and Pitx3. Development *140*, 4116–4116.

Voorn, P., Kalsbeek, A., Jorritsma-Byham, B., and Groenewegen, H.J. (1988). The pre- and postnatal development of the dopaminergic cell groups in the ventral mesencephalon and the dopaminergic innervation of the striatum of the rat. Neuroscience *25*, 857–887.

Xu, M., Moratalla, R., Gold, L.H., Hiroi, N., Koob, G.F., Graybiel, A.M., and Tonegawa, S. (1994). Dopamine D1 receptor mutant mice are deficient in striatal expression of dynorphin and in dopamine-mediated behavioral responses. Cell *79*, 729–742.

'Once you accept that science is the only source of human knowledge, you have adopted a philosophical position (scientism) that cannot be verified, or falsified, by science itself.'

- Thomas Burnett

Addendum

SAMENVATTING IN HET NEDERLANDS

Het centraal zenuwstelsel is opgebouwd uit miljoenen zenuwcellen (neuronen) die op een zeer specifieke wijze met elkaar verbonden zijn. Deze connectiviteit is cruciaal voor het correct functioneren van het zenuwstelsel. Opmerkelijk is dat een groot deel van de verbindingen tussen neuronen worden aangelegd tijdens de embryonale en postnatale ontwikkeling. Dit is een zeer complex proces waarbij de uitlopers van zenuwcellen (axonen) over relatief lange afstanden naar specifieke hersengebieden worden gestuurd. In deze hersengebieden maken ze zeer selectief verbinding met de juiste partner neuronen, welke veelal in specifieke subdomeinen liggen en worden omgeven door andere type neuronen.

De sturing van axonen wordt gereguleerd door een combinatie van moleculaire signalen (zie **hoofdstuk 1**). Moleculen in de extracellulaire omgeving sturen axonen door ze aan te trekken (attractie) of ze af te stoten (repulsie) en functioneren zo als wegwijzers. Axonen maken ook gebruik van al eerder aangelegde zenuwbanen door ze te volgen naar de juiste hersengebieden. In deze hersengebieden leidt een combinatie van moleculen, die op zeer specifieke locaties tot expressie komen, axonen naar de juiste partner neuronen om synaptische verbindingen mee te vormen.

Het complexe patroon van neuronale connecties bepaalt voor een groot deel de functionele eigenschappen van het zenuwstelsel. Begrijpen hoe deze connecties worden gevormd is daarom van groot belang om te begrijpen hoe het zenuwstelsel zich ontwikkelt en functioneert. Bovendien speelt de foutieve aanleg van neuronale verbindingen een rol bij de ontwikkeling van neurologische en psychiatrische aandoeningen, zoals de ziekte van Parkinson, autisme en schizofrenie. Echter, voor veel hersengebieden is nog onbekend hoe de connectiviteit wordt aangelegd en welke cellulaire en moleculaire processen hierbij betrokken zijn. Het onderzoek beschreven in dit proefschrift richt zich op het ontdekken welke moleculaire mechanismen ten grondslag liggen aan de vorming van neuronale connecties. Hierbij ligt de nadruk op het mesodiencephalisch dopamine (mdDA) systeem, omdat: (1) het mdDA systeem een goed beschreven en toegankelijk systeem is, waardoor het zeer geschikt is om de vorming van connecties in het zenuwstelsel te bestuderen; (2) het mdDA systeem direct en indirect betrokken is bij verschillende neurologische en psychiatrische aandoeningen. Kennis over hoe verbindingen in dit hersengebied worden aangelegd is cruciaal voor het begrijpen hoe deze ziekten ontstaan en voor de ontwikkeling van therapeutische strategieën gericht op deze ziekten.

BEVINDINGEN VAN DIT PROEFSCHRIFT

MdDA neuronen projecteren hun axonen via de mediale voorhersenbundel (MFB) naar verschillende gebieden in de voorhersenen, waaronder het striatum. De vorming van deze verbindingen wordt gereguleerd door moleculen die worden uitgescheiden langs de route die mdDA axonen volgen (zie **hoofdstuk 1**). Zoals beschreven in **hoofdstuk 2** kunnen deze moleculen *in vitro* bestudeerd worden door weefsel van het mdDA systeem en doelgebieden, zoals het striatum, samen in een collageen matrix te groeien. De collageen matrix functioneert als een driedimensionale omgeving die de extracellulaire matrix nabootst. Daarnaast biedt het de mogelijkheid voor uitgescheiden moleculen om een stabiele gradiënt te vormen. Op deze manier kan de invloed die moleculen hebben op de groei van mdDA axonen bestudeerd worden en biedt het een methode om de uitgroei van axonen en/of de attractieve of repulsieve respons te kwantificeren. Dit maakt deze methode uitermate geschikt om de cellulaire en moleculaire mechanismen die de groei van mdDA axonen en striatale axon reguleren *in vitro* te analyseren.

Om de mechanismen te onderzoeken die de ontwikkeling van mdDA connectiviteit reguleren, hebben we in **hoofdstuk 3** de mdDA axonen bestudeerd die de habenula innerveren. Deze axonen zijn zeer geschikt om mdDA connectiviteit te bestuderen, omdat het hier gaat om een geïsoleerde groep axonen die goed herkenbaar zijn en waarvan het innervatiepatroon volledig bekend is. Bovendien laten recente studies zien hoe deze axonen een rol spelen bij beloningsgedrag en verschillende psychiatrische aandoeningen. Echter, de ontwikkeling van deze axonen en de moleculaire mechanismen die dit proces reguleren zijn nagenoeg onbekend.

De habenula ligt dorsaal van de thalamus en bestaat uit twee subdomeinen, de mediale habenula (mHb) en laterale habenula (lHb), waarbij mdDA axonen specifiek de lHb innerveren. Een belangrijk resultaat van deze studie is de ontdekking dat mdDA axonen gebruik maken van al eerder aangelegde axonen uit de lHb. Door lHb axonen te volgen worden mdDA axonen naar de lHb gestuurd. Deze axon-axon interactie tussen mdDA en lHb axonen wordt gemedieerd door het *Limbic-system associated membrane protein* (LAMP) molecuul. LAMP is aanwezig op zowel lHb als mdDA axonen en verstoringen van het expressieniveau of de locatie van LAMP veroorzaken defecten in de innervatie van de lHb door mdDA axonen. Opmerkelijk is dat eerdere studies naar de ontwikkeling van depressieve stoornissen een rol hebben gevonden voor enerzijds de hyperactivteit van de habenula en anderzijds

verstoringen in LAMP. De bevindingen beschreven in **hoofdstuk 3** bieden een mogelijke verklaring door te laten zien dat verstoringen in LAMP verlies van dopaminerge innervatie in de habenula veroorzaakt. Dit verlies van innervatie zou kunnen leiden tot hyperactivieit van de habenula.

Axonen van het mdDA systeem brengen ook het molecuul *Deleted in Colorectal Carcinoma* (DCC) tot expressie. Deze receptor stelt mdDA axonen in staat om een ander molecuul, Netrin-1, te detecteren. Netrin-1 wordt uitgescheiden door de lHb, en collageen matrix assays (zoals beschreven in **hoofdstuk 2**) laten zien dat Netrin-1, uitgescheiden door de lHb, een attractieve respons bij mdDA axonen veroorzaakt. Verlies van Netrin-1 in de lHb, of DCC op mdDA axonen, resulteert in verlies van dopaminerge innervatie van de lHb, waarbij mdDA axonen tot aan de lHb groeien, maar deze niet binnen gaan.

De resultaten in deze studie laten voor het eerst zien hoe een subdomein van een hersengebied via axon-axon interacties en secretie van attractieve moleculen zijn eigen innervatie patroon bepaalt. Daarnaast werpen deze bevindingen nieuw licht op een mogelijk algemeen mechanisme voor het sturen van mdDA axonen, bijvoorbeeld naar structuren in het voorbrein, zoals het striatum (zie ook **hoofdstuk 5**).

Receptoren voor Netrin-1 spelen ook een belangrijke rol bij de ontwikkeling van mdDA projecties naar de prefrontaal cortex (PFC). *DCC* haploinsufficiënte muizen hebben afwijkingen in de dopaminerge innervatie van de PFC en zijn minder gevoelig voor amfetamine en cocaïne, zoals blijkt uit een minder sterke locomotor respons na toediening van deze stoffen. Echter, deze effecten ontstaan pas na de adolescentie. Dit is opvallend, aangezien de DCC receptor al tot expressie komt vanaf de embryonale ontwikkeling. Naast DCC is ook de Unc5 receptor in staat om Netrin-1 te binden. De expressie van Unc5 wordt in mdDA neuronen sterk gereguleerd en komt tot expressie vanaf de adolescentie. Dit suggereert een mogelijke rol voor het DCC/Unc5 receptor complex bij de vorming van mdDA circuits in de PFC en kan verklaren waarom de defecten in *DCC* haploinsufficiënte muizen pas zichtbaar worden na de adolescentie. De resultaten beschreven in **hoofdstuk 4** tonen de expressie van *Unc5C*, een homoloog van Unc5, specifiek in neuronen in het ventraal tegmentum (VTA) van het mdDA systeem. De verlaging van Unc5C expressie in *Unc5C* haploinsufficiënte dieren leidt tot een verstoorde respons na toediening van amfetamine en cocaïne. Dit gaat gepaard met een sterke toename in expressie van tyrosine hydroxylase (TH), het enzym dat essentieel is voor de productie van dopamine, in de PFC.

Dit fenotype is sterk vergelijkbaar met wat in eerdere studies is gevonden bij *DCC* haploinsufficiënte dieren. Bovendien is dit tegenovergesteld aan wat in diermodellen voor schizofrenie en in patiënten met schizofrenie is gevonden. Deze bevindingen geven een sterke aanwijzing dat het DCC/Unc5C receptor complex een belangrijke rol speelt bij de vorming en stabiliteit van mdDA circuits in de PFC en wijst op een mogelijke betrokkenheid van deze receptoren bij de ontwikkeling van psychiatrische aandoeningen, zoals schizofrenie.

Zoals beschreven in de voorgaande hoofdstukken, bestaat het mdDA systeem uit verschillende neuronen die naar verscheidene hersengebieden projecteren (waaronder de habenula, het striatum en de PFC). Deze heterogeniteit van mdDA neuronen speelt ook een rol in verschillende neurologische en psychiatrische aandoeningen. Zo is een kenmerk van de ziekte van Parkinson de selectieve degeneratie van neuronen in de substantia nigra van het mdDA systeem, en spelen neuronen in de VTA een belangrijke rol bij de ontwikkeling van verslavingsgedrag. Onderzoek naar de ontwikkeling van het mdDA systeem wordt bemoeilijkt door gebrek aan de juiste middelen om de verschillende mdDA subtypes de identificeren en te markeren. In **hoofdstuk 5** beschrijven we een nieuwe, transgene methode waarbij gebruik wordt gemaakt van het Cre/*lox* en Flp/*frt* recombinatie systeem dat selectieve expressie van verschillende fluorescente eiwitten mogelijk maakt. Met deze methode, genaamd ITC (IFP/tdTomato/Citrine) kunnen twee verschillende mdDA subsets worden gemarkeerd met het fluorescente eiwit Citrine of tdTomato, waarbij tdTomato expressie afhankelijk is van Cre recombinase en Citrine expressie van Flp recombinase. In de ITC muizen is een groot deel van de mdDA neuronen ITC-positief, hoewel neuronen in de mediale VTA geen expressie vertonen. Expressie is ook zichtbaar in axonen die projecteren naar het striatum. Deze ITC-positieve axonen zijn echter niet homogeen verspreid in het striatum, maar zijn verrijkt in specifieke compartimenten van het striatum. Dit type innervatie is niet zichtbaar wanneer alle mdDA axonen aangekleurd zijn en is mogelijk een gevolg van het niet aankleuren van ITC-negatieve axonen vanuit de mediale VTA. Naast dit specifieke innervatiepatroon blijkt in deze muizen ook dat dopaminerge axonen in specifieke domeinen van de MFB groeien. Mogelijk is deze organisatie belangrijk voor de ontwikkeling van deze projecties (zie **hoofdstuk 3**).

Omdat de ITC strategie afhankelijk is van de juiste expressie van Cre en Flp in mdDA subsets, zijn in **hoofdstuk 5** ook subset-specifieke Cre en Flp muizen gegenereerd. Hierbij is gebruik gemaakt van *Neuropilin-2* (*Nrp2)* en *Guanylyl Cyclase 2C* (*Gucy2c)* promotor sequencies om *Nrp2-Flp* en *Gucy2c-Cre* dieren te genereren. Tegen verwachting in leidt de kruising van *Nrp2-Flp* of *Gucy2c-Cre* muizen met ITC muizen tot de markering van enkele, individuele neuronen in plaats van een volledige groep neuronen. Hierdoor is de complete structuur van deze neuronen, inclusief de dendritische projecties, goed zichtbaar. Voor het eerst kan met deze benadering de ontwikkeling van het mdDA systeem op individueel celniveau bestudeerd worden. Een eerste analyse van deze neuronen onthult specifieke verschillen in pre- en postsynaptische connectiviteit. Subtypen van mdDA neuronen kunnen worden herkend door verschillen in de dendritische organizatie. Daarnaast kan in deze muizen de complexe innervatie van het striatum door individuele mdDA axonen gevisualiseerd en bestudeerd worden. Dit opent nieuwe mogelijkheden om te onderzoeken welke moleculaire mechanismen betrokken zijn bij de ontwikkeling van dendritische structuren in het mdDA systeem en hoe synaptische specificiteit wordt gereguleerd in het striatum.

De ITC strategie biedt nieuwe mogelijkheden voor het bestuderen van de ontwikkeling en functie van mdDA circuits. Processen als migratie, de groei van axonen en ontwikkeling van dendrieten kunnen in deze muizen bestudeerd worden, maar ook of en hoe bepaalde gedragspatronen en farmacologische interventies structurele verandering van dopaminerge circuits veroorzaken. Daarnaast biedt het markeren van verschillende groepen van mdDA neuronen in dezelfde muis de mogelijkheid om subset-specifieke effecten van kandidaatmoleculen te testen in een enkele *ex vivo* of *in vitro* experimentele opstelling. Ook kunnen *in vivo* manipulaties geanalyseerd worden op het niveau van specifieke groepen van mdDA neuronen. Door deze nieuwe mogelijkheden zal deze strategie een belangrijke bijdrage leveren aan toekomstige studies naar de ontwikkeling van het mdDA systeem.

De studies beschreven in dit proefschrift bieden nieuwe inzichten in de mechanismen die betrokken zijn bij de ontwikkeling van mdDA circuits (zie **hoofdstuk 6**). Axon-axon interacties spelen een belangrijke rol bij de vorming van een deel van deze connecties en toekomstige studies moeten uitwijzen of dit ook voor andere mdDA axonen geldt. Netrin-1, en de receptoren die dit molecuul binden, zijn ook nauw betrokken bij de ontwikkeling van mdDA circuits. Verstoringen in

mdDA connectiviteit spelen een mogelijke rol bij de ontwikkeling van verschillende neurologische en psychiatrische aandoeningen. Dit maakt zowel LAMP als Netrin-1 interessante kandidaatmoleculen voor het ontwikkelen van therapieën. Ook is een nieuwe transgene strategie ontwikkeld om studies naar de ontwikkeling van het mdDA systeem te faciliteren. Deze bevindingen en nieuwe methoden dragen bij aan het ontdekken van hoe verstoringen in de ontwikkeling van het mdDA systeem betrokken zijn bij de ontwikkeling van neurologische en psychiatrische aandoeningen. Daarnaast bieden ze nieuwe uitgangspunten voor de ontwikkeling van therapieën gericht op het manipuleren of herstellen van deze connecties.

CURRICULUM VITAE

Ewoud Roberto Eduard Schmidt is geboren op 5 februari 1985 te Rotterdam. Na het behalen van zijn VWO diploma in 2003 aan het Wartburg College, Guido de Brès in Rotterdam begon hij met zijn studie Biomedische Wetenschappen aan de Universiteit Utrecht. Hij behaalde zijn bachelor diploma in 2006, waarna hij zijn opleiding vervolgde met de master Neurowetenschappen & Cognitie aan dezelfde universiteit. Als onderdeel van zijn master deed Ewoud een stage van 9 maanden in het laboratorium van Jeroen Pasterkamp onder supervisie van Dianne van den Heuvel in het Rudolf Magnus Instituut voor Neurowetenschappen van het Universitair Medische Centrum Utrecht. Hierna deed hij een stage van 6 maanden in het laboratorium van Antonella Riccio in het Medical Research Council Laboratory of Molecular and Cell Biology, University College London, Groot-Brittannië. Ewoud behaalde zijn master diploma in 2008 (cum laude). In hetzelfde jaar verkreeg hij een Toptalent onderzoeksbeurs van de Nederlandse Organisatie voor Wetenschappelijk Onderzoek (NWO) voor de financiering van zijn promotieonderzoek. Hij voerde dit onderzoek uit in de groep van Jeroen Pasterkamp in het Rudolf Magnus Instituut voor Neurowetenschappen in Utrecht. De resultaten van dit onderzoek staan beschreven in dit proefschrift. Hij zal zijn wetenschappelijk onderzoek voortzetten als postdoc in het laboratorium van Franck Polleux aan Columbia University in New York, de Verenigde Staten van Amerika.

Ewoud Roberto Eduard Schmidt was born on February 5th 1985 in Rotterdam, the Netherlands. After graduation from secondary school (Wartburg College, Guido de Brès in Rotterdam, the Netherlands) in 2003, he studied Biomedical Sciences at Utrecht University. He obtained his Bachelor of Science degree in 2006 and continued with the Master Neuroscience & Cognition at the same university. As part of the Master program he did a 9 month internship in the laboratory of Jeroen Pasterkamp under supervision of Dianne van den Heuvel at the Rudolf Magnus Institute of Neuroscience of the University Medical Center Utrecht. This was followed by a 6 month internship in the laboratory of Antonella Riccio at the Medical Research Council Laboratory for Molecular and Cell Biology, University College London, United Kingdom. Ewoud obtained his Master of Science degree in 2008 (cum laude). In the same year he acquired a Toptalent research grant from the Netherlands Organisation for Scientific Research (NWO) to fund his own PhD research project. He performed this research project in the laboratory of Jeroen Pasterkamp at the Rudolf Magnus Institute for Neuroscience in Utrecht. The results of this research project are presented in this thesis. He will continue with his postdoctoral research in the laboratory of Franck Polleux at Columbia University in New York, USA.

A

'Science is organized knowledge. Wisdom is organized life.'

- Immanuel Kant

LIST OF PUBLICATIONS

Schmidt ERE, Brignani S, Adolfs Y, Demmers J, Vidaki M, Donahoo AS, Richards LJ, Karagogeos D, Kolk SM, Pasterkamp RJ (2013). Subdomain-mediated axon-axon signaling and chemoattraction cooperate to regulate afferent innervation of the lateral habenula. *Neuron, Under Revision.*

Manitt C, Eng C, Pokinko M, Ryan RT, Torres-Berrio A, Lopez JP, Yogendran SV, Daubaras MJ, Grant A, **Schmidt ERE**, Tronche F, Krimpenfort P, Cooper HM, Pasterkamp RJ, Kolb B, Turecki G, Wong TP, Nestler EJ, Giros B, Flores C (2013). DCC orchestrates the development of the prefrontal cortex during adolescence and is altered in psychiatric patients. *Translational Psychiatry* 3, e338.

Auger ML, **Schmidt ERE**, Manitt C, Dal-Bo G, Pasterkamp RJ, Flores C (2013). Unc5c haploinsufficient phenotype: striking similarities with the dcc haploinsufficiency model. *European Journal of Neuroscience*, 38, 2853-2863.

Schmidt ERE, Morello F, Pasterkamp RJ (2012). Dissection and culture of mouse dopaminergic and striatal explants in three-dimensional collagen matrix assays. *Journal of Visualized Experiments*. 61, e3691, doi: 10.3791/3691.

Vorstman JA, van Daalen E, Jalali GR, **Schmidt ERE**, Pasterkamp RJ, de Jonge M, Hennekam EA, Janson E, Staal WG, van der Zwaag B, Burbach JP, Kahn RS, Emanuel BS, van Engeland H, Ophoff RA (2010). A double hit implicates DIAPH3 as an autism risk gene. *Molecular Psychiatry* 16, 442-451.

Schmidt ERE, Pasterkamp RJ, van den Berg LH (2009). Axon guidance proteins: novel therapeutic targets for ALS? *Progress in Neurobiology* 88, 286-301.

A

'The most important task of philosophy in the modern world is to resurrect the human person, to rescue it from trivializing science, and to replace the sarcasm which knows that we are merely animals, with the irony that sees we are not.'

- Roger Scruton

DANKWOORD

De afgelopen vijf jaar heb ik mogen merken dat wetenschap één grote sociale activiteit is, waarmee ik niet alleen op alle zeer gewaardeerde borrelmomenten doel. Zonder de mensen waarmee ik heb mogen samenwerken, en de mensen die direct om mij heen staan, had dit proefschrift nooit tot stand gekomen. En nu is het zover, het boekje is geschreven, de laatste woorden staan op papier. Dit boek kan letterlijk en figuurlijk afgesloten worden met het meest gelezen hoofdstuk waarin ik mijn dank wil uitspreken.

Allereerst mijn promotor, Jeroen Pasterkamp. Beste Jeroen, hartelijk dank voor je begeleiding en expertise de afgelopen jaren. Tijdens mijn verblijf in het Pasterkamplab, zowel als master student en als promovendus, heb ik veel geleerd over hoe een goed onderzoeksproject uit te voeren. Ik heb je ambitie om vernieuwend en kwalitatief hoogstaand onderzoek te doen zeer gewaardeerd. Dit bleek ook uit je steun bij het zoeken naar een buitenland stage en later bij het aanvragen van mijn Toptalent beurs. Ook je wetenschappelijke houding vond ik zeer prettig en herkenbaar. De vasthoudendheid om met die extra stap de publicatie op een hoger niveau te brengen, met alle risico's en frustraties die daarbij horen, heeft geleid tot zeer mooie resultaten.

Mijn tweede promotor, Peter Burbach. Beste Peter, hartelijk dank voor je begeleiding en ondersteuning. De gesprekken over mijn toekomstplannen en jouw inzet en hulp bij het zoeken naar een postdoc positie heb ik zeer op prijs gesteld. Ook jouw inzicht en visie over de inhoud van dit proefschrift waren zeer waardevol.

Ik bedank de leden van mijn leescommissie, prof. dr. Casper Hoogenraad, prof. dr. Alain de Bruin, prof. dr. Sander van den Heuvel, prof. dr. Joost Verhaagen en prof. dr. Vincent Christoffels voor het beoordelen van mijn proefschrift.

Alle (voormalig) leden van het Pasterkamplab. Julie hartelijk dank voor de input en wetenschappelijke discussies. Dianne, bedankt voor de begeleiding tijdens mijn masterstage. Uiteindelijk is dit een mooi begin gebleken van mijn – nu nog prille – onderzoekscarrière. Youri, bedankt voor je enorme inzet en het meedenken met de projecten. Het nemen van verschillende praktische drempels was niet altijd even

makkelijk, maar onder andere jouw doorzettingsvermogen heeft ons er doorheen geholpen. Mark, jij ook bedankt bij de hulp met experimenten en het muiswerk. Leo, je zou in het dankwoord moeten staan van elk proefschrift dat van onze afdeling komt. Hartelijk dank voor al je hulp op het lab. Eljo en Anna, jullie ook bedankt om het toch een tijdje uit te houden met mij op de kamer. Het was een leuke tijd, maar ik kon zo'n grote kamer met aquarium uiteraard niet afslaan.

Bart, het was een voorrecht om het laatste jaar de kamer met je te delen. De muziek was altijd dik in orde, de sfeer, met het prachtige aquarium, was prima, en de gesprekken over wetenschap en andere zaken had ik niet willen missen. Ook de 'metal-momenten' op het lab en het 'klokhuis kijken met een biertje' waren zeer effectief tegen de frustraties die onlosmakelijk met labwerk verbonden zijn. Ook zeer bedankt voor je hulp bij het bouwen van mijn eerste 'fixie'. Jouw sportieve inslag gecombineerd met een 'doe-het-zelf' mentaliteit (vliegers naaien, longboards zagen, fietsen bouwen etc.) heeft mooie – en misschien een paar minder mooie – fietsmomenten opgeleverd!

Francesca, thanks for all your help on setting up many experiments and making our awesome JoVE video. I very much appreciated our talks in which we critically reviewed science and life. They were great, much fun, and sometimes even hilarious. I wish you all the best with your new postdoc position, I am sure you can do it! And hopefully it gives you exactly what you are looking for.

Sara, thank you very much for your help with completing the habenula project and all the best in continuing with the ITC mice! Thanks for your incredible enthusiasm and the many insights into the Dutch culture. Try to keep up your motivation, even when it's raining or the results are not up to your expectations!

De afgelopen jaren zijn er ook genoeg mensen weer vertrokken. Desalniettemin hebben ze, direct of indirect, een belangrijke bijdrage geleverd aan dit proefschrift. Sharon, zeer bedankt voor jouw bijdrage aan het 'habenula-hoofdstuk'. De Smidt groep, Marten, Marco, Jesse, Elisa en Lars, hartelijk dank voor jullie expertise op het gebied van het dopamine systeem en de feedback en discussies die hieruit voortkwamen. Frank, Koushik, Anup, Arjen, Kristel, and Ruud, thanks for all the

conversations and discussions, often accompanied by one or many drinks, that we had over the years.

Krista, Ria, Joke, Vicki en Sandra, jullie bedankt voor alle hulp en ondersteuning. Marjolein, jij zeer bedankt voor de goede zorg van alle dieren.

De masterstudenten die ik heb mogen begeleiden bij hun stage. Jitte Groothuis, Camille Okom en Marieke Martens, hartelijk dank voor jullie bijdrage aan dit onderzoek en heel veel succes met jullie toekomstige carrières.

Familie en vrienden. Jullie allemaal heel erg bedankt voor de momenten waarbij ik even uit de wetenschappelijke bubbel kon stappen. Deze momenten waren zeer belangrijk om te kunnen relativeren en te reflecteren.

Bart en Jerre, zeer bedankt dat jullie mij willen ondersteunen als paranimf tijdens mijn verdediging. Toch fijn dat ik tijdens mijn verdediging het één en ander kan overleggen.

Lieve ouders, hartelijk dank voor jullie steun en onvoorwaardelijke liefde. Zonder jullie had ik dit punt nooit kunnen bereiken. Dit proefschrift gaat over mijn werk, maar het is zeer belangrijk om daar een thuis tegenover te hebben staan. En hoewel ik al geruime tijd mijn eigen plek heb gevonden, hebben jullie mij altijd een thuis geboden om op terug te vallen.

Lieve Susanne, niet alleen wil ik je bedanken wat je voor mij betekent, maar voornamelijk om wie je bent. Je manier van denken, doorzien en voelen zijn uniek en heel bijzonder. Ik verwonder mij over de integriteit, ambitie en liefde die je in je hebt. En je moet een enorm incasseringsvermogen hebben om het met mij uit te houden. Dank voor je steun, je begrip en dat je mij helpt herinneren wat écht belangrijk is.

'The universe is big. It's vast and complicated and ridiculous. And sometimes, very rarely, impossible things just happen and we call them miracles.'

- The Doctor

'Heb ik mijn rol goed gespeeld? Zo ja, applaudiseer dan, want de komedie is voorbij!'

- Keizer Augustus